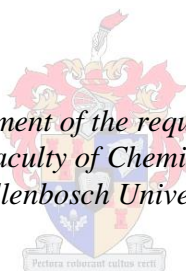


Dendrimer Encapsulated Gold Nanoparticles as Catalyst Precursors for Oxidative Transformations of Unsaturated Hydrocarbons

by
Ené Slazus

*Thesis presented in fulfilment of the requirements for the degree of
Master of Science in the Faculty of Chemistry and Polymer Science at
Stellenbosch University*



Supervisor: Prof Selwyn Frank Mapolie
Co-supervisor: Dr Rehana Malgas-Enus

March 2015

Declaration

By submitting this thesis electronically, I declare that the entirety of the work contained therein is my own, original work, that I am the sole author thereof (save to the extent explicitly otherwise stated), that reproduction and publication thereof by Stellenbosch University will not infringe any third party rights and that I have not previously in its entirety or in part submitted it for obtaining any qualification.

February 2015

Copyright © 2015 Stellenbosch University

All rights reserved

Abstract

In an attempt to produce active catalysts for the oxidation of alkanes, hydrophobic dendritic micelle encapsulated gold nanoparticles were prepared. Dendrimers are well suited as templates for the encapsulation of metal nanoparticles as they can control the size and distribution of the particles. Using hydrophobic dendritic micelles it was found that the mode of encapsulation is driven by the solubility of the metal ions and not complexation of these ions, as is the case with conventional dendrimers. The dendritic micelles also provide the possibility of producing the dendrimer encapsulated nanoparticles in organic solvents, simplifying the encapsulation process as well as their subsequent application in catalysis.

With this in mind, two types of dendritic micelles were synthesized. The first type, based on commercially available DAB PPI dendrimers, contained a diaminobutane core while the second type, containing a PAMAM interior architecture, has a cyclam core. Three generations of DAB PPI dendrimers were modified on their periphery with palmitoyl chloride to give the alkyl chain terminated hydrophobic DAB PPI dendritic micelles. The PAMAM-type cyclam-cored dendrimers were synthesized from the core outwards to produce two generations of cyclam-cored amine-terminated dendrimers. Their periphery could then be modified with palmitoyl chloride to produce two generations of alkyl chain terminated hydrophobic cyclam-cored dendritic micelles.

The dendritic micelles were used as templates for the encapsulation of gold nanoparticles and these were fully characterized by UV/Vis spectroscopy and HR-TEM. Au₁₃, Au₃₁ and Au₅₅ nanoparticles were encapsulated in each dendrimer template by varying the dendrimer to gold ratio. HR-TEM results indicate relatively uniform particles with an average particle size falling in the range of 4-6 nm.

Finally, the dendrimer encapsulated nanoparticles (DENs) were applied as catalysts in the oxidation of n-octane. To the best of our knowledge DENs have not been applied as catalysts in the oxidation of linear alkanes. High substrate conversions, falling in the range of 70-90%, were achieved with all of the catalysts. Longer reaction times and lower catalyst loadings resulted in higher conversions with the optimum condition determined to be 0.1 mol% catalyst and 72 hours reaction time. It was also concluded that the nanoparticle size has a

bigger influence on the conversion than the nature and generation of the dendrimer template. Overall the gold DENs show great potential as oxidation catalysts.

Opsomming

In die poging om aktiewe katalisators vir die oksidasie van alkane te produseer is goud nanopartikels in die binne ruimtes van hidrofobiese dendritiese miselle ge-enskapsuleer. Dendrimere is geskikte template vir die enkapsulering van metaal nanopartikels a.g.v die feit dat dit die grootte en distribusie van die partikels kan beheer. Deur gebruik te maak van hidrofobiese dendritiese miselle verander die wyse van enkapsulering van kompleksing van metaal ione (die geval in konvensionele dendrimere) na oplossing gedrewe enkapsulering. Dendritiese miselle bied ook die moontlikheid om die dendrimer-ge-enskapsuleerde nanopartikels in organiese oplosmiddels voor te berei wat die enkapsulerings proses sowel as die toepassing in katalise vergemaklik.

Met hierdie in gedagte is twee verskillende tipe dendritiese miselle gesintetiseer. Die eerste tipe, gebaseer op kommersieel beskikbare DAB PPI dendrimere, bevat 'n diaminobutaan kern, terwyl die tweede tipe, bestaande uit 'n PAMAM binne-struktuur, 'n siklaam kern bevat. Drie generasies van DAB PPI dendrimere was gemodifiseer op die periferie met palmitoïelchloried om alkiel ketting getermineerde hidrofobiese DAB PPI dendritiese miselle te produseer. Die PAMAM siklaam kern bevattende dendrimere was gesintetiseer van die kern uitwaarts om twee generasies amien getermineerde dendrimere te produseer. Dit was toe moontlik om die periferie met palmitoïelchloried te modifiseer om twee generasies van alkiel getermineerde siklaam kern bevattende hidrofobiese dendritiese miselle op te lewer.

Die dendritiese miselle was gebruik as template vir die enkapsulasie van goud nanopartikels en volledig gekarakteriseer deur UV/Vis spektroskopie en HR-TEM. Au₁₃, Au₃₁ and Au₅₅ nanopartikels was ge-enskapsuleer in elk van die dendrimeer template deur die verhouding van dendrimeer tot goud te wissel. HR-TEM resultate dui aan dat die partikels goed versprei is met 'n gemiddelde partikel grootte tussen 4-6 nm.

Die dendrimeer ge-enskapsuleerde goud nanopartikels (DENS) was as katalisators in die oksidasie van n-oktaan toegepas. Volgens ons kennis is DENSs nog nie toegepas as katalisators in die oksidasie van lineêre alkane nie. Hoë substraat omskakelings, tussen 70 en 90%, was deur al die katalisators bereik. 'n Langer reaksie tyd en laer katalisator konsentrasies het hoër omsettings tot gevolg gehad. Die optimale kondisies sluit 'n 0.1 mol% katalisator konsentrasie en 72 uur reaksie tyd in. Die gevolgtrekking was gemaak dat die

nanopartikel grootte 'n groter invloed op die substraat omsetting het as die aard en generasie van die dendrimeer templaar. Alles in ag geneem, wys die goud DENs groot potensiaal as oksidasie katalisators.

Acknowledgements

Firstly and most importantly I would like to thank my two supervisors, Prof S. F. Mapolie and Dr R. Malgas-Enus. Without their guidance, encouragement and patience this project would not be what it is. Their doors were always open for me to bother them with silly questions and concepts and for that I'm truly grateful.

I would not have survived the past two years were it not for friends and family. The students in the Organometallic Research Group have not only become close friends through the last two years but have provided guidance and support where needed as well as laughter. Jacquin and Cassiem, thank you for lightening the mood and giving the lab a fun environment. Corli, Hennie, Derik and Angelique thank you for all of your guidance and patience, I would not have survived without it. Anna, thank you for always being willing to go for coffee and provide some much needed distractions from all the work.

André, you kept me sane, lifted my spirits when I needed it most and never let a day go by without telling me that I am more than capable and should start believing more in myself. You were there through the good and the bad and never stopped believing in me, this means the world to me.

I would not be where I am today were it not for my family. Thank you for your love, encouragement, support and just being there when I needed some family time. Mom, you have been through so much these last few years and have come out stronger. You are and will always be my role model and I love you with all of my heart. Thank you for the home made food and the enthusiasm in trying to understand my project, it means a lot. Dad, you have stood by me, paid for studies, accommodation, petrol and so much more. You have provided me with more than I could ever dream of and I am truly grateful for that. Lastly to my sister, Cecile, although you are far away I could always count on you for some sisterly love, support and encouragement, thank you.

Conference Contributions

E. Slazus, R. Malgas-Enus and S.F. Mapolie

Poster Titled: *Catalytic metal nanoparticles stabilized by novel micelle-like dendrimers*

Catalysis Society of South Africa (CATSA) annual conference, Port Edward (Wild Coast Sun Hotel), South Africa, 2013

E. Slazus, R. Malgas-Enus and S.F. Mapolie

Oral Presentation Titled: *The application of dendritic micelle encapsulated gold nanoparticles as oxidation catalysts*

SACI Young Chemists Symposium, Cape Town (University of Cape Town), South Africa, 2014

E. Slazus, R. Malgas-Enus and S.F. Mapolie

Oral Presentation Titled: *Au nanoparticles encapsulated in dendritic micelles as catalysts for the oxidation of octane*

Catalysis Society of South Africa (CATSA) annual conference, Johannesburg (St Georges Hotel and Conference Centre), South Africa, 2014

Table of Contents

Declaration	i
Abstract	ii
Opsomming	iv
Acknowledgements	vi
Conference Contributions	vii
Table of Contents	viii
List of Figures	xii
List of Schemes	xvi
List of Tables	xvii
List of Abbreviations and Symbols	xviii
Chapter one: An introduction to Dendrimer Encapsulated Nanoparticles and their Application in Catalysis	
1.1. Synthesis, Stabilization and Application of Metal NPs	1
1.1.1. Ligand-stabilized NPs	2
1.1.1.1. Preparation of ligand-stabilized NPs	3
1.1.1.2. Applications of ligand-stabilized NPs	5
1.1.2. Dendrimer Stabilized NPs	7
1.1.2.1. Dendrimer Synthesis and Application	8
1.1.2.2. Stabilization techniques	13
1.2. Dendrimer Encapsulated NPs in Catalysis	14
1.2.1. The use of DENs in coupling reactions.....	15

1.2.2. The use of DENs in hydrogenation reactions	17
1.2.3. Oxidation Reactions	18
1.3. Summary and Objectives	19
1.4. References.....	21
Chapter two: Synthesis of Unimolecular Dendritic Micelles	
2.1. Introduction.....	24
2.2. Modification of DAB PPI dendrimers with long aliphatic chains.....	26
2.2.1. Characterization	27
2.2.1.1. Infrared Spectroscopy (ATR-IR).....	27
2.2.1.2. ¹ H-NMR and ¹³ C-NMR Spectroscopy	27
2.2.1.3. Mass Spectrometry, Elemental Analysis and Thermal stability.....	28
2.3. Synthesis of cyclam-cored unimolecular dendritic micelles	28
2.3.1. Characterization	31
2.3.1.1. Infrared Spectroscopy (ATR-IR).....	31
2.3.1.2. ¹ H-NMR and ¹³ C-NMR Spectroscopy	32
2.3.1.3. Mass Spectrometry, Elemental Analyses and Thermal Stability	34
2.4. Conclusion	36
2.5. Experimental Section.....	37
2.5.1. General Consideration and Materials.....	37
2.5.2. Instrumentation	37
2.5.3. Procedures and Characterization.....	37
2.6. References.....	44

Chapter three: Encapsulation of Gold Nanoparticles in Dendritic Micelles

3.1. Introduction.....	45
3.2. UV/Vis binding study	45
3.3. Encapsulation of Au nanoparticles in dendritic micelles.....	49
3.3.1. Method	49
3.3.2. Characterization	50
3.3.2.1. Au ₁₃ Dendrimer Encapsulated Nanoparticles.....	50
3.3.2.2. Au ₃₁ Dendrimer Encapsulated Nanoparticles.....	54
3.3.2.3. Au ₅₅ Dendrimer Encapsulated Nanoparticles.....	57
3.3.3. Cluster size vs average particle size.....	61
3.4. Conclusion.....	64
3.5. Experimental Section.....	64
3.5.1. General Consideration and Materials.....	64
3.5.2. Instrumentation	64
3.5.3. Procedures and Characterization.....	65
3.6. References.....	68

Chapter four: Application of Dendritic Micelle Encapsulated Gold Nanoparticles as Alkane Oxidation Catalysts

4.1. Introduction.....	69
4.1.1. Oxidation of cyclic hydrocarbon substrates	69
4.1.2. Oxidation of linear hydrocarbon substrates	70
4.2. Catalysed oxidation of n-octane.....	72
4.2.1. Mechanistic insight into the product selectivity.....	79

4.2.2. Possibility of catalyst recovery	80
4.3. Conclusion	81
4.4. Experimental Section	82
4.4.1. General Considerations and Materials	82
4.4.2. Instrumentation	82
4.4.3. Procedures and Characterization	82
4.5. References	83
Chapter five: A Summary of the Preceding Chapters and Suggestions for Future Work	
5.1. Summary of preceding chapters.....	84
5.2. Suggestions for future work.....	86

List of Figures

Chapter one

Figure 1.1-1: Routes to metal nanoparticle formation	1
Figure 1.1-2: A dendrimer consists of a core, branching units and terminal groups	7
Figure 1.1-3: Schematic representation of amine- and folate-terminated PAMAM dendrimer of generation 5 and its complexation with the anesthetics	12
Figure 1.1-4: The three different approaches to metal NP stabilization via dendrimers	13
Figure 1.2-1: Formation of DENs	14

Chapter two

Figure 2.1-1: Comparison between a classic micelle and a dendrimer.....	24
Figure 2.1-2: 1,4,8,11-Tetraazacyclotetradecane or more commonly cyclam	25
Figure 2.3-1: Synthesis of G 0.5 dendrimer.....	28
Figure 2.3-2: (a) Linking of two dendrimer arms through ethylenediamine (b) Polymer type by-product.....	29
Figure 2.3-3: G 0.5 (1) and G1.5 (3) cyclam-cored dendrimers	32
Figure 2.3-4: G1 (2) and G2 (4) cyclam-cored dendrimers	33
Figure 2.3-5: G1 cyclam-cored dendritic micelle	34

Chapter three

Figure 3.2-1: UV/Vis titration binding study results for DAB-dendr-(palmitoyl) ₄	47
Figure 3.2-2: UV/Vis titration binding study results for DAB-dendr-(palmitoyl) ₈	47
Figure 3.2-3: UV/Vis titration binding study results for DAB-dendr-(palmitoyl) ₁₆	47
Figure 3.2-4: UV/Vis titration binding study results for Cyclam-dendr-(palmitoyl) ₄	48
Figure 3.2-5: UV/Vis titration binding study results for Cyclam-dendr-(palmitoyl) ₈	48

Figure 3.3-1: General method for the preparation of dendrimer encapsulated Au nanoparticles.....	49
Figure 3.3-2: UV/Vis spectrum of Au ₁₃ DENs.....	51
Figure 3.3-3: HR-TEM images of G1 Cyclam-dendr-(palmitoyl) ₄ -Au ₁₃	51
Figure 3.3-4: HR-TEM images of G2 Cyclam-dendr-(palmitoyl) ₈ -Au ₁₃	51
Figure 3.3-5: Particle size distribution (a) Average particle size: 3.41 ± 1.03 nm ; Max: 8.44 nm; Min: 1.45 nm (b) Average particle size: 2.66 ± 0.589 nm; Max: 5.03 nm; Min: 1.43 nm	52
Figure 3.3-6: HR-TEM images of G1 DAB-dendr-(palmitoyl) ₄ -Au ₁₃	52
Figure 3.3-7: HR-TEM images of G2 DAB-dendr-(palmitoyl) ₈ -Au ₁₃	53
Figure 3.3-8: HR-TEM images of G3 DAB-dendr-(palmitoyl) ₁₆ -Au ₁₃	53
Figure 3.3-9: Particle distribution (a) 4.26 ± 1.31 nm; Max: 11.11 nm; Min: 1.79 nm (b) 8.98 ± 3.87 nm; Max: 24.82 nm; Min: 1.71 nm (c) 4.54 ± 2.02 nm; Max: 13.49 nm; Min: 1.62 nm	53
Figure 3.3-10: UV/Vis spectrum of Au ₃₁ DENs.....	54
Figure 3.3-11: HR-TEM images of G1 Cyclam-dendr-(palmitoyl) ₄ -Au ₃₁	55
Figure 3.3-12: HR-TEM images of G2 Cyclam-dendr-(palmitoyl) ₈ -Au ₃₁	55
Figure 3.3-13: Particle distribution (a) Average particle size: 4.41 ± 1.31 nm; Min: 2.33 nm; Max: 14.43 nm (b) Average particles size: 4.83 ± 2.00 nm; Min: 1.36 nm; Max: 11.93 nm.....	55
Figure 3.3-14: HR-TEM images of G1 DAB-dendr-(palmitoyl) ₄ -Au ₃₁	56
Figure 3.3-15: HR-TEM images of G2 DAB-dendr-(palmitoyl) ₈ -Au ₃₁	56
Figure 3.3-16: HR-TEM images of G3 DAB-dendr-(palmitoyl) ₁₆ -Au ₃₁	56
Figure 3.3-17: Particle distribution (a) Average particle size: 6.72 ± 2.69 nm; Min: 1.71 nm; Max: 17.20 nm (b) Average particle size: 6.06 ± 2.42 nm;	

Min: 1.64 nm; Max: 13.66 nm (c) Average particle size: 5.68 ± 1.54 nm; Min: 1.86 nm; Max: 10.62 nm	57
Figure 3.3-18: UV/Vis spectrum of Au ₅₅ DENs.....	58
Figure 3.3-19: HR-TEM images of G1 Cyclam-dendr-(palmitoyl) ₄ -Au ₅₅	58
Figure 3.3-20: HR-TEM images of G2 Cyclam-dendr-(palmitoyl) ₈ -Au ₅₅	59
Figure 3.3-21: Particle distribution (a) Average particle size: 4.63 ± 1.29 nm; Min: 2.03 nm; Max: 10.55 nm (b) Average particle size: 4.27 ± 1.23 nm; Min: 1.87 nm; Max: 8.76 nm.....	59
Figure 3.3-22: HR-TEM images of G1 DAB-dendr-(palmitoyl) ₄ -Au ₅₅	60
Figure 3.3-23: HR-TEM images of G2 DAB-dendr-(palmitoyl) ₈ -Au ₅₅	60
Figure 3.3-24: HR-TEM images of G3 DAB-dendr-(palmitoyl) ₁₆ -Au ₅₅	60
Figure 3.3-25: Particle distribution (a) Average particle size: 4.57 ± 1.12 nm; Min: 2.18 nm; Max: 9.62 nm (b) Average particle size: 4.44 ± 1.14 nm; Min: 1.94 nm; Max: 8.33 nm (c) Average particle size: 4.61 ± 1.53 nm; Min: 1.66 nm; Max: 10.01 nm	61
Figure 3.3-26: The organization of full shells of atoms around a central core atom to produce ‘magic number’ cluster sizes	62
Chapter four	
Figure 4.1-1: Photocatalysed oxidation of cyclohexane via (a) Au/CQD composites in the presence of H ₂ O ₂ and (b) C ₃ N ₄ /Au using water as oxidant.....	70
Figure 4.1-2: Product distribution and % conversion achieved for the oxidation of ethane using a Fe/ZSM-5 catalyst prepared by calcination and reduction	70
Figure 4.2-1: Results of the effect of metal loading experiments.....	73
Figure 4.2-2: Results of the effect of time experiments.....	74
Figure 4.2-3: Effect of the dendrimer template on the conversion for the Au ₁₃ DENs.....	74

Figure 4.2-4: Effect of the dendrimer template on the conversion for the Au₃₁ DENs75

Figure 4.2-5: Effect of the dendrimer template on the conversion for the Au₅₅ DENs76

Figure 4.2-6: Effect of the different Au/dendrimer ratios used for each specific
dendrimer template on the conversion achieved76

List of Schemes

Chapter one

Scheme 1.1-1: Ligand exchange reaction on thioether stabilized Pd-NP with LC-NHCs	3
Scheme 1.1-2: The two synthetic approaches (a) divergent and (b) convergent	8
Scheme 1.1-3: Synthesis of PPI dendrimer by Vögtle <i>et al</i> in 1978.....	9
Scheme 1.2-1: Heck coupling of aryl halides with n-butylacrylate.....	15
Scheme 1.2-2: Suzuki-reaction with palladium DENs	16

Chapter two

Scheme 2.2-1: Modification of G3 DAB PPI dendrimer with palmitoyl chloride	26
Scheme 2.3-1: Synthesis of G1 dendrimer	29
Scheme 2.3-2: (a) Synthesis of G 1.5 ester-terminated dendrimer (b) Synthesis of G 2 amine terminated dendrimer.....	30
Scheme 2.3-3: (a) Modification of G 1 tetra-amine dendrimer (b) Modification of G 2 octa-amine dendrimer.....	30

Chapter four

Scheme 4.1-1: General scheme for the photocatalytic oxidation of cyclohexane	69
Scheme 4.1-2: Au/SBA-15 catalysed oxidation of ethylbenzene	71
Scheme 4.2-1: General reaction for the oxidation of n-octane	72
Scheme 4.2-2: Iron-induced radical chain decomposition of TBHP	79
Scheme 4.2-3: CeNR induced decomposition of TBHP.....	79
Scheme 4.2-4: The mechanism proposed by Biradar <i>et al</i>	80

List of Tables

Chapter one

Table 1.1-1: Examples of ligand-stabilized NPs.....	4
Table 1.1-2: Dendrimers used for the TA binding studies.....	10

Chapter three

Table 3.3-1: Approximate size of specific Pt nanoparticle cluster sizes	62
Table 3.3-2: Approximate theoretical size of Au ₁₃ and Au ₅₅ nanoparticles	63
Table 3.3-3: Calculated cluster sizes of Au nanoparticles synthesized	63
Table 3.5-1: Amount of the dendrimer template used	65
Table 3.5-2: Amount of HAuCl ₄ solution required	66
Table 3.5-3: Amount of dendrimer template used	66
Table 3.5-4: Amount of HAuCl ₄ solution required	66
Table 3.5-5: Amount of dendrimer template used	67
Table 3.5-6: Amount of HAuCl ₄ required	67

Chapter four

Table 4.1-1: Oxidation of n-hexadecane catalyzed by Au/SBA-15 under various reaction conditions	71
Table 4.2-1: Summary of catalyst activity in turn over number (TON) and percentage conversion	77

List of abbreviations and Symbols

Units

J	coupling constant
°	degrees
°C	degrees Celsius
g	gram
Hz	Hertz
kV	kiloVolts
m/z	mass to charge ratio
MHz	Megahertz
MPa	Megapascal
μL	microlitre
mg	milligram
mL	millilitre
mM	millimolar
mmol	millimole
M	Molar concentration
nm	nanometre
ppm	parts per million
%	percentage
W	Watt
cm ⁻¹	wavenumber (inverse centimetre)

wt% weight percent

Chemicals

DMSO-*d*₆ deuterated dimethyl sulfoxide

DAB diaminobutane

DAD diaminododecane

DAH diaminohexane

DCM dichloromethane

EDA ethylenediamine

PAMAM poly(amidoamine)

PPI poly(propyleneimine)

TBHP tert-butyl hydroperoxide

Cyclam 1,4,8,11-Tetraazacyclotetradecane

THF tetrahydrofuran

Instrumentation

ATR attenuated total reflectance

¹³C NMR carbon-13 nuclear magnetic resonance

ESI-MS electron spray ionisation-mass spectrometry

FT-IR fourier transform infrared (spectroscopy)

GC-FID gas chromatography – flame ionization detector

HR-TEM high resolution transmission electron microscopy

¹H NMR proton nuclear magnetic resonance

UV/Vis ultraviolet/visible (spectroscopy)

NMR spectra peak descriptions

bm	broad mutiplet
bt	broad triplet
bs	broad singlet
d	doublet
dd	doublet of doublets
dt	doublet of triplets
m	multiplet
s	singlet
t	triplet

Other

cal	calculated
DENs	dendrimer encapsulated nanoparticles
DSNs	dendrimer stabilized nanoparticles
exp	experimental
G	generation
HSAB	hard-soft acid base
MP	melting point
NPs	nanoparticles
NCDs	nanoparticle cored dendrimers
R.T	room temperature
TON	turn over number

Chapter 1: An introduction to Dendrimer Encapsulated Nanoparticles and their Application in Catalysis

1.1. Synthesis, Stabilization and Application of Metal NPs

Nanoparticles (NPs) are defined as particles with a dimension smaller than 100 nm, placing them in between isolated atoms and bulk solids. ^[1] The chemical and physical properties of transition metal NPs can differ from that of the bulk materials resulting in a possible appearance of catalytic ability. A good example of this is gold. The bulk material is known to be catalytically inactive while particles in the nanometer region show much more promising activity. ^[2,3] Another reason why these particles are extensively used as catalysts is that with the decrease in particle size NPs have an increase in surface to volume ratio, which could have an influence on their catalytic activity. The problem one faces when using metal NPs is that because of their reactivity, they are relatively unstable and tend to aggregate having a negative impact on their activity. The challenge is thus to find a method of stabilization that will eliminate agglomeration of the particles without reducing their catalytic activity as well as control their size and distribution. ^[4]

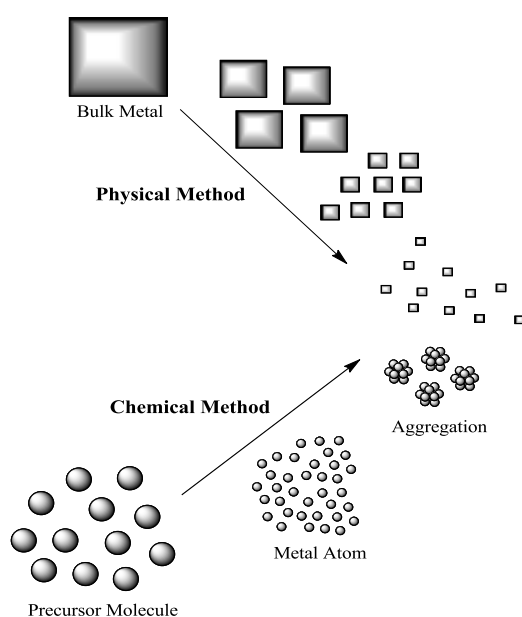


Figure 1.1-1: Routes to metal nanoparticle formation ^[5]

Chapter 1

An Introduction to Dendrimer Encapsulated Nanoparticles and their Application in Catalysis

There are two routes that can be followed when synthesizing metal NPs, the chemical or “bottom-up” approach and the physical or “top-down” approach as shown in Figure 1.1-1.

The physical method involves breaking down particles in the bulk material to NPs by using mechanical, thermal or chemical decomposition methods. This method has the advantage that it produces large amounts of nanocrystals, but controlling the size and uniformity of the synthesized particles is problematic. The chemical route starts with a metal salt or organometallic precursor being reduced to metal atoms and then aggregating to metal NPs of a certain size. This method provides better control over the nanoparticle shape, size and uniformity achieved. ^[5,6,7] The chemical route can be further subdivided into three different synthetic approaches:

1. Chemical reduction of metal salt precursors
2. Electrochemical synthesis
3. Thermal decomposition of metal salts

The most common of the three methods is the chemical reduction of metal salt precursors. In this approach a metal salt is reduced in the presence of a stabilizer to give stabilized metal NPs. Stabilization of metal NPs can be accomplished with or without the use of a solid support. There are three types of interactions that play a role in support free stabilization: electrostatic, steric and electrosteric stabilization. The more common methods of stabilization for application in catalysis are through the use of a solid support or preparation of the NPs in the presence of a steric stabilizer or template which will then prevent the particles from aggregating. ^[6]

1.1.1. Ligand-stabilized NPs

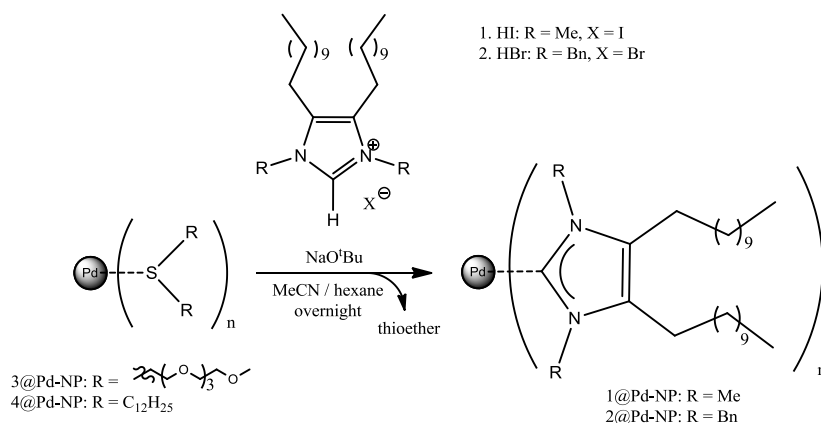
Ligands are commonly used as steric stabilizers for the preparation of metal NPs. Ligands containing functional groups like amines, thiols, phosphines etc. on their periphery can bind to the particles and in this way passivate its surface to prevent aggregation. Binding usually occurs through covalent bonding, electrostatic interactions or physical adsorption and is governed by hard-soft acid base (HSAB) rules. The strength of the bond between the particle and the ligand, depending on HSAB rules, as well as the concentration of the ligand present, has an effect on the particle size. A stronger bond between the particle and the ligand as well as a higher concentration of ligand can result in better stability of the particles and thus smaller NPs. The nature of the ligand also has an effect on the shape of the formed NPs. ^[8,9]

Chapter 1

An Introduction to Dendrimer Encapsulated Nanoparticles and their Application in Catalysis

1.1.1.1. Preparation of ligand-stabilized NPs

There are a variety of different approaches to the preparation of ligand-stabilized metal NPs with the most common being the reduction method where the metal salt is reduced in the presence of a stabilizer. This method can also be approached in different ways for example: Rahme *et al* ^[10] prepared polyethylene glycol-based thiol ligand-stabilized gold NPs in the presence of the stabilizer as well as by ligand exchange, utilizing different reducing agents. Gold NPs were prepared from HAuCl_4 in the presence of a thiol terminated poly(ethylene glycol) methyl ether (mPEG-SH) stabilizer using NaBH_4 as reducing agent. This resulted in NPs with a diameter of 5 ± 1.5 nm. The next approach involved using a milder reducing agent compared to NaBH_4 , sodium citrate, as both reducing agent and electrostatic stabilizer resulting in larger gold NPs with a diameter of 15 ± 1.5 nm. Even larger (30 ± 4 nm) gold NPs were obtained when using sodium citrate as a stabilizer and ascorbic acid as the reducing agent in a similar process as the first approach. Other than synthesizing the NPs in the presence of the stabilizer they also formed mPEG-SH stabilized gold NPs by ligand exchange. For this approach they exchanged the citrate ligand with the mPEG-SH ligand. They found that the mPEG-SH stabilized NPs were much more stable than those stabilized by sodium citrate in a high salt concentration solution as this causes the citrate stabilized particles to aggregate.



Scheme 1.1-1: Ligand exchange reaction on thioether stabilized Pd-NP with LC-NHCs ^[11]

Richter *et al* ^[11] also used the ligand exchange approach when synthesizing N-heterocyclic carbene (NHC) stabilized palladium NPs. They developed a NHC ligand containing small methyl or flexible benzyl substituents on the nitrogen atoms to minimize steric repulsion between the ligand and the particle surface (Scheme 1.1-1). They also hypothesized that

Chapter 1

An Introduction to Dendrimer Encapsulated Nanoparticles and their Application in Catalysis

attaching long aliphatic chains to positions 4 and 5 of the heterocycle would provide steric repulsion between particles and thus eliminate possible aggregation. Didodecylsulfide as well as bis(tetraethylene glycol monomethyl ether) sulphide stabilized palladium NPs were used in the ligand exchange reaction. The ligand exchange reaction was done in a two phase hexane and acetonitrile system by mixing the thioether stabilized palladium NPs, NaO^tBu and the designed long chain imidazolium salt. The isolated NHC ligand (LC-NHC) stabilized palladium NPs were found to be stable for over 4 months. NMR analysis of the LC-NHC stabilized palladium NPs showed that the ligand exchange occurred completely and that binding occurred through the carbene. TEM analysis showed that the palladium NPs had an average size of 4.4 nm and that the ligand exchange caused no particle aggregation. These authors also determined the influence of the long aliphatic chains and the small nitrogen substituents on the particle stability and ligand exchange ability. When NHC ligands without the long aliphatic chains were used in the exchange reaction, the ligand exchange occurred but the stability of the resulting system was extremely poor. The strength of the coordination between the particles and the ligand was tested by adding an excess of competing thiol or thioether ligands. The results indicated that the NHC ligand can be replaced by stronger thiol ligands but not by weaker thioether ligands.

Many other examples of ligand-stabilized NPs are reported, some of which are provided in Table 1.1-1.

Table 1.1-1: Examples of ligand-stabilized NPs

Metal	Ligand type	Ligand	Reference
Ru	N-donor	β -amino alcohol, amino(oxazolines), hydroxy(oxazolines), bis(oxazolines)	12
	O-Ru	Ferrocenecarboxylate	13
	Polymer or bidentate phosphine	Polyvinylpyrrolidone (PVP), bisdiphenylphosphinobutane (dppe)	14
	Phosphine	Roof-shaped monophosphines & diphosphines	15
Rh	Thiol	1-octadecanethiol	16
	P-donor	Mono and bidentate phosphines and phosphites	17

Chapter 1

An Introduction to Dendrimer Encapsulated Nanoparticles and their Application in Catalysis

Pt	Mono and bifunctional amine	Hexadecylamine, aniline, 1,8-diaminooctane, <i>p</i> -phenylenediamine, 4,4'-bipyridine	18
	Polymer	Polyvinylpyrrolidone (PVP)	19
Pd	Selenium	Didocosyl selenide	20
Au	Polysaccharide	Pullulan (neutral glucan produced by yeast)	21
	Phosphine	2,2'-bis(diphenylphosphino)-1,1'-binaphthyl (binap)	22
	Thiol	Mixed self-assembled ligand monolayer with intercalating PEG chains containing -SH and -OH groups	23

1.1.1.2. Applications of ligand-stabilized NPs

Ligand-stabilized nanoparticles are used in a variety of applications including biological and catalytic applications. They are however predominantly applied as catalyst.

An interesting approach to nanoparticle stabilization was that taken by Yu *et al* ^[24] in a recently published article. These authors set out to stabilize nickel NPs using an ionic liquid triblock copolymer mixed micelle. Imidazolium-based ionic liquids and the water soluble poly(ethylene oxide)-poly(propylene oxide)-poly(ethylene oxide) triblock copolymer (PEO-PPO-PEO or P123) was used for this investigation. The P123 triblock copolymer was chosen as it does not only stabilize the NPs but also increases their water solubility. The P123-stabilized nickel NPs were tested in the hydrogenation of α , β -unsaturated aldehydes and a variety of olefins. The study was started by first investigating the influence of different ionic liquids on the catalytic activity. This was done by studying the hydrogenation of citral. It was found that with an increase in the basicity of the ionic liquid additive there is an increase in the catalytic activity with conversions up to 99.5% being achieved when the 1-Butyl-2,3-dimethylimidazolium acetate [BMMIm]OAc is used as ionic liquid. The traditionally used Raney nickel catalyst also shows a very high conversion in the reaction but has a lower selectivity towards the intended product than the nickel NP system. The next part of the investigation dealt with studying the P123 concentration effect on the nickel catalyst in

Chapter 1

An Introduction to Dendrimer Encapsulated Nanoparticles and their Application in Catalysis

the hydrogenation of cyclohexene. It was found that when no P123 was used the nickel NPs aggregated easily and no significant conversion was achieved. With an increase in the P123 concentration from 0.5-2.5 mM there was an increase in conversion from 24.5 to 99.9%, but when the P123 concentration was increased above 2.5 mM the activity of the catalyst once again decreased. This trend was attributed to the fact that when the P123 is introduced it stabilizes the NPs. The more P123 introduced, the more micelles can be formed which results in better solubility and better stability of the NPs. The catalytic activity does however decrease again at some point because the active sites on the nickel NPs become blocked by the micelle present. It was also shown that the addition of the ionic liquid results in a modification of the micelle to form an ionic liquid-P123 mixed micelle. This catalytic system was also tested in the hydrogenation of several other α , β -unsaturated aldehydes and ketones with great success. This highlights the possible wide application of this system.

The group of Li *et al* ^[25] prepared rhodium NPs stabilized with thermoregulated $\text{Ph}_2\text{P}(\text{CH}_2\text{CH}_2\text{O})_{16}\text{CH}_3$ ligands as catalysts for application in the hydroaminomethylation of olefins with di-*n*-propylamine in a biphasic aqueous/1-butanol system. Hydroaminomethylation involves the hydroformylation of an olefin to an aldehyde, the reaction of the resulting aldehyde with a primary or secondary amine to produce the corresponding imine or enamine, followed by the hydrogenation of this product to the desired amine. The catalyst was prepared by reducing $\text{RhCl}_3 \cdot 3\text{H}_2\text{O}$ with hydrogen under 4 MPa pressure at 70 °C in an autoclave using the biphasic aqueous/1-butanol solvent system. TEM analysis showed well dispersed particles with an average size of 2.4 ± 0.3 nm. Thermoregulated phase transfer catalysis was used for the hydroaminomethylation reaction. This approach involves a biphasic aqueous/1-butanol system with the catalyst in the aqueous phase and the substrate in the organic phase. With an increase in temperature above the cloud point of the ligand, the catalyst will transfer to the organic phase where the reaction can take place. With a decrease in temperature below the cloud point of the ligand, the catalyst transfers back to the aqueous phase. This approach provides the advantage of easy catalyst recovery and recyclability. The effect of temperature on the conversion and selectivity was the first parameter investigated. The results showed that an increase in temperature has little effect on the conversion of 1-octene. The selectivity towards the amine product increased while the normal to branched ratio decreased. The effect of syngas pressure was also studied and found that again the conversion of 1-octene was not influenced but that the amine

Chapter 1

An Introduction to Dendrimer Encapsulated Nanoparticles and their Application in Catalysis

selectivity increased with an increase in pressure. Reusability of the catalyst was also explored and it was found that the recovered catalyst can be used up to three times with only a slight decrease in the amine selectivity and almost no change in the particle size. They also found that 2.7 wt% of the rhodium leached into the organic (1-butanol phase) which could account for the slight decrease in amine selectivity when reusing the catalyst.

1.1.2. Dendrimer-Stabilized NPs

Vögtle defines dendrimers or cascade molecules as “highly branched yet structurally perfect molecules”.^[26] The name ‘dendrimer’ was first proposed by Tomalia *et al*^[27] and is based on the greek words *dendri-* (tree branch-like) and *meros* (part of). Although they are considered macromolecules, the fact that they are known to be discrete and monodisperse distinguishes them from other polymeric molecules.^[28]

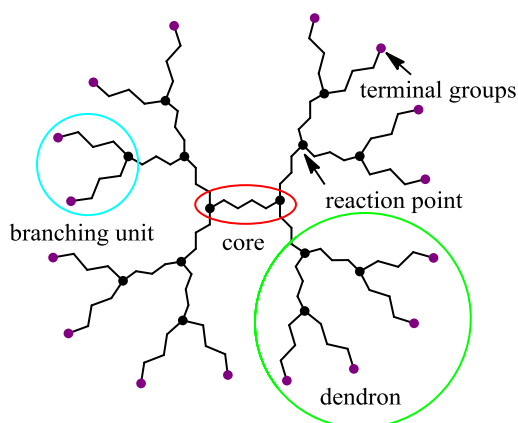


Figure 1.1-2: A dendrimer consists of a core, branching units and terminal groups

These types of molecules generally consist of a core, an interior architecture of repeat branching units and terminal functional groups on the periphery (Figure 1.1-2), each component having their own function and properties. The core molecule will determine the shape of the dendrimer as well as provide directionality. The terminal groups on the periphery can serve as a means of functionalizing the dendrimer for specific applications. The size and shape of these terminal groups can also act as selective gates for the entry of guest molecules.^[27]

The number of reaction points between the core and the terminal groups is known as the generation of the dendrimer and this also defines its size and molecular weight.^[29] As example, the dendrimer shown in Figure 1.1-2 is a generation 3 (G3) dendrimer. With an

Chapter 1

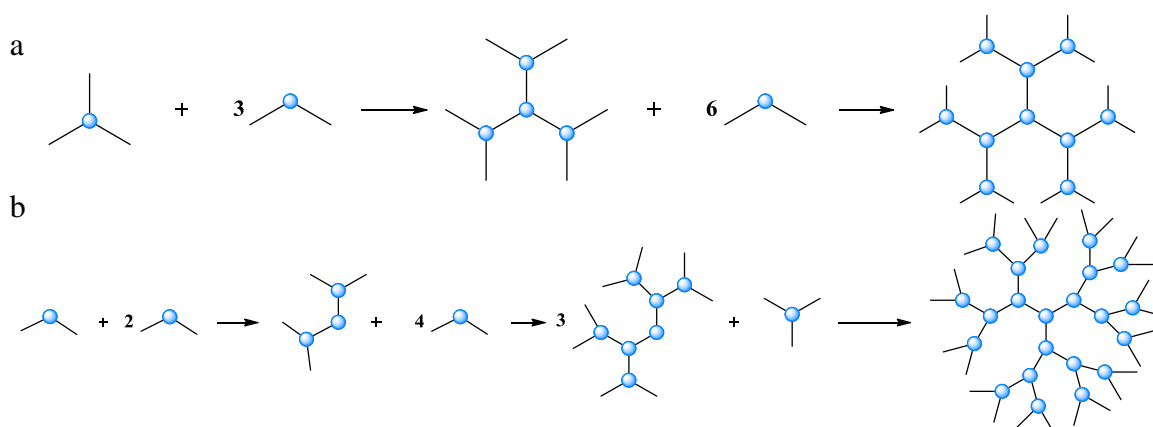
An Introduction to Dendrimer Encapsulated Nanoparticles and their Application in Catalysis

increase in dendrimer generation there is a change in the size, properties and shape of the dendrimer, from a more ellipsoidal to a more spherical shape. Higher generation dendrimers also have a much more densely packed periphery and a more open interior structure which can play as host to guest molecules.^[30]

1.1.2.1. Dendrimer Synthesis and Application

Vögtle, Tomalia and Fréchet can be considered the fathers of dendrimer chemistry as they discovered the two synthetic approaches that are used most often today.

Currently there are two general approaches to dendrimer synthesis^[31]: the divergent method developed by Vögtle and Tomalia independently and the convergent method developed by Fréchet. In the divergent approach the dendrimer is built from the multifunctional core outwards to the periphery by the attachment of branching units [Scheme 1.1-2 (a)]. The dendrimer can be grown outwards until steric effects prevent the interaction of the terminal groups with another branching unit, also known as the “starburst dense packing” state.^[31]



Scheme 2.1-1: The two synthetic approaches (a) divergent and (b) convergent

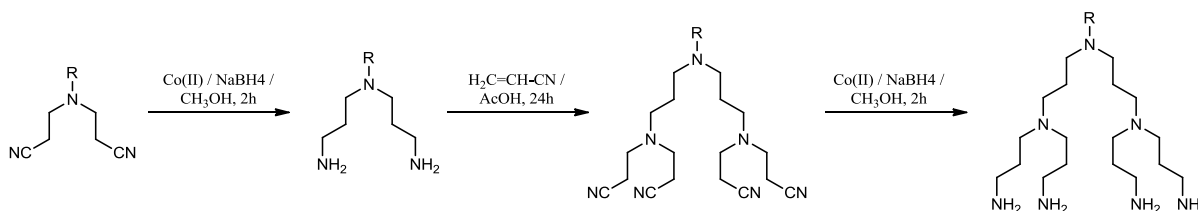
The convergent approach is the opposite of the divergent approach. This approach involves the formation of a dendritic wedge or dendron which is then reacted with the core molecule in the last step of the dendrimer synthesis [Scheme 1.1-2 (b)]. Divergently synthesized dendrimers are considered to contain structural defects as a result of incomplete reactions with the terminal groups. These defects accumulate with increasing dendrimer generation and because they are so similar to the desired product are very difficult to remove. The divergent approach does however give the opportunity to develop dendrimers with very high generations. In comparison it would be difficult to produce high generation dendrimers with

Chapter 1

An Introduction to Dendrimer Encapsulated Nanoparticles and their Application in Catalysis

the convergent approach because of steric hindrance when reacting the dendrons and the core molecule. Convergently produced dendrimers are however considered to be free of structural defects and by-products as these are more easily removed through purification methods at each step.

The first reported synthesis of a dendrimer was that of the poly(propyleneimine) (PPI) dendrimers by Vögtle *et al* in 1978^[32] leading the way for many to come. In the quest to develop a molecule containing large cavities, which can be utilised in the binding of guest molecules, through a stepwise repetitive synthetic approach Vögtle *et al* synthesized the first PPI dendrimer. They approached this synthesis by starting with either a monoamine or a diamine as the core and then building the dendrimer out from there with consecutive steps that includes the reaction with acrylonitrile followed by the reduction of the resulting nitrile groups to amines (Scheme 1.1-3). The idea behind this was to produce molecules with an increasing cavity size as the generation increases.



Scheme 1.1-3: Synthesis of PPI dendrimer by Vögtle *et al* in 1978

This discovery was followed by Tomalia *et al*, who also used this stepwise repetitive divergent approach, for the synthesis of poly(amido amine) (poly(β -alanine)) (PAMAM) dendrimers in 1986.^[33] The synthesis involved a two-step reaction sequence. An amine core was completely reacted with methyl acrylate to produce the ester-terminated G 0.5 dendrimer. This is followed by the addition of an excess of ethylenediamine to give the amine-terminated G 1 dendrimer. This process can then be repeated to produce higher generation dendrimers.

In 1990 the first report of a dendrimer synthesized through a convergent approach was published by Fréchet and Hawker.^[34] According to the authors the divergent approach had two setbacks:

1. Incomplete reactions will lead to imperfections in the dendrimer which will increase as the generation increases.

Chapter 1

An Introduction to Dendrimer Encapsulated Nanoparticles and their Application in Catalysis

2. Purification difficulties are caused by the need for an excess of reagents in each step. They proposed that the convergent approach would minimize the chance of imperfections, provide easier control over the synthesis and eliminate the need for excess reagents and in this way simplify the purification required. They used 3,5-dihydroxybenzyl alcohol as the monomer unit and produced polyether dendrimers. The process involved the dialkylation of the 3,5-dihydroxybenzyl monomer with the G1 benzylic bromide resulting in a hydroxymethyl terminated product. The hydroxymethyl was then converted to its corresponding bromomethyl to produce the G2 dendritic wedge. This G2 wedge can be extended to higher generations by following the same two-step procedure. The final dendrimer is produced by coupling the desired generation dendritic wedge with the polyfunctional core 1,1,1-tris(4'-hydroxyphenyl)ethane. They found that with an increase in the generation the steric hindrance on the periphery increases and the purification gets more difficult. Although the convergent method may not be superior to the divergent method where the production of high generation dendrimers are concerned it still has advantages such as minimum defects when producing lower generation dendrimers.

These three fundamental developments paved the road for many new dendrimers and synthetic approaches to dendrimers to be discovered.

The fact that dendrimers are monodisperse, can be tailored to a specific need and can play host to a high amount of guests make them popular for application in a variety of fields including drug delivery and catalysis.

Table 1.1-2: Dendrimers used for the TA binding studies ^[35]

Dendrimer	Core	Generation	End-group
PAMAM-G4	EDA	4	-NH ₂
PAMAM-G5	EDA	5	-NH ₂
PPI-G3	DAB	3	-NH ₂
PPI-G4	DAB	4	-NH ₂
PPI-G5	DAB	5	-NH ₂
PAMAM-tris-OH-G3	DAD	3	Tris(hydroxymethyl)-amidomethane
PAMAM-tris-OH-G4	DAH	4	Tris(hydroxymethyl)-amidomethane
PAMAM-G2.5-Me	EDA	2.5	-COOMe
PAMAM-G3.5-Me	EDA	3.5	-COOMe
PAMAM-G3.5-Me	EDA	3.5	-COONa
PAMAM-G4.5	EDA	4.5	-COONa
PAMAM-Suc-G3	DAB	3	Succinamic acid
PAMAM-Suc-G4	DAB	4	Succinamic acid

Chapter 1

An Introduction to Dendrimer Encapsulated Nanoparticles and their Application in Catalysis

Schramm *et al*^[35] took advantage of the guest-host properties of dendrimers to investigate the removal and recovery of tartaric acid (TA) from wine samples. The authors screened a variety of dendrimers with different cores and terminal groups (Table 1.1-2) and found that the functionality on the periphery of the dendrimers greatly influenced the binding of tartaric acid. The amine-terminated dendrimers showed a high affinity for the tartaric acid while the hydroxyl terminated dendrimers showed moderate binding. They also found that more tartaric acid could be bound with higher generation dendrimers, in fact there seems to be a correlation between the number of amino terminal groups on the dendrimer and the maximum amount of tartaric acid that could be bound. This linear correlation starts to deviate when higher generations (example G5) are used and could be explained by the increased steric bulk on the periphery. The correlation between the binding ability of the dendrimers and pH was also investigated and they found that the pH has a great influence on the binding of tartaric acid to the dendrimers decreasing from about 90% at pH 5 to almost 0% at pH 2 and pH 11. After conducting all the previously mentioned studies in an aqueous tartaric acid solution, they decided to investigate the binding capabilities of the tartaric acid to the dendrimers in wine samples (both white and red). A slight decrease in the binding capacity was observed in both the red and the white wine samples when compared to the aqueous tartaric acid solution but the decrease was not as much as expected considering the number of competing compounds in the wine samples. So in conclusion, the authors proved that dendrimers can be used to recover compounds like tartaric acid from complex samples like wine.

Carrasco-Sánchez *et al*^[36] investigated the use of amine (PAMAM G5) and folate terminated G5 PAMAM (PAMAM G5-FA) dendrimers to play host to drugs like morphine and tramadol. In this way the dendrimer should aid in the controlled release of these drugs which would prevent the need to ingest the drug every few hours (Figure 1.1-3). The use of dendrimers as drug carriers has many advantages as it could help improve drug solubility, play a role in controlled release and possible drug targeting as well as increase the circulation time of the drug. The authors determined that the PAMAM G5 and the PAMAM G5-FA dendrimers encapsulate morphine and tramadol and that the folate-terminated dendrimer has the ability to encapsulate more of these drugs than the amine-terminated dendrimer. They also established that more molecules of morphine could be encapsulated by the dendrimers than tramadol molecules. After determining that the dendrimers do in fact encapsulate the drug molecules, the authors moved on to determining the drug release capabilities of the dendrimers at a pH of 1.5, 7.4 and 8.5. They found that for both morphine and tramadol the

Chapter 1

An Introduction to Dendrimer Encapsulated Nanoparticles and their Application in Catalysis

amine-terminated and the FA-terminated dendrimers showed an inverse release rate. At a low pH the drug release is much slower for the FA-terminated dendrimers compared to the amine-terminated dendrimers which indicates that the FA-terminated dendrimers have a higher affinity for the drugs.

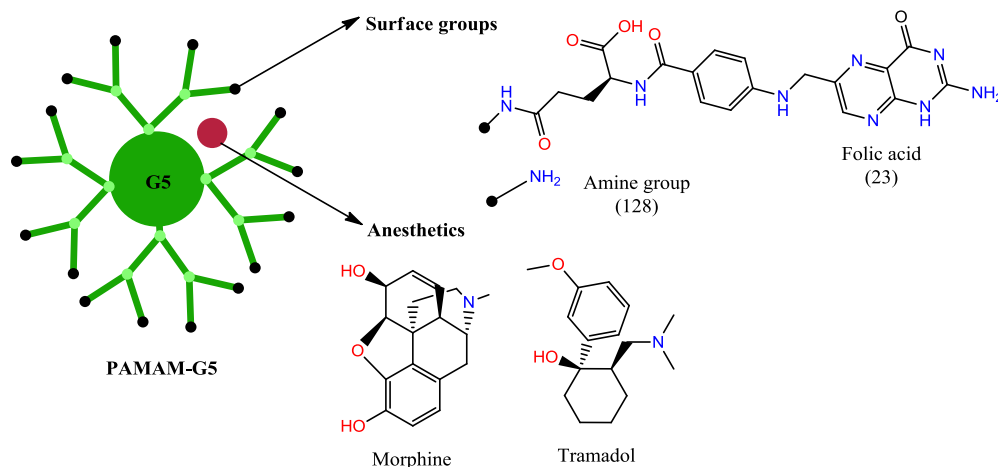


Figure 1.1-3: Schematic representation of amine- and folate-terminated PAMAM dendrimer of generation 5 and its complexation with the anesthetics morphine and tramadol. The chemical structures of the surface groups and the drugs are shown on the right. ^[36]

They also found that the drug release occurs in two phases: a rapid release of the molecules on the periphery of the dendrimers followed by a slower release of the drug molecules situated in the interior of the dendrimer. These results show the potential of dendrimers as drug carriers.

Another field in which dendrimers are applied is to mimic the catalytic properties of enzymes which could result in the use of greener reaction conditions. Fhayli *et al* ^[37] synthesized generation 1-5 PPI dendrimers functionalized with glycerol. The functionalized dendrimers were complexed to Cu(II) and used to activate molecular oxygen in the aerobic oxidation of 3,5-ditert-butylcatechol (3,5-DTBC) to 3,5-di-tert-butyl-o-quinone (3,5-DTBQ). They investigated the influence of the dendrimer and the ratio of Cu(OAc)₂ to dendrimer on the conversion. They found that when no dendrimer was present the conversion decreased significantly indicating that the dendrimer has an influence on the rate of the reaction. When using a higher ratio of Cu(OAc)₂ to dendrimer the conversion also increased. In summary they showed that by complexing Cu(II) to dendrimers provides a catalyst capable of activating molecular oxygen resulting in possible greener conditions for oxidation reactions.

Chapter 1

An Introduction to Dendrimer Encapsulated Nanoparticles and their Application in Catalysis

1.1.2.2. Stabilization techniques

There are three different approaches to the use of dendrimers as stabilizers for metal NPs (Figure 1.1-4):

1. Nanoparticle-cored dendrimers (NCD)
2. Dendrimer stabilized NPs (DSN)
3. Dendrimer encapsulated NPs (DEN)

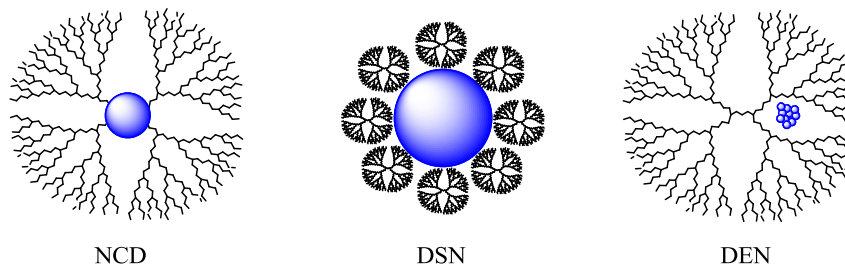


Figure 1.1-4: The three different approaches to metal NP stabilization via dendrimers

Dendritic wedges containing coordinating groups can be attached to metal NPs to assist with preparation and stabilization of the NPs much like ligands. These types of dendritic structures are called nanoparticle-cored dendrimers (NCDs). Because of the highly branched and sterically encumbered nature of dendrimers, a smaller number of dendritic wedges are required for stabilization compared to small molecule ligands. This means that a larger section of the particle surface is unpassivated by the ligand and hence active to take part in catalysis. [38,39] Wu *et al* used this stabilization approach to synthesize palladium-cored phosphine dendrimers. G1-3 Fréchet-type polyaryl ether dendrons were modified at their focal points by reacting the dendritic bromide with potassium diphenylphosphine ($G_n\text{DenP}$). Fréchet-type polyaryl ether dendrons were chosen because of their inability to coordinate to palladium and because they are so unreactive. To prepare the stabilized palladium NPs, $\text{Pd}(\text{acac})_2$ was reduced with hydrogen in the presence of the dendritic ligand producing NPs with sizes between 5.0 and 3.2 nm ($G_n\text{DenP-Pd}$). The size of the NPs decreased when the higher generation dendritic ligands were used. They applied these catalysts in Suzuki coupling and hydrogenation reactions and found that the catalysts were highly active and reusable resulting in high yields for all coupling products. They also found that the dendritic wedge plays the role of not only stabilizer but also has an effect on the catalytic activity and helps with the recoverability of the catalysts.

Chapter 1

An Introduction to Dendrimer Encapsulated Nanoparticles and their Application in Catalysis

Another approach to the stabilization of NPs through the use of dendrimers is by the preparation of dendrimer stabilized NPs (DSNs). DSNs and dendrimer encapsulated NPs (DENs) are closely related. DSNs usually consist of one nanoparticle surrounded by several dendrimers to provide stabilization. DENs are the opposite, consisting of one dendrimer molecule stabilizing several NPs in its interior voids.^[40] The preparation for both of these systems are essentially the same, the only difference would be the ratio of dendrimer to metal salt being used. An example of this can be seen in the research reported by Yuan *et al*^[41]. The authors used G5 ethylenediamine cored PAMAM dendrimers with NH_2 terminal groups for the formation of silver DSNs which could then be applied in the sensitive and selective colorimetric detection of mercury in aqueous solutions. In short, an aqueous AgNO_3 solution was added to an aqueous dendrimer solution with vigorous stirring, followed by the addition of NaBH_4 to reduce the metal ions to zero valent metal NPs. In a previous study a silver salt/dendrimer ratio of 50:1 was used to form the DENs which was changed to a ratio of 100:1 in this study resulting in the formation of DSNs instead of DENs.

1.2. Dendrimer-Encapsulated NPs in Catalysis

The use of dendrimers as templates for the encapsulation of metal NPs has become a popular method of stabilization in the last few years. Dendrimers can be tailored to the application by changes to their core and periphery. By functionalizing the periphery with different types of terminal groups the solubility of the dendrimer can be changed and when used in applications such as catalysis these terminal groups can act as selective gates to molecules resulting in possible selectivity improvements. When NPs are used in catalysis they ideally need to be monodisperse, small in size and their surface should not be passivated by the stabilizing agent as this could reduce their activity. Dendrimers can provide a means of size and distribution control and provide stability against aggregation without reducing their active sites.^[42]

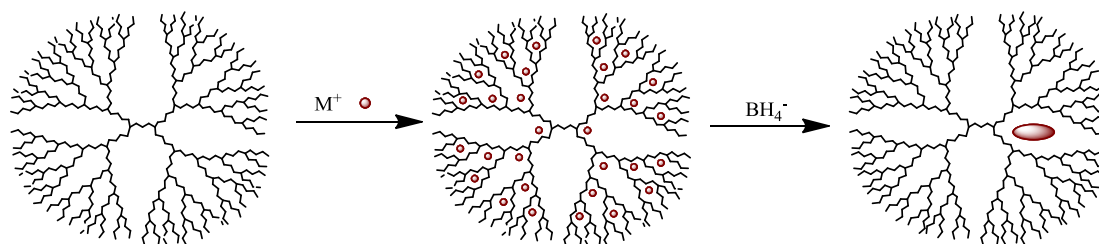


Figure 1.2-1: Formation of DENs

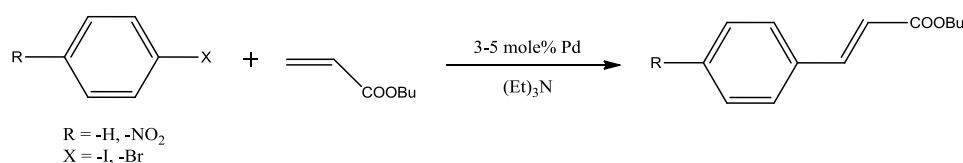
Chapter 1

An Introduction to Dendrimer Encapsulated Nanoparticles and their Application in Catalysis

The first report of dendrimer encapsulated NPs (DENs) was published in 1998 by the group of Crooks.^[43] They did a proof of concept with copper NPs showing that dendrimers can be loaded with Cu^{2+} which can then be reduced to form Cu^0 nanoparticle clusters inside the dendrimer. They followed this by UV/Vis spectroscopy and also in this way determined that dendrimers have a maximum loading limit that if reached results in bigger aggregates on the outside of the dendrimers. This then provided the basic method to form dendrimer encapsulated NPs: The dendrimer template is reacted with a metal salt and after complexation of the metal inside the dendrimers, the metal ions are reduced to zerovalent metal clusters or NPs (Figure 1.2-1).

1.2.1. The use of DENs in coupling reactions

In 2001 Yeung and Crooks^[44] reported the first application of DENs as catalysts in a Heck heterocoupling reaction. This study in several ways showed how these types of systems can be manipulated to give the best catalyst for a specific need. They prepared palladium NPs encapsulated in G4 and G5 PPI dendrimers modified on their periphery with perfluorinated polyether chains to be applied in a biphasic fluorocarbon/hydrocarbon Heck reaction. The biphasic solvent system was chosen so that the catalyst and coupling products could be separated and that the catalyst could be recovered and reused. They chose PPI dendrimers rather than the normal PAMAM dendrimers as these are more thermostable and thus more applicable for these types of reactions. The same Pd^{2+} /dendrimer ratio was used when forming both generation DENs as they wanted to investigate the influence of the dendrimer template on the particle size and catalytic activity. From HR-TEM data they concluded that the average particle size formed is independent of the template size used when the Pd^{2+} /dendrimer ratio is kept constant.



Scheme 1.2-1: Heck coupling of aryl halides with n-butylacrylate^[44]

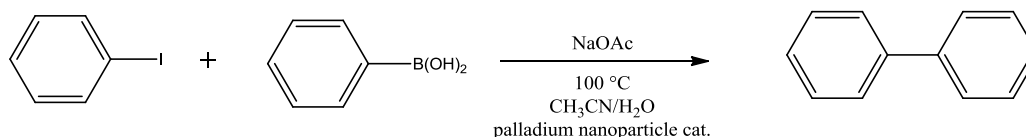
Other studies^[45,46] using palladium NPs in a fluoruous biphasic system reports the selectivity towards the *trans* isomer of *n*-butyl-formylcinnamate between 74 and 98%. Using the palladium DEN catalyst this selectivity was found to be 100% showing that the nature of the environment inside the dendrimer can impart regio-selectivity in the product distribution.

Chapter 1

An Introduction to Dendrimer Encapsulated Nanoparticles and their Application in Catalysis

Another interesting observation was that the G5 DEN catalyst gave a 70% yield of the product while the G4 DEN catalyst under the same conditions could only yield 38% of product. This was attributed to the fact that the G5 dendrimer has a more open interior structure and thus it is easier for the reactants to come into contact with the catalytic Pd particles. The catalyst could be recovered and reused although there was a decrease in activity in the second catalytic cycle. They also determined that the catalyst is very stable as no leaching of palladium took place and the catalyst could be stored in solution without any deactivation occurring.

Lemo *et al* ^[47] also prepared palladium NPs encapsulated in DAB PPI dendrimers but for the application as catalysts in the Suzuki-Miyaura reaction between iodobenzene and phenylboronic acid (Scheme 1.2-5).



Scheme 1.2-2: Suzuki-reaction with palladium DENs ^[47]

DAB PPI dendrimers of G1-5 was used for the encapsulation of the palladium NPs by two different methods. The first method involved the adjustment of the solution pH before reduction of Pd²⁺ to Pd⁰ while the other involved no pH adjustment. NPs with an average diameter of 1.7-1.9 nm were formed using the first method without the formation of palladium black in most cases while using the second method particles with an average diameter of 1.8-2.8 nm were formed with palladium black forming in all cases. All 5 generations of Pd-DENs prepared by method 1 were tested as catalysts in the Suzuki reaction and showed good activity. DENs prepared with the lower generation 1-3 dendrimers were found to be the most active with the product being isolated in 100% yield after just 1 hour while 24 hours led to a 98% yield for the G4 catalyst and 4 days led to only a 40% yield for the G5 catalyst. Small amounts of palladium black formation was observed for the G4 and G5 catalysts while a reasonable amount formed with the lower generation catalysts. DENs prepared by method 2 with G2-4 DAB PPI dendrimers showed a lower activity for the cross-coupling reaction after 20 hours and palladium black formed in all cases during the reaction. The reduced catalytic activity and palladium black formation with higher generation dendrimers were attributed to the high stability of the encapsulated particles in these dendrimers as well as the steric crowding preventing access for the substrate molecules. The

Chapter 1

An Introduction to Dendrimer Encapsulated Nanoparticles and their Application in Catalysis

catalysts could also be recovered but re-use led to a decrease in activity because of particle aggregation. To improve the recoverability and reactivity of these catalysts the authors suggested the addition of alkyl chains on the periphery of the dendrimers.

Deraedt *et al* ^[48] designed two generations of click ferrocenyl dendrimers terminated with triethyleneglycol groups to host palladium NPs for the use as catalysts in the Suzuki-Miyaura reaction between halogenoarenes and phenylboronic acid. They focused mainly on the coupling using bromoarenes with the G0 catalyst and found that low amounts of palladium leads to high turn of numbers (TON) and product yields. The G1 catalyst lead to much lower yields which can be attributed to the fact that the particles in the G1 dendrimer were slightly larger than those in the G0 dendrimer. These DENs were also found to be stable for several months and could easily be recovered and re-used indefinitely.

1.2.2. The use of DENs in hydrogenation reactions

Ooe *et al* ^[49] reported the use of G3-5 tri-ethoxybenzamide-terminated PPI dendrimers as templates for the encapsulation of palladium NPs to be applied in the substrate-specific hydrogenation of olefins. The authors looked at the effect that the substrate size and the dendrimer generation has on the rate of hydrogenation. With all the substrates tested, the rate of hydrogenation decreased with an increase in dendrimer generation. When comparing the rate of hydrogenation of cyclic conjugated dienes using the G5 catalyst it was found that with an increase in ring size there is a decrease in the rate of hydrogenation (cyclopentadiene > 1,3-cyclohexadiene > 1,3-cyclooctadiene). The same trend was seen for acrylates as well as allylic alcohols. When using Pd/C as catalyst these hydrogenation rates weren't affected much by the size of substrate. From these results the authors concluded that the steric crowding on the periphery of higher generation dendrimers could suppress the entry of large substrates into the interior where the catalytic palladium NPs are situated. This is most prominent for the G5 catalyst. They also investigated whether the dendritic catalytic system can be substrate specific by looking at the hydrogenation of an equimolar mixture of two substrates. The first example was done with 3-cyclohexene-1-methanol and cyclohexene. They found that by using the G5 catalyst cyclohexane methanol was formed selectively as product. This selectivity decreased slightly when using the smaller G3 catalyst as 7% cyclohexane was also formed. Similarly, when using N-methyl-3-cyclohexene-1-carboxamide and cyclohexene in the competitive hydrogenation reaction with the G5 catalyst

Chapter 1

An Introduction to Dendrimer Encapsulated Nanoparticles and their Application in Catalysis

only the former was reduced to yield N-methyl-cyclohexane carboxamide. These results indicated that this dendrimer system can be selective to more polar substrates. The results show that dendrimers do not only act as templates for the formation of stable NPs but can also have an influence on substrate specificity or act as “nanoreactors” as the authors referred to it.

Chechik and Crooks ^[50] reported the application of palladium NPs encapsulated in dendrimers as catalysts in the biphasic hydrogenation of alkenes. They modified PAMAM dendrimers with perfluoropolyethers to render them soluble in fluoruous solvents and found that the palladium DENs are active and recyclable in this simple biphasic system.

A more recent report of the application of DENs is by Johnson *et al.* ^[51] These authors studied the activity of palladium DENs in the hydrogenation of *p*-nitrophenol and found that the dendrimer generation and cluster size have a significant impact on the reaction kinetics. The use of higher generation dendrimers show a slower reaction rate compared to smaller dendrimers which can be attributed to the increase in steric crowding as the dendrimer generation increases. Nanoparticle clusters with an average size of 1.7 nm containing between 10 and 200 palladium atoms were formed. It was found that using particles containing between 10 and 50 atoms, the per-atom rate constant for the hydrogenation reaction stays relatively constant while it decreases in the atom range of 50 to 200.

1.2.3. Oxidation Reactions

As far as it could be ascertained there are only a handful of reports where DENs have been employed as catalysts in oxidation reactions without making use of a solid support. One example was published by Kracke *et al* ^[52] in 2010 for the oxidation of carbon monoxide. This study was conducted to test the activity of unsupported gold NPs as catalysts in CO oxidations. Hydroxyl-terminated G5 PAMAM dendrimers were used as templates for the encapsulation of Au₅₅ NPs in aqueous solutions. UV/Vis and TEM data indicate the formation of gold NPs with an average size of 2.2 ± 0.8 nm. The catalyst was found to be active at room temperature for the CO oxidation with the activity increasing with an increase in storage time of the catalyst.

Meijboom and Nemanashi ^[53] reported the use of G4 NH₂-terminated PAMAM dendrimers to encapsulate gold NPs. These gold DENs were then immobilised onto TiO₂ supports via the sol-gel and wet impregnation methods and used as catalysts for the oxidation of styrene. The

Chapter 1

An Introduction to Dendrimer Encapsulated Nanoparticles and their Application in Catalysis

gold NPs formed in the dendrimers were found to increase from 2.3 ± 0.4 nm to 2.4 ± 0.5 nm for the sol-gel method and 1.9 ± 0.4 nm to 2.3 ± 0.4 nm for the wet impregnation method after immobilization. A further increase in particle size to 7.1 ± 2.0 nm (sol-gel) and 7.6 ± 2.2 nm (wet impregnation) occurred after calcination as the dendrimer stabilizer decomposed leaving the particles unstable and prone to agglomeration. In the catalytic study it was observed that the catalyst amount, reaction temperature and time, solvent and oxidant influenced the styrene conversion and the selectivity of the reaction. Styrene conversion as well as the selectivity towards styrene oxide increased with an increase in temperature although the selectivity towards benzaldehyde remained favoured for both catalysts. The highest conversions achieved were 16% for the sol-gel prepared catalyst and 21% for the wet impregnation prepared catalyst at 70°C . With an increase in reaction time from 12 to 15 hours the styrene conversion could be increased to 18% and 25% respectively. The choice of solvent also had a significant effect on the conversion causing an increase to 43% for the sol-gel prepared catalyst when using toluene instead of acetonitrile.

1.3. Summary and Objectives

Dendrimers are versatile, monodisperse molecules with the ability to play host to different types of smaller molecules. They can act as templates for the encapsulation of metal NPs providing stability against aggregation as well as a means of size and size distribution control. DENs have successfully been used as catalyst in carbon coupling, hydrogenation and some oxidation reactions. Not only can they act as catalysts but the dendrimer system could possibly influence selectivity towards certain substrates or products. Taking all of this into account the aims of this project were:

1. Preparation of hydrophobic dendrimer hosts based on commercially available dendrimers. Generation 1, 2 and 3 commercially available DAB PPI dendrimers were modified with palmitoyl chloride to provide hydrophobic dendrimer hosts.
2. Preparation of novel hydrophobic dendrimer hosts based on synthesized cyclam-cored dendrimers. Generation 1 and 2 cyclam-cored dendrimers were synthesized via the divergent approach and modified with palmitoyl chloride to give novel hydrophobic dendrimer hosts.
3. Characterize all synthesized dendrimers with FT-IR, $^1\text{H-NMR}$ and $^{13}\text{C-NMR}$, mass spectrometry and elemental analysis.

Chapter 1

An Introduction to Dendrimer Encapsulated Nanoparticles and their Application in Catalysis

4. Encapsulate gold NPs in all synthesized dendrimer hosts. Gold NPs of different sizes were encapsulated in all the hydrophobic dendrimer hosts and characterized by UV/Vis spectroscopy and HR-TEM.
5. Apply the prepared DENs as catalysts in the oxidation of alkanes. The DENs were evaluated based on dendrimer generation and nanoparticle size in the oxidation of alkanes.

1.4. References

1. A. Castonguay, A. K. Kakkar, *Adv. Colloid Interface Sci.*, **160** (2010) 76
2. K. Bhattacharyya, S. Varma, A. K. Tripathi, S.R. Bharadwaj, A. K. Tyagi, *J. Phys. Chem. C*, **112** (2008) 19102
3. A. Corma, H. Garcia, *Chem. Soc. Rev.*, **37** (2008) 2096
4. M. Zhao, L. Sun, R. M. Crooks, *J. Am. Chem. Soc.*, **120** (1998) 4877
5. N. Toshima, T. Yonezawa, *New J. Chem.*, **22** (1998) 1179
6. C. Jia, F. Schüth, *Phys. Chem. Chem. Phys.*, **13** (2011) 2457
7. M. Zahmakiran, S. Özkar, *Nanoscale*, **3** (2011) 3462
8. S. Nath, S. Jana, M. Pradhan, T. Pal, *J. Colloid Interface Sci.*, **341** (2010) 333
9. K. Na, Q. Zhang, G. A. Somorjai, *J. Clust. Sci.*, **25** (2014) 83
10. K. Rahme, M. T. Nolan, T. Doody, G. P. McGlacken, M. A. Morris, C. O'Driscoll, J. D. Holmes, *RSC Advances*, **3** (2013) 21016
11. C. Richter, K. Schaepe, F. Glorius, B. J. Ravoo, *Chem. Commun.*, **50** (2014) 3204
12. S. Jansat, D. Picurelli, K. Pelzer, K. Philippot, M. Gómez, G. Muller, P. Lecantec, B. Chaudret, *New J. Chem.*, **30** (2006) 115
13. L. Chen, Y. Song, P. Hu, C. P. Deming, Y. Guo, S. Chen, *Phys. Chem. Chem. Phys.*, **16** (2014) 18736
14. F. Novio, K. Philippot, *Catal. Lett.*, **140** (2010) 1
15. D. González-Gálvez, P. Nolis, K. Philippot, B. Chaudret, P. W. N. M. van Leeuwen, *ACS Catal.*, **2** (2012) 317
16. L. M. Rossi, L. L. R. Vono, M. A. S. Garcia, T. L. T. Faria, J. A. Lopez-Sanchez, *Top Catal.*, **56** (2013) 1228
17. J. L. Castelbou, A. Gual, E. Mercadé, C. Claver, C. Godard, *Catal. Sci. Technol.*, **3** (2013) 2828
18. E. Morsbach, E. Brauns, T. Kowalik, W. Lang, S. Kunz, M. Bäumer, *Phys. Chem. Chem. Phys.*, **16** (2014) 21243
19. J. M. Krier, W. D. Michalak, L. R. Baker, K. An, K. Komvopoulos, G. A. Somorjai, *J. Phys. Chem. C*, **116** (2012) 17540
20. G. K. Rao, A. Kumar, B. Kumar, A. K. Singh, *Dalton Trans.*, **41** (2012) 4306
21. M. Ganeshkumar, T. Ponrasu, M. D. Raja, M. K. Subamekala, L. Suguna, *Spectrochim. Acta, Part A*, **130** (2014) 64

Chapter 1

An Introduction to Dendrimer Encapsulated Nanoparticles and their Application in Catalysis

22. J. Ramírez, M. Sanaffl, E. Fernández, *Angew. Chem. Int. Ed.* **47** (2008) 5194
23. S. Avvakumova, E. Galbiati, L. Pandolfi, S. Mazzucchelli, M. Cassani, A. Gori, R. Longhi, D. Prospero, *Bioconjugate Chem.*, **25** (2014) 1381
24. Y. Yu, W. Zhu, L. Hua, H. Yang, Y. Qiao, R. Zhang, L. Guo, X. Zhao, Z. Hou, *J. Colloid Interface Sci.*, **415** (2014) 117
25. K. Li, Y. Wang, Y. Xu, W. Li, M. Niu, J. Jiang, Z. Jin, *Catal. Commun.*, **34** (2013) 73
26. A. Archut, F. Vötle, *Chem. Soc. Rev.*, **27** (1998) 233
27. D. A Tomalia, *Prog. Polym. Sci.*, **30** (2005) 294
28. T. Emrick, J. M. J Fréchet, *Curr. Opin. Colloid Interface Sci.*, **4** (1999) 15
29. U. Boas, J. B. Christensen, P. M. H. Heegaard, *J. Mater. Chem.*, **16** (2006) 3785
30. V. Percec, W. D. Cho, P. E. Mosier, G. Ungar, D. J. P. Yearley, *J. Am. Chem. Soc.*, **120** (1998) 11061
31. F. Vögtle, M. Fischer, *Angew. Chem. Int. Ed.*, **38** (1999) 884
32. E. Buhleier, W. Wehner, F. Vögtle, *Synthesis*, (1978) 155
33. D. A. Tomalia, E. Baker, J. Dewald, M. Hall, G. Kalla, S. Martin, J. Raeck, J. Ryder, P. Smith, *Macromolecules*, **19** (1986) 2466
34. C. J. Hawker, J. M. J. Fréchet, *J. Am. Chem. Soc.*, **112** (1990) 7638
35. O. G. Schramm, X. L'opez-Cort'es, L. S. Santos, V. F. Laurie, F. D. G. Nilo, M. Krolik, R. Fischer, S. D. Fiorea, *Soft Matter*, **10** (2014) 600
36. V. Carrasco-Sánchez, A. Vergara-Jaque, M. Zuñiga, J. Comer, A. John, F. M. Nachtigall, O. Valdes, E. F. Duran-Lara, C. Sandoval, L. S. Santos, *Eur. J. Med. Chem.*, **73** (2014) 250
37. K. Fhayli, S. Gatard, A. Mohamadou, L. Dupont, S. Bouquillon, *Inorg. Chem. Commun.*, **27** (2013) 101
38. L. Wu, B. Li, Y. Huang, H. Zhou, Y. He, Q. Fan, *Org. Lett.*, **8** (2006) 3605
39. V. K. R. Kumar, S. Krishnakumar, K. R. Gopidas, *Eur. J. Org. Chem.*, (2012) 3447
40. X. Shi, I. Leeb, J. R. Baker Jr, *J. Mater. Chem.*, **18** (2008) 586
41. X. Yuan, S. Wen, M. Shena, X. Shi, *Anal. Methods*, **5** (2013) 5486
42. R. W. J. Scott, O. M. Wilson, R. M. Crooks, *J. Phys. Chem. B*, **109** (2005) 692
43. M. Zhao, L. Sun, R. M. Crooks, *J. Am. Chem. Soc.*, **120** (1998) 4877
44. L. K. Yeung, R. M. Crooks, *Nano Lett.*, **1** (2001) 14
45. J. Moineau, G. Pozzi, S. Quici, D. Sinou, *Tetrahedron Lett.*, **40** (1999) 7683

Chapter 1

An Introduction to Dendrimer Encapsulated Nanoparticles and their Application in Catalysis

46. R. Kling, D. Sinou, G. Pozzi, A. Choplin, F. Quignard, S. Busch, S. Kainz, D. Koch, W. Leitner, *Tetrahedron Lett.*, **39** (1998) 9439
47. J. Lemo, K. Heuzé, D. Astruc, *Inorg. Chim. Acta*, **359** (2006), 4909
48. C. Deraedt, L. Salmon, L. Etienne, J. Ruiz, D. Astruc, *Chem. Commun.*, **49** (2013) 8169
49. M. Ooe, M. Murata, T. Mizugaki, K. Ebitani, K. Kaneda, *Nano Lett.*, **2** (2002) 999
50. V. Chechik, R. M. Crooks, *J. Am. Chem. Soc.*, **122** (2000) 1243
51. J. A. Johnson, J. J. Makis, K. A. Marvin, S. E. Rodenbusch, K. J. Stevenson, *J. Phys. Chem. C*, **117** (2013) 22644
52. P. Kracke, T. Haas, H. Saltsburg, M. Flytzani-Stephanopoulos, *J. Phys. Chem. C*, **114** (2010) 16401
53. M. Nemanashi, R. Meijboom, *Catal. Lett.*, **143** (2011) 324

Chapter 2 : Synthesis of Unimolecular Dendritic Micelles

2.1. Introduction

Traditionally micelles (Figure 2.1-1) are formed when surfactant molecules, containing a hydrophobic and hydrophilic component, in an aqueous solution are above their critical micelle concentration (cmc). The surfactant molecules arrange themselves with their hydrophobic “tails” facing inward, away from the water molecules, and their hydrophilic “heads” facing outwards towards the water molecules.^[1] Micelles also have the ability to solubilize other molecules and it is this property that makes them useful in host-guest chemistry.

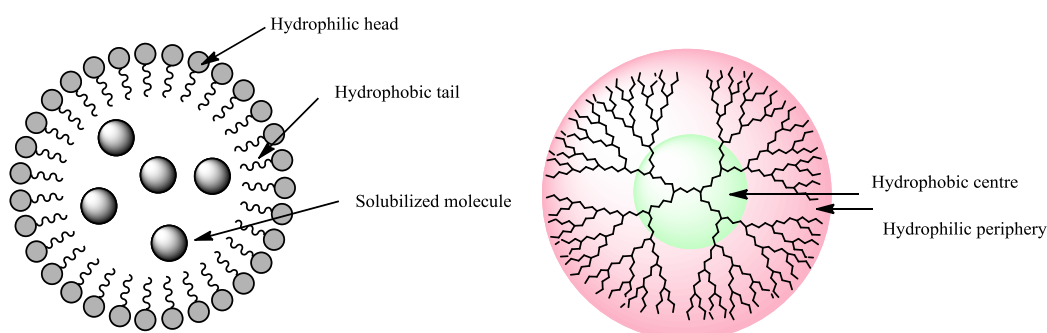


Figure 2.1-1: Comparison between a classic micelle and a dendrimer

These systems can easily be compared with dendrimers when considering their 3-dimensional architecture. Dendrimers can be tailored to produce structures containing a hydrophilic periphery and a hydrophobic interior or vice versa resulting in a similar system to that of micelles or reverse micelles. These types of molecules are usually referred to as unimolecular dendritic micelles. Compared to traditional polymeric micelles these types of molecules are better candidates for applications such as drug delivery agents because of their ability to accommodate guest molecules as well as their stable structures in dilute solutions. Polymeric micelles will dissociate in dilute solutions abruptly releasing the guest located within its interior while dendritic molecules are more stable in these dilute solutions and thus slower release of the guest is possible. Fréchet *et al* ^[2] designed dendritic unimolecular micelles using 4, 4-bis (4'-hydroxyphenyl)-pentanol as a building block for the hydrophobic dendritic hypercore and functionalized these with poly(ethylene glycol) mesylate to provide a

Chapter 2

Synthesis of Unimolecular Dendritic Micelles

hydrophilic outer shell. The drug loading and release capabilities of this micelle was tested using Indomethacin as the guest molecule. They found a drug loading of 11 wt%, corresponding to about nine to ten drug molecules, could be achieved and the release of these drugs were slow showing about 98% of the drug released only after 27 hours. Stevelmans *et al* ^[3] reported the synthesis of inverted unimolecular micelles which were tested as hosts for guest molecules by trapping of the hydrophilic dye Bengal Rose. The inverted micelles were synthesized by peripheral modification of DAB PPI dendrimers with a variety of long alkyl chains. Similar hydrophobic unimolecular dendritic micelles were used in the preparation of gold nanoparticles by Knecht *et al.* ^[4] Instead of DAB PPI modified dendrimers these authors used PAMAM dendrimers modified on their periphery with dodecyl groups. These types of systems give the host-guest advantages of unimolecular dendritic micelles as well as provide a means of nanoparticle synthesis in organic solvents.

When designing any dendritic system one should decide which core molecule is appropriate for the desired application. 1, 4, 8, 11-Tetraazacyclotetradecane (cyclam) has been used as a core molecule in a variety of dendrimers designed for different applications such as phenylazomethine dendrimers, ^[5] dimethoxybenzene and naphthyl containing dendrimers ^[6] as well as cyclam-based propyl imine Schiff base dendritic ligands ^[7] to name a few. Cyclam (Figure 2.1-2) has the ability to coordinate a variety of metal ions and also contains nitrogen atoms which can easily be functionalized. ^[8,9]

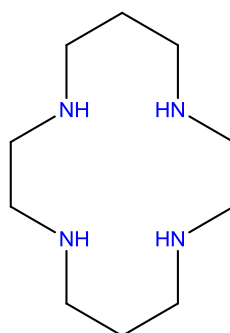
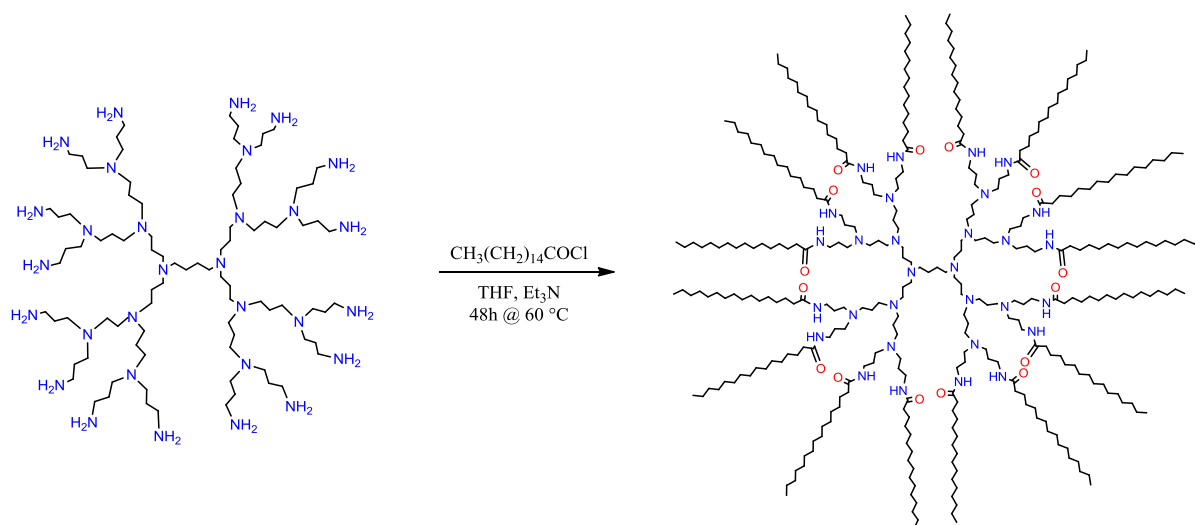


Figure 2.1-2: 1,4,8,11-Tetraazacyclotetradecane or more commonly cyclam

Taking all of this into account we decided to develop unimolecular dendritic micelles based on commercially available DAB PPI dendrimers as well as to synthesize novel cyclam-cored dendritic micelles.

2.2. Modification of DAB PPI dendrimers with long aliphatic chains



Scheme 2.2-1: Modification of G3 DAB PPI dendrimer with palmitoyl chloride

In this project, commercially available DAB PPI dendrimers were used as a starting material for the formation of the unimolecular dendritic micelles (Scheme 2.2-1). The aim was to compare the linear diaminobutane core of the DAB PPI dendrimer, which is more flexible, to the more rigid and spherical cyclam-cored dendrimers that would also be synthesized.

The synthetic route reported by Stevelmans *et al* ^[3] was utilised to modify the periphery of generation 1, 2 and 3 DAB PPI dendrimers with palmitoyl chloride. The particular generation DAB PPI dendrimer was completely dissolved in THF in a round bottom flask. A base, triethylamine, was added followed by the dropwise addition of a small excess palmitoyl chloride resulting in a colour change from clear to milky white. The palmitoyl chloride reacts with the amine groups on the periphery of the dendrimer via a nucleophilic substitution. This is followed by the elimination of the chloride ion which results in the formation of hydrochloric acid. The hydrochloric acid immediately reacts with the base, triethylamine, to form triethylamine hydrochloride. After stirring the reaction for 48 hours the excess solvent was removed. Diethyl ether was then added and the reaction mixture was heated under reflux for 30 minutes and filtered to remove the excess palmitoyl chloride left in the reaction mixture. To the residue was added sodium carbonate and water and the mixture was heated under reflux overnight, cooled and filtered to remove the remaining ammonium salt. The final product in all cases is an off-white powder.

Chapter 2

Synthesis of Unimolecular Dendritic Micelles

2.2.1. Characterization

All of the products were fully characterized by FT-IR spectroscopy, ^1H -NMR and ^{13}C -NMR spectroscopy, mass spectrometry and elemental analysis. The FT-IR, ^1H -NMR and ^{13}C -NMR characterization data for all three generations are similar and so the discussion will be limited to results relating to the generation 1 modified product, G1 DAB-PPI-(palmitoyl)₄.

2.2.1.1. Infrared Spectroscopy (ATR-IR)

To determine if the modification process was successful we had to establish if an amide functionality was present in the product. The IR spectrum of the product shows a band at 1635 cm^{-1} . This band can be assigned to an amide carbonyl functionality providing initial proof that the modification was successful. Another characteristic band can be found at around 3280 cm^{-1} corresponding to the N-H in an amide functionality. At approximately 2915 cm^{-1} a band corresponding to the saturated hydrocarbon chain is also present. The results correspond well with literature data for similar amide-functionalized dendrimer. ^[3]

2.2.1.2. ^1H -NMR and ^{13}C -NMR Spectroscopy

To establish with more certainty that the product formation was successful ^1H and ^{13}C NMR spectra were recorded and referenced to chloroform-*d*. The most characteristic resonance peaks in the ^1H NMR spectrum would be those found for the terminal methyl protons of the palmitoyl chain and the amide protons. At 0.87 ppm a triplet corresponding to the terminal methyl protons can be found while at 6.56 ppm a triplet corresponding to the amide protons is found. In the range of 1.24-2.15 ppm several peaks corresponding to the methylene protons in the saturated hydrocarbon chain are observed. The peaks found at 2.41 ppm and 3.27 ppm corresponds to the methylene protons situated next to the tertiary and secondary amines in the interior architecture of the dendrimer. They are situated close to the electronegative nitrogen atoms which lead to a deshielding effect and thus a downfield shift. The ^1H -NMR data for all of the products correspond well with the literature data for similar compounds. ^[3]

In the ^{13}C -NMR spectrum the most characteristic resonance peaks would once again be those indicating the presence of the amide as well as the terminal methyl group. Here we observed a peak at 14.26 ppm corresponding to the chemically equivalent terminal methyl carbons as well as a peak at 173.58 ppm corresponding to the carbonyl carbon in the amide functionality. The different methylene carbons can be found in the range of 22.83-53.81 ppm. The ^{13}C -NMR data also corresponds well with the literature data for similar compounds. ^[3]

Chapter 2

Synthesis of Unimolecular Dendritic Micelles

2.2.1.3. Mass Spectrometry, Elemental Analysis and Thermal stability

Mass spectrometry and elemental analysis were performed as final proof that the desired product was formed successfully. The mass spectrum for G1 DAB-PPI-(palmitoyl)₄ shows the presence of the molecular ion at $m/z = 1270.3$ and the doubly charged ion at $m/z = 635.6$. Elemental analysis results indicate the entrapment of water molecules in the dendrimer cavities. Further details are available in the experimental section (section 2.5.3).

2.3. Synthesis of cyclam-cored unimolecular dendritic micelles

To synthesize the cyclam-cored unimolecular dendritic micelles a divergent synthetic approach was chosen. The generation 1 and 2 amino functionalized dendrimers were first synthesized and then modified with palmitoyl chloride to result in two generations of cyclam-cored unimolecular dendritic micelles.

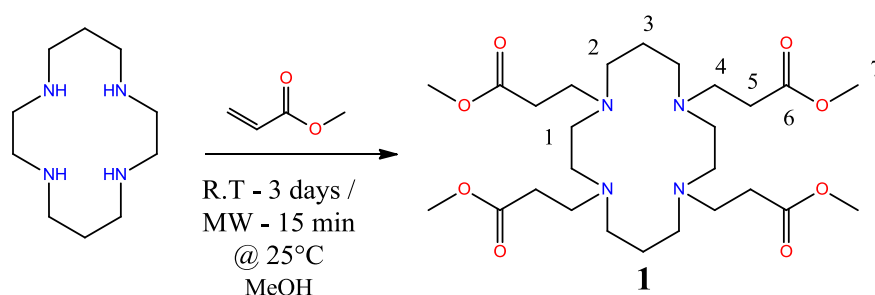


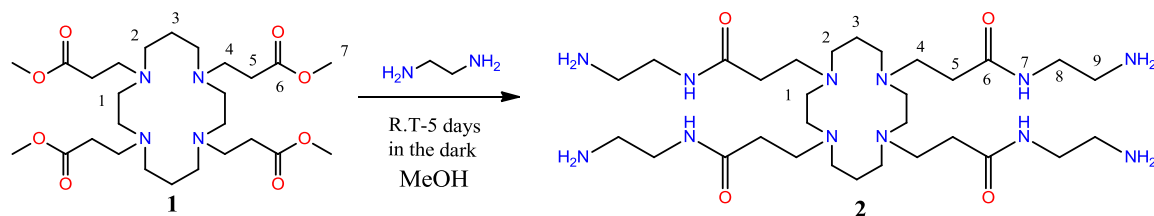
Figure 2.3-1: Synthesis of G 0.5 dendrimer

The first step in the synthetic sequence involved the Michael addition of methyl acrylate to 1,4,8,11-tetraazacyclotetradecane (cyclam) to give the generation 0.5 dendrimer with ester functionalities on the periphery (Figure 2.3-1). The conventional synthetic route was adapted from the procedure reported by Subik et al ^[10]. The Michael addition reaction was performed in MeOH under an inert atmosphere for three days resulting in white crystals as the final product. We also developed an optimized synthetic procedure by making use of a microwave reactor. Using this approach the reaction time was reduced to 15 minutes. Cyclam and methyl acrylate were added to a 10 mL reaction vial and dissolved in MeOH. The reaction was run for 15 minutes at 25 °C and 300 W power. After removal of the excess solvent and methyl acrylate a clear oil is obtained. Purification was performed as with the conventional procedure by recrystallization from DCM and hexane resulting in white crystals as the final product.

Chapter 2

Synthesis of Unimolecular Dendritic Micelles

The second step in the reaction sequence involved an amidation reaction between ethylenediamine and the generation 0.5 ester-terminated dendrimer **1** to yield the generation 1 amine-terminated cyclam-cored dendrimer **2** (Scheme 2.3-1).



Scheme 2.3-1: Synthesis of G1 dendrimer

The synthetic method was adapted from the method reported by Stephan et al.^[11]. The reaction was performed under an argon atmosphere using standard Schlenk techniques. In short, **1** was fully dissolved in MeOH followed by the slow addition of a large excess of ethylenediamine. The reaction was stirred for 5 days in the dark. A large excess of ethylenediamine was used to prevent unwanted side reactions occurring. If a smaller excess is used there is a possibility that two G 0.5 dendrimer molecules could link through ethylenediamine forming a polymer-type product. Another possibility is that two of the arms on the G 0.5 dendrimer could link through an ethylenediamine molecule. Examples of these types of side reaction products are given in Figure 2.3-2. The reaction is also done in the dark to prevent polymerization from taking place.

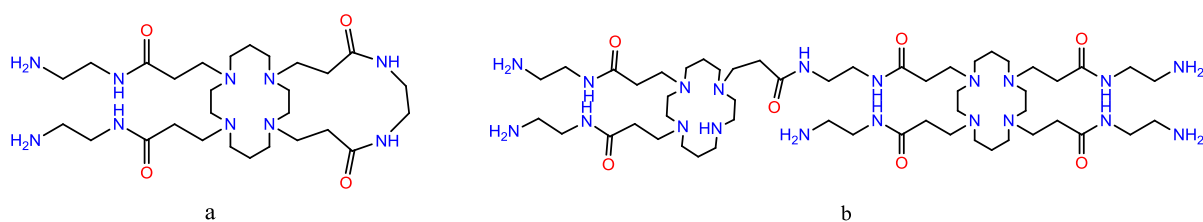
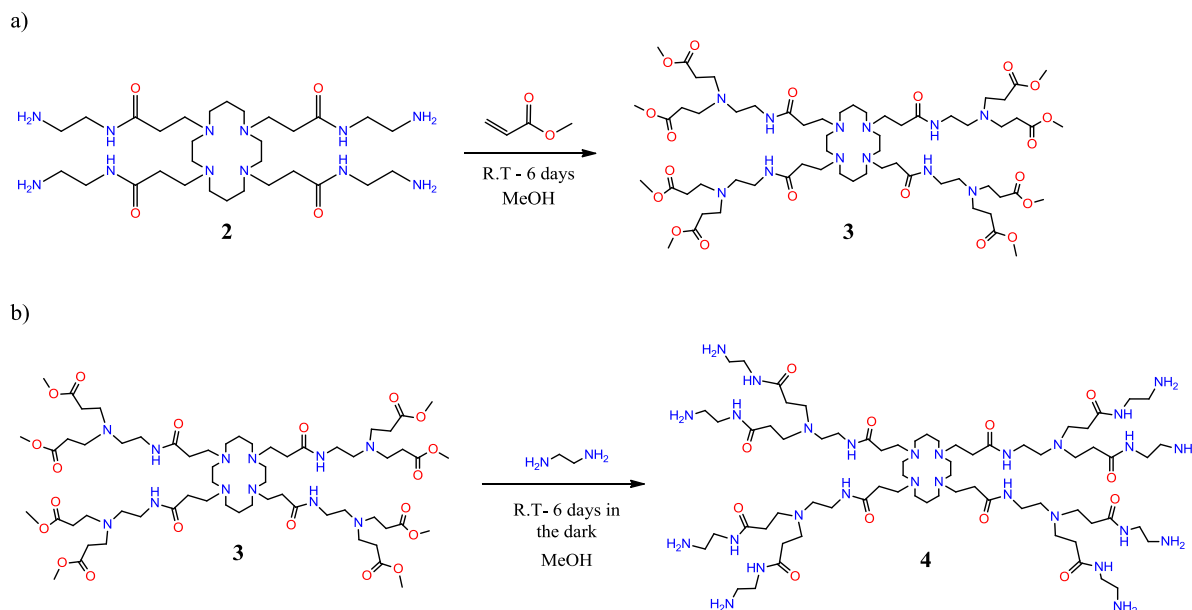


Figure 2.3-2: (a) Linking of two dendrimer arms through ethylenediamine (b) Polymer type by-product

After the reaction had run to completion the excess solvent and ethylenediamine was removed under reduced pressure resulting in a yellow oil. Diethyl ether is added for purification purposes resulting in the precipitation of the final product, a light yellow-coloured sticky solid.

Chapter 2

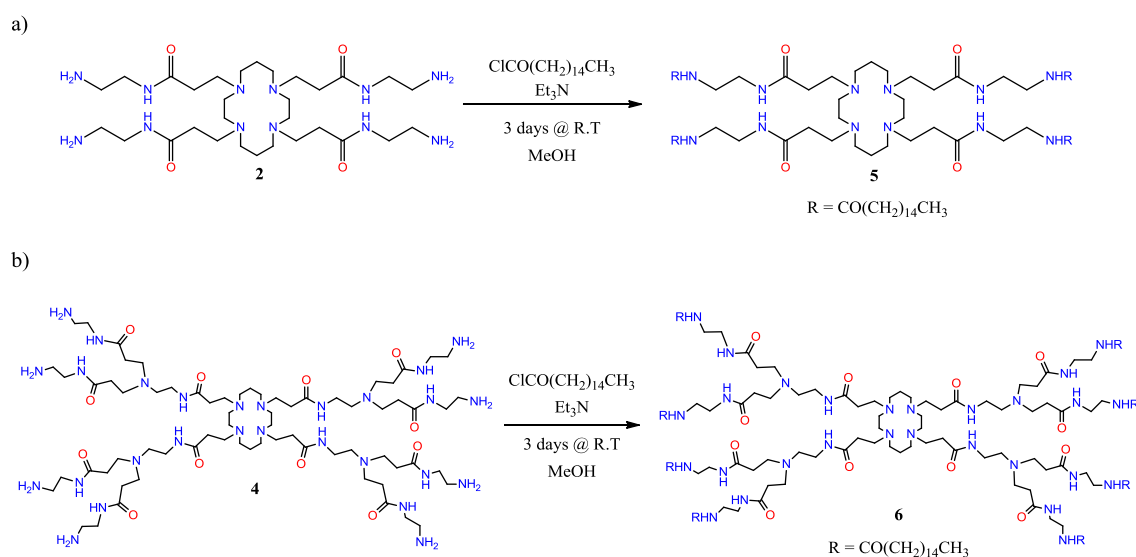
Synthesis of Unimolecular Dendritic Micelles



Scheme 2.3-2: (a) Synthesis of G 1.5 ester-terminated dendrimer (b) Synthesis of G2 amine-terminated dendrimer

The generation 2 dendrimer was synthesized by reacting **2** with methyl acrylate in a Michael addition [Scheme 2.3-2 (a)] followed by the amidation reaction with ethylenediamine [Scheme 2.3-2 (b)]. The reaction conditions were similar to those used for the synthesis of compounds **1** and **2** and so will not be repeated. The most significant change in conditions was the slightly longer reaction times used for the synthesis of G 1.5 and G 2 as these compounds are so much larger.

The last step in the reaction sequence was the modification of the G 1 and G 2 polyamine dendrimers with palmitoyl chloride to give the final unimolecular dendritic micelles **5** and **6**.



Scheme 2.3-3: (a) Modification of G 1 tetra-amine dendrimer (b) Modification of G 2 octa-amine dendrimer

Chapter 2

Synthesis of Unimolecular Dendritic Micelles

The modification method was again adapted from the procedure reported by Stevelmans *et al* [3]. The specific generation cyclam-cored amine-terminated dendrimer was reacted with an excess of palmitoyl chloride (Scheme 2.3-3). The alkyl chain terminated product was isolated as an off-white powder in all cases.

2.3.1. Characterization

All of the products were fully characterized by FT-IR spectroscopy, $^1\text{H-NMR}$ and $^{13}\text{C-NMR}$ spectroscopy, mass spectrometry and elemental analysis.

2.3.1.1. Infrared Spectroscopy (ATR-IR)

To confirm the successful Michael addition reaction between cyclam and methyl acrylate, the IR spectrum of the G0.5 dendrimer is expected to show a carbonyl band around 1700 cm^{-1} indicating that an ester functionality is present. This was found to be the case for the synthesized G 0.5 acrylate-functionalized dendrimer. A band at 1732 cm^{-1} was present in the IR spectrum of the product. The next step in the dendrimer synthesis involved an amidation reaction between the synthesized G0.5 acrylate-functionalized dendrimer and ethylenediamine. The IR spectrum of this product should therefore not contain any carbonyl band for the ester functionality present in the starting material but should contain a carbonyl band for the amide functionality present in the desired G1 product. This was observed as a band at 1628 cm^{-1} for the amide carbonyl as well as a band at 3292 cm^{-1} corresponding to an N-H stretch and a band at 1545 cm^{-1} corresponding to an N-H bend. To elaborate the dendrimer to G2 the first two steps were repeated. To synthesize the G1.5 dendrimer the G1 dendrimer was reacted with methyl acrylate in a Michael addition resulting in the formation of an ester-terminated dendrimer. This dendrimer would then contain both an amide and an ester functionality. This is again observed in the IR spectrum as a band at 1728 cm^{-1} for the ester carbonyl and 1642 cm^{-1} for the amide carbonyl is present. The last step in the dendrimer synthesis involves an amidation between the G1.5 dendrimer and ethylenediamine to give the final G2 polyamine dendrimer containing no ester functionality. The IR spectrum showed exactly this as the only band in the carbonyl region was found at 1633 cm^{-1} for the amide carbonyl. An N-H bend is also present at 1540 cm^{-1} and an N-H stretch at 3269 cm^{-1} .

As the generation 1 and generation 2 modifications are performed similarly only the G1 IR spectrum will be discussed. The IR spectrum of this product looks similar to that of the modified DAB PPI dendritic micelle. An N-H bend is found at 1549 cm^{-1} and an N-H stretch

Chapter 2

Synthesis of Unimolecular Dendritic Micelles

at 3295 cm^{-1} . The amide carbonyl band could be found at 1632 cm^{-1} as expected along with a band at 2915 cm^{-1} corresponding to the saturated hydrocarbon chain.

2.3.1.2. $^1\text{H-NMR}$ and $^{13}\text{C-NMR}$ Spectroscopy

All of the synthesized products were characterized by $^1\text{H-NMR}$ and $^{13}\text{C-NMR}$ and referenced to chloroform-*d*, dimethyl sulfoxide-*d*₆ or D₂O.

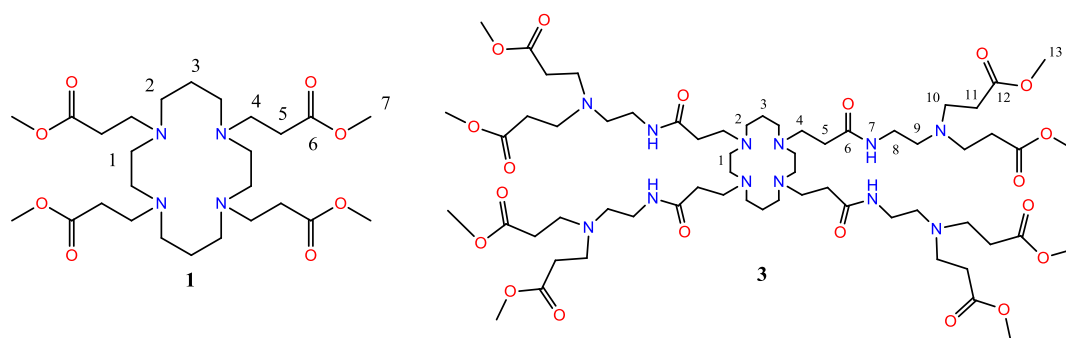


Figure 2.3-3: G 0.5 (1) and G1.5 (3) cyclam-core dendrimers

Considering compounds **1** and **3** (Figure 2.3-3), the ester-terminated dendrimers, the most characteristic resonances would be those corresponding to the methoxy protons on the periphery and the carbonyl carbons indicating that the Michael addition was successful. The $^1\text{H-NMR}$ spectrum of **1** showed all the expected peaks integrating to the estimated amounts. The most significant peak can be found at 3.64 ppm integrating for 12 protons representing the 12 methoxy protons. The $^{13}\text{C-NMR}$ spectrum shows a resonance at 173.34 ppm corresponding to C₆ and representing the carbonyl carbon.

In the $^1\text{H-NMR}$ spectrum of compound **3**, the ester-terminated G 1.5 dendrimer, a singlet is observed at 3.65 ppm corresponding to the methoxy protons. A broad peak at 7.23 ppm is also present for the amide protons. Considering the ^{13}C NMR spectrum, in the region of 170 ppm where a resonance for the carbonyl carbons of esters and amides are expected, two signals are observed. As the product does contain both ester and amide functionalities this is desired. The most downfield peak found at 173.1 ppm corresponds to the ester carbonyl carbon while the signal at 172.5 ppm corresponds to the amide carbonyl carbon.

The $^1\text{H-NMR}$ spectrum of the G1 dendrimer **2** (Figure 2.3-4) shows all the expected signals. A triplet corresponding to the amide proton H₇ can be seen at 7.92 ppm. Signals representing the cyclam core protons are found at 1.50, 2.40 and 2.43 ppm respectively. H₃ is the most shielded signal at 1.50 ppm represented by the expected quintet. The triplet at 2.40 ppm

Chapter 2

Synthesis of Unimolecular Dendritic Micelles

representing the H₂ equivalent protons and the singlet at 2.43 ppm representing the H₁ equivalent protons overlaps slightly because they are so similar considering their chemical environment. The ¹³C NMR spectrum shows the expected resonance at 171.44 ppm for C₆, the amide carbonyl carbon, as well as signals at 23.53 (C₃), 50.16 (C₁) and 50.55 (C₂) ppm for the carbons present in the cyclam core. All other carbons are also accounted for. The ¹H NMR and ¹³C NMR data correspond well with literature data for similar compounds. [10,11]

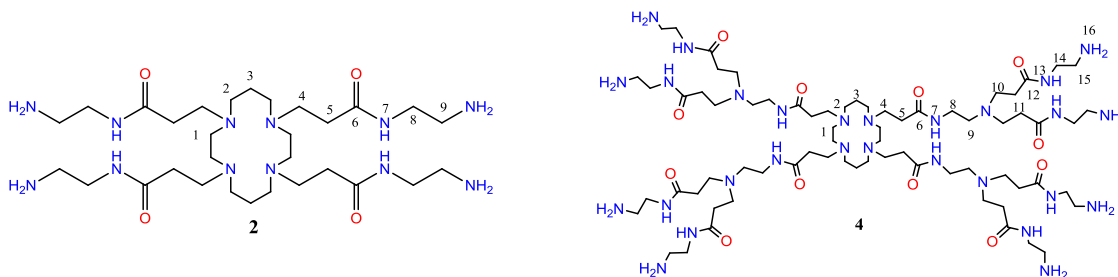


Figure 2.3-4: G1 (2) and G2 (4) cyclam-cored dendrimers

For the G2 amine-terminated dendrimer **4** (Figure 2.3-4), a broad singlet representing the four H₃ protons in the cyclam core is found at 1.49 ppm. A broad peak with a small shoulder on the left and a larger shoulder on the right is found at 2.42 ppm representing H₁ and H₂. A singlet and a triplet are expected for H₁ and H₂ respectively. This peak can thus be better defined as an overlap between the two signals. A broad triplet is found at 2.19 ppm representing the H₅ and H₁₁ protons. These protons are found in chemically similar environments however the slight differences in their chemical environments causes the poorly resolved signal. The branched nature of this compound also contributes to the broadness of some of the signals. Although it is expected that, for example, the H₁₁ protons are equivalent on all eight branches of the dendrimer this could in fact not be the case. The dendrimer has a three dimensional structure with branches that are flexible. The same thing is observed for the triplet at 2.64 ppm representing H₄ and H₉. This triplet is more defined as it represents a smaller number of protons. In the range of 2.52 - 2.59 ppm several signals representing H₉, H₁₅ and H₁₆ and in the range of 3.01 – 3.08 ppm several signals representing H₈ and H₁₄ are observed. A cluster of unresolved signals is observed in both cases. A characteristic signal is the one representing the amide protons. Two overlapping signals with a large broad shoulder are observed at 7.91 and 7.92 ppm representing H₇ and H₁₃. In the ¹³C NMR spectrum signals representing the carbons present in the cyclam core can be found at 23.52 ppm (C₃), 50.02 ppm (C₁) and 50.48 ppm (C₂). The most characteristic carbon signals are however those found at 171.56 and 171.62 ppm representing the two amide carbonyls.

Chapter 2

Synthesis of Unimolecular Dendritic Micelles

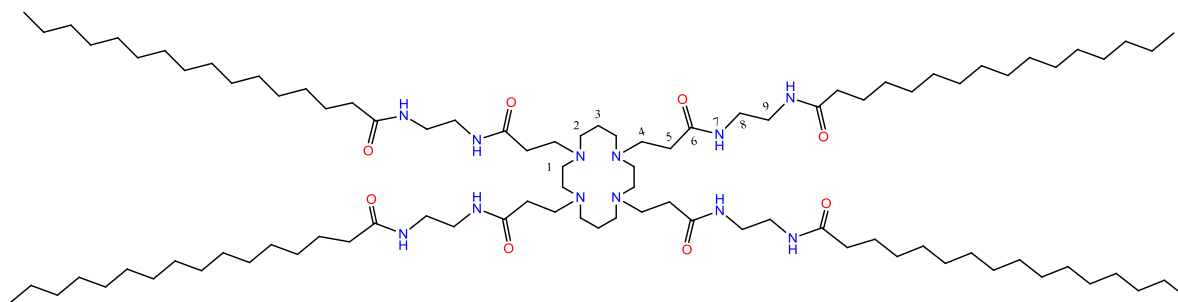


Figure 2.3-5: G1 cyclam-cored dendritic micelle

The modified G1 and G2 dendrimers are very similar and so only the NMR data of the G1 dendrimer (Figure 2.3-5) will be discussed. Considering the vast number of methylene protons in several different chemical environments it is not difficult to understand that the ^1H NMR spectrum of this product is quite complex. The product is also poorly soluble resulting in an NMR spectrum with broad unresolved peaks. Nonetheless, there is a well-defined triplet found at 0.88 ppm representing the chemically equivalent methyl protons on the periphery of the dendrimer. The signals representing the protons in the interior architecture of the dendrimer can be found in the range of 1.25-3.36 ppm with the most intense peak found at 1.25 ppm. At 7.26 ppm a split peak can be found which we have attributed to the solvent (chloroform) peak as well as a peak for the amide proton appearing close to each other. The ^{13}C NMR spectrum shows a signal at 14.27 ppm representing the methyl carbons at the end of the hydrocarbon chain. The carbons present in the cyclam core are represented by signals found at 25.97 ppm (C_3), 40.37 ppm (C_2) and 51.59 ppm (C_1). Signals representing the methylene carbons present in the alkyl chain are found in the range of 29.31-29.86 ppm. The length of the hydrocarbon chains and the flexible three dimensional architecture of the dendrimer lead to a range of broad unresolved and overlapping signals. Finally the signal found at 174.69 ppm shows the presence of an amide carbonyl in the structure.

2.3.1.3. Mass Spectrometry, Elemental Analyses and Thermal Stability

Mass spectrometry and elemental analysis were performed on all intermediate and final products. The mass spectrum of the first intermediate G0.5 ester-terminated dendrimer (**1**) showed the molecular ion at a m/z ratio of 546.4 and the doubly charged ion as the base peak at a m/z ratio of 273.2 m/z ratio. The isotopic pattern found in both of these regions corresponds well with simulated data. The compound is relatively stable considering that the molecular ion is present in the spectrum and little to no fragmentation occurs. The doubly charged molecular ion appears to be the more stable form as this is found as the base peak. The experimental elemental analysis data corresponds well with the calculated values thus

Chapter 2

Synthesis of Unimolecular Dendritic Micelles

confirming the purity of this product. The white crystalline solid melts in the range of 45.0 – 50.5 °C.

The mass spectrum of the G1 amine-terminated dendrimer (**2**) shows the molecular ion at a m/z of 657.53 as well as the sodium adduct at a m/z of 679.50. The isotopic pattern of both of these clusters correlates well with the calculated data. The base peak is found at a m/z ratio of 543.4 corresponding to a loss of one pendant arm $[\text{C}_{25}\text{H}_{54}\text{N}_{10}\text{O}_3 + \text{H}]^+$. The doubly charged molecular ion is also observed at a m/z ratio of 329.26. The elemental analysis indicates the entrapment of water molecules within the cavities of the dendrimer. This product is a relatively hygroscopic sticky solid and thus it is difficult to sufficiently remove all the water from it.

The mass spectrum of the G1.5 ester-terminated dendrimer shows the molecular ion at a m/z ratio of 1345.80 and a sodium adduct with a slight lower intensity at a m/z ratio of 1367.78. The fragmentation pattern found in both of these clusters corresponds well with the calculated data. At a m/z ratio of 1145.69 and 1167.69 the $[\text{C}_{53}\text{H}_{97}\text{N}_{11}\text{O}_{16} + \text{H}]^+$ ion and sodium adduct of this fragment are seen respectively. Another fragment that can be identified is found at a m/z ratio of 1059 and corresponds to the molecular ion with the loss of one pendant arm $[\text{C}_{49}\text{H}_{90}\text{N}_{10}\text{O}_{15} + \text{H}]^+$. This fragment is seen at a very low intensity. The base peak was identified as the doubly charged molecular ion found at a m/z ratio of 673.41. The elemental analysis points to the entrapment of solvent (DCM) molecules. DCM is used in the purification process of this product.

The mass spectrum for the generation 2 amine-terminated dendrimer shows the molecular ion at a m/z ratio of 1570.1 with a fragmentation pattern corresponding to the calculated data. Other ions that are present are the doubly charged ion, m/z 285.6, the triply charged ion, m/z 524.1, and the quadruply charged ion which is also the base peak at a m/z ratio of 393.3. A fragment corresponding to $[\text{C}_{47}\text{H}_{98}\text{N}_{18}\text{O}_7 + \text{H}]^+$ is found at a m/z of 1027.4. Once again this amine-terminated product is relatively hygroscopic and contains a fair amount of water. Elemental analysis data indicates the entrapment of water molecules within the cavities of the dendrimer.

The two final products are the generation 1 and 2 modified cyclam-cored unimolecular dendritic micelles. The mass spectrum of the generation 1 dendrimer modified with the hydrocarbon chain shows that this product is relatively unstable under the mass spectrometry

Chapter 2

Synthesis of Unimolecular Dendritic Micelles

conditions. The molecular ion peak found at a m/z ratio of 1611.99 has a very low intensity and fragmentation occurs easily. The triply charged molecular ion and its sodium adduct is found at a m/z ratio of 537.46 and 559.52 respectively. The loss of one pendant arm resulting in a molecule with the formula $C_{73}H_{144}N_{10}O_6$ corresponds to a peak found at a m/z ratio of 1258.14. Another fragment that can be identified is found at a m/z ratio of 1074.06 and corresponds to a fragment with the formula $C_{60}H_{118}N_{10}O_6$. This mass corresponds to a fragment that lost one pendant arm and a part of one of the hydrocarbon chains. Elemental analysis indicates the entrapment of solvent molecules (diethyl ether and water) in the cavities of the dendritic micelle. These solvents are used in the work-up procedure when preparing this compound. The product was found to decompose at 200 °C.

The mass spectrometry result for the generation 2 hydrophobic dendrimer was inconclusive. It seems that this compound is unstable under the conditions used for the analysis. Mostly low molecular weight peaks are seen indicating that the compound fragments easily. The only peak that can be identified is found at a m/z ratio of 819.71 with a relatively high intensity and corresponds to one complete pendant arm. The elemental analysis data conforms to a species in which solvent molecules (DCM and H_2O) are entrapped within the dendrimer. The melting point range for this product is between 153.3 – 170 °C. The product starts to melt at 153.3 °C and then decomposes when the temperature increases to 170 °C.

2.4. Conclusion

The synthesis and characterization of 2 types of unimolecular dendritic micelles have been outlined in this chapter. Previously reported unimolecular dendritic micelles with a DAB PPI interior structure as well as novel cyclam-cored micelles with a PAMAM interior structure were synthesized and fully characterized. Generation 1, 2 and 3 commercially available DAB dendrimers were modified with palmitoyl chloride to give hydrophobic micelles containing long aliphatic chains on their periphery. To synthesize the cyclam-cored version of these micelles generation 1 and generation 2 cyclam-cored dendrimers were synthesized, using a divergent approach, by successive Michael addition and amidation reactions and finally modified with palmitoyl chloride resulting in hydrophobic dendrimers with long aliphatic chains on their periphery. All products were fully characterized by FT-IR, Mass spectrometry, 1H NMR, ^{13}C NMR and elemental analysis. These two types of unimolecular

dendritic micelles will play host to metal nanoparticles to form dendrimer encapsulated metal nanoparticles.

2.5. Experimental Section

2.5.1. General Consideration and Materials

All reactions were performed using standard Schlenk techniques under argon or nitrogen atmosphere unless stated otherwise. In the case of microwave-assisted reactions a CEM Microwave reactor was used. All reagents were acquired from Sigma-Aldrich and used without any further purification. All solvents were purchased from Sigma-Aldrich or Kimix and purified by a Pure SolvTM Micro solvent purifier fitted with activated alumina columns with the exception of MeOH which was purified by distillation over a mixture of magnesium filings and iodine.

2.5.2. Instrumentation

Infrared spectra were recorded using a Nicolet Avatar 330 FT-IR spectrometer equipped with a Smart Performer ATR attachment with a Zn/Se crystal. ¹H-NMR (300, 400, 600 MHz) and ¹³C-NMR (75, 300, 400 MHz) spectroscopy was performed on a Varian Unity Inova spectrometer. ESI-MS was performed using a Waters Synapt G2 Mass Spectrometer. Elemental Analysis was performed at the University of Cape Town. Melting point data was recorded with a Stuart Scientific melting point apparatus SMP3.

2.5.3. Procedures and Characterization

DAB-dendr-(palmitoyl)₄

G1-DAB (0.258 g, 0.815 mmol) was dissolved in THF (20 mL) while stirring. Et₃N (0.7 mL, 5.02 mmol) was added followed by the dropwise addition of palmitoyl chloride (1.25 mL, 4.08 mmol). The reaction was stirred for 22 hours after which the solvent was evaporated under reduced pressure. Diethyl ether (50 mL) was added and the mixture was refluxed for 30 min and filtered to remove excess palmitoyl chloride. Na₂CO₃ (0.504 g) and H₂O (50 mL) were added to the residue and the mixture was refluxed for 24 hours to remove residual ammonium salts and to deprotonate the dendrimers, followed by filtration. The product was dried in an oven resulting in a cream coloured solid (0.914 g, 87.88% yield) as final product. ¹H-NMR (300 MHz, CDCl₃): δ 0.87 (12H, t, CH₃, *J* = 6.7 Hz), 1.24-1.40 (108H, s & bs,

Chapter 2

Synthesis of Unimolecular Dendritic Micelles

$\text{CH}_2\text{-CH}_3 + \text{CH}_2\text{-CH}_2\text{-CH}_2$), 1.61 (8H, dt, $\text{NHCO-CH}_2\text{-CH}_2$), 2.15 (8H, t, NHCO-CH_2 , $J = 7.7 \text{ Hz}$), 2.41 (12H, m, $\text{CH}_2\text{-N-(CH}_2)_2 + \text{CH}_2\text{-N-(CH}_2)_2$), 3.27 (8H, dd, $\text{CH}_2\text{-NHCO}$), 6.56 (4H, t, NHCO , $J = 5.5 \text{ Hz}$). ^{13}C NMR (300 MHz, CDCl_3): δ 14.26 (CH_3), 22.83 ($\text{CH}_2\text{-CH}_3$), 24.89 ($\text{N-CH}_2\text{-CH}_2\text{-CH}_2\text{-CH}_2\text{-N} + \text{N-CH}_2\text{-CH}_2\text{-CH}_2\text{-N}$), 26.05 ($\text{NHCO-CH}_2\text{-CH}_2$), 27.05 ($\text{N-CH}_2\text{-CH}_2\text{-CH}_2\text{-NHCO}$), 29.51-29.86 ($\text{CH}_2\text{-(CH}_2)_n\text{-CH}_2$), 32.07 ($\text{CH}_2\text{-CH}_2\text{-CH}_3$), 36.96 (NHCO-CH_2), 38.22 ($\text{CH}_2\text{-NHCO}$), 51.93 ($\text{N-CH}_2\text{-CH}_2\text{-CH}_2\text{-NHCO}$), 53.81 ($\text{N-CH}_2\text{-CH}_2\text{-CH}_2\text{-CH}_2\text{-N} + \text{N-CH}_2\text{-CH}_2\text{-CH}_2\text{-N}$), 173.58 (NHCO) ppm. IR (ATR) $\nu = 3280.18 \text{ cm}^{-1}$ (N-H amide); 3080.30 cm^{-1} (sec. amide); 2915.83 cm^{-1} (C-H sat.); 1635.46 cm^{-1} (C=O amide); 1543.56 cm^{-1} (N-H bend). Elemental analysis $\text{C}_{80}\text{H}_{160}\text{N}_6\text{O}_4 \cdot 2\text{H}_2\text{O}$: $C_{\text{cal}} = 73.56\%$; $C_{\text{exp}} = 73.88\%$; $H_{\text{cal}} = 12.66\%$; $H_{\text{exp}} = 10.56\%$; $N_{\text{cal}} = 6.57\%$; $N_{\text{exp}} = 6.43\%$. ESI-MS: $\text{C}_{80}\text{H}_{160}\text{N}_6\text{O}_4$ (1270.16); m/z 1270.3 (mol. ion); m/z 635.6 $[\text{M}+2\text{H}]^{2+}$. MP: 114.5°C - 119.1°C

DAB-dendr-(palmitoyl)₈

G2 DAB (0.269 g, 0.383 mmol) was dissolved in THF (20 mL) while stirring. Et_3N (0.7 mL, 5.02 mmol) was added followed by the dropwise addition of palmitoyl chloride (1 mL, 3.45 mmol). The reaction mixture was stirred for 48 hours after which the solvent was evaporated. Diethyl ether (55 mL) was added to the residue and the mixture was refluxed for 40 min followed by filtration to remove excess palmitoyl chloride. To the residue Na_2CO_3 (0.530 g) and H_2O (60 mL) were added and the mixture was refluxed for 23 hours to remove residual ammonium salts and deprotonate the dendrimer. The mixture was filtered and the residue dried in an oven to obtain the product as a cream coloured solid (0.225g, 21.84 % yield). ^1H -NMR (300 MHz, CDCl_3): δ 0.87 (24H, t, CH_3 , $J = 6.7 \text{ Hz}$), 1.24-1.51 (220H, s & bs, $\text{CH}_2\text{-CH}_3 + \text{CH}_2\text{-CH}_2\text{-CH}_2$), 1.60 (16H, m, $\text{NHCO-CH}_2\text{-CH}_2$), 2.17 (16H, t, NHCO-CH_2 , $J = 7.6 \text{ Hz}$), 2.37 (36H, d, $\text{CH}_2\text{-N-(CH}_2)_2 + \text{CH}_2\text{-N-(CH}_2)_2$, $J = 5.0 \text{ Hz}$), 3.26 (16H, dd, $\text{CH}_2\text{-NHCO}$), 6.95 (8H, t, NHCO , $J = 5.8 \text{ Hz}$) ppm. ^{13}C -NMR (75 MHz, CDCl_3): δ 14.27 (CH_3), 22.83 ($\text{CH}_2\text{-CH}_3$), 26.1 ($\text{NHCO-CH}_2\text{-CH}_2$), 27.17 ($\text{N-CH}_2\text{-CH}_2\text{-CH}_2\text{-NHCO}$), 29.52-29.88 ($\text{CH}_2\text{-(CH}_2)_n\text{-CH}_2$), 32.07 ($\text{CH}_2\text{-CH}_2\text{-CH}_3$), 36.86 (NHCO-CH_2), 38.01 ($\text{CH}_2\text{-NHCO}$), 51.67 ($\text{N-CH}_2\text{-CH}_2\text{-CH}_2\text{-NHCO}$), 52.26 ($\text{N-CH}_2\text{-CH}_2\text{-CH}_2\text{-CH}_2\text{-N} + \text{N-CH}_2\text{-CH}_2\text{-CH}_2\text{-N}$), 173.77 (NHCO) ppm. IR (ATR) $\nu = 3293.78 \text{ cm}^{-1}$ (N-H amide); 3075.46 cm^{-1} (sec. amide); 2915.40 cm^{-1} (C-H sat.); 1635.27 cm^{-1} (C=O amide); 1551.37 cm^{-1} (N-H bend). Elemental analysis $\text{C}_{168}\text{H}_{336}\text{N}_{14}\text{O}_8 \cdot 3\text{H}_2\text{O}$: $C_{\text{cal}} = 73.79\%$; $C_{\text{exp}} = 73.93\%$; $H_{\text{cal}} = 12.61\%$; $H_{\text{exp}} = 9.57\%$; $N_{\text{cal}} = 7.17\%$; $N_{\text{exp}} = 7.13\%$. ESI-MS: $\text{C}_{168}\text{H}_{336}\text{N}_{14}\text{O}_8$ (2680.55); m/z 1340.8 $[\text{M}+2\text{H}]^{2+}$; m/z 894.2 $[\text{M}+3\text{H}]^{3+}$; m/z 670.9 $[\text{M}+4\text{H}]^{4+}$. MP: 86°C - 93.8°C

Chapter 2

Synthesis of Unimolecular Dendritic Micelles

DAB-dendr-(palmitoyl)₁₆

G1-DAB (0.284 g, 0.168 mmol) was dissolved in THF (20 mL) while stirring. Et₃N (3 mL, 0.0215 mol) was added followed by the dropwise addition of palmitoyl chloride (0.9 mL, 2.86 mmol). The reaction mixture was stirred for 46 hours and the solvent was evaporated. Diethyl ether (50 mL) was added, the mixture was refluxed for 30 min after which it was cooled and filtered to remove excess palmitoyl chloride. Na₂CO₃ (0.504 g) and H₂O (60 mL) was added and the mixture was refluxed overnight to remove residual ammonium salts and to deprotonate the dendrimer. The mixture was filtered and dried in an oven resulting in a cream coloured solid (0.675 g, 73.05% yield). ¹H-NMR (400 MHz, CDCl₃): δ 0.87 (48H, t, CH₃, *J* = 6.8 Hz), 1.25-1.52 (444H, s & bs, CH₂-CH₃ + CH₂-CH₂-CH₂), 1.61 (32H, t, NHCO-CH₂-CH₂, *J* = 6.06 Hz), 2.18 (32H, m, NHCO-CH₂), 2.36 (84H, bm, CH₂-N-(CH₂)₂ + CH₂-N-(CH₂)₂), 3.25 (32H, d, CH₂-NHCO, *J* = 5.5 Hz), 7.17 (16H, t, NHCO, *J* = 5.2 Hz). ¹³C NMR (400 MHz, CDCl₃): δ 14.28 (CH₃), 22.85 (CH₂-CH₃), 24.77 (N-CH₂-CH₂-CH₂-CH₂-N + N-CH₂-CH₂-CH₂-N), 26.15 (NHCO-CH₂-CH₂), 27.25 (N-CH₂-CH₂-CH₂-NHCO), 29.54-29.91 (CH₂-(CH₂)_n-CH₂), 32.09 (CH₂-CH₂-CH₃), 36.83 (NHCO-CH₂), 37.90 (CH₂-NHCO), 51.56 (N-CH₂-CH₂-CH₂-NHCO), 52.30 (N-CH₂-CH₂-CH₂-CH₂-N + N-CH₂-CH₂-CH₂-N), 173.93 (NHCO) ppm. IR (ATR) ν = 3295.66 cm⁻¹ (N-H amide); 3078.63 cm⁻¹ (sec. amide); 2915.32 cm⁻¹ (C-H sat.); 1635.23 cm⁻¹ (C=O amide); 1551.57 cm⁻¹ (N-H bend). Elemental analysis C₃₄₄H₆₈₈N₃₀O₁₆·7H₂O: C_{cal} = 73.42%; C_{exp} = 73.46%; H_{cal} = 12.57%; H_{exp} = 11.13%; N_{cal} = 7.47%; N_{exp} = 7.83%. ESI-MS: C₃₄₄H₆₈₈N₃₀O₁₆ (5501.33); m/z 2613.27 [C₁₆₁H₃₂₇N₁₇O₇ + H]⁺; m/z 1372.37 [C₈₂H₁₇₂N₁₂O₃]⁺; m/z 274.27 [C₁₄H₃₅N₅]⁺. MP: 89.3 °C-97.5 °C

N,N,N,N-tetrakis[2-(methoxycarbonyl)eth-1-yl]-1,4,8,11 tetraazacyclotetradecane (1)

Cyclam (0.0496 g, 0.248 mmol) was dissolved in MeOH (2 mL) in a 10 mL microwavable reaction vial. Methyl acrylate (1.4 mL, 0.0149 mmol) was added and the reaction was run in a microwave reactor for 15 min at 25 °C and 300 W. Excess solvent was removed under reduced pressure resulting in a clear oil. Purification was performed by recrystallization from DCM and hexane. The final product was isolated as white crystals (1.177 g, 87.25 %). ¹H NMR (300 MHz, CDCl₃): δ 1.53 (4H, quintet, H₃), 2.38-2.44 (16H, m, H₂, H₅), 2.47 (8H, s, H₁), 2.72 (8H, t, H₄, *J* = 7.2 Hz), 3.64 (12H, s, H₇) ppm. ¹³C NMR (300 MHz, CDCl₃): δ 24.1 (CH₂, C₃), 32.5 (CH₂, C₅), 50.6 (CH₂, C₄), 51.3 (CH₂, C₁), 51.3 (CH₂, C₂), 51.6 (CH₃-O, C₇), 173.3 (C=O, C₆) ppm. IR (ATR) ν = 1732.85 cm⁻¹ (C=O, ester). Elemental analysis C₂₆H₄₈N₄O₈: C_{cal} = 57.33%; C_{exp} = 57.04%; H_{cal} = 8.88%; H_{exp} = 9.29%; N_{cal} = 10.29%; N_{exp}

Chapter 2

Synthesis of Unimolecular Dendritic Micelles

= 10.44%. ESI-MS: $C_{26}H_{48}N_4O_8$ (544.68); m/z 546.4 $[m+H]^+$; m/z 273.2 $[M+2H]^{2+}$. MP: 45.0 – 50.5 °C.

N,N,N,N-tetrakis{2-[N-(2-aminoethyl)aminocarbonyl]-eth-1-yl}-1,4,8,11-tetraazacyclotetradecane (2)

1 (0.605 g, 1.11 mmol) was dissolved in MeOH (4 mL) in a Schlenk flask. Ethylenediamine (7.5 mL, 0.139 mol) was added and the reaction mixture was stirred for 4 days in the dark. The excess solvent was removed under reduced pressure resulting in a yellow oil. The crude product was stirred in diethyl ether resulting in the product, a yellow sticky solid, precipitating out. This purification process was repeated three times. The final product was dried under vacuum at 40 °C and isolated as a light yellow sticky solid (0.650 g, 90% yield). 1H -NMR (600 MHz, DMSO- d_6): δ 1.50 (4H, quintet, H_3), 2.17 (8H, t, H_5 , $J = 6.9$ Hz), 2.40 (8H, t, H_2 , $J = 6.7$ Hz), 2.43 (8H, s, H_1), 2.54 (8H, t, H_9 , $J = 6.4$ Hz), 2.59 (8H, t, H_4 , $J = 7.0$ Hz), 3.01 (8H, dd, H_8), 7.92 (4H, t, H_7 , $J = 5.3$ Hz) ppm. ^{13}C NMR (400 MHz, DMSO- d_6): δ 23.53 (C_3), 33.21 (C_5), 41.43 (C_9), 42.26 (C_8), 50.16 (C_1), 50.55 (C_2), 50.80 (C_4), 171.44 (C_6) ppm. IR (ATR) $\nu = 3292.18$ cm^{-1} (N-H stretch); 1628.77 cm^{-1} (C=O, amide); 1545.39 cm^{-1} (N-H bend). Elemental analysis $C_{30}H_{64}N_{12}O_4 \cdot 5H_2O$: $C_{cal} = 48.24\%$; $C_{exp} = 48.42\%$; $H_{cal} = 9.99\%$; $H_{exp} = 9.79\%$; $N_{cal} = 25.50\%$; $N_{exp} = 22.23\%$. ESI-MS: $C_{30}H_{64}N_{12}O_4$ (656.92); m/z 679.50 $[M+Na]^+$; m/z 657.52 $[M+H]^+$; m/z 543.45 $[C_{25}H_{54}N_{10}O_3 + H]^+$.

G 1.5 cyclam-cored dendrimer (3)

2 (0.334 g, 0.508 mmol) was dissolved in MeOH (6 mL) in a Schlenk flask. Methyl acrylate (0.46 mL, 5.08 mmol) was added and the reaction mixture was stirred for 5 days. Excess solvent was removed resulting in a golden yellow oil. Purification was performed through precipitation from DCM and hexane. The final product was isolated as a golden yellow oil (0.633 g, 92.5 %). 1H NMR (300 MHz, $CDCl_3$): δ 1.63 (4H, bt, H_3), 2.20 (16H, bs, H_5), 2.32 (8H, t, H_2 , $J = 6.9$ Hz), 2.42 (8H, t, H_{11} , $J = 6.7$ Hz), 2.47-2.55 (24H, m, H_1 , H_4 , H_9), 2.74 (16H, t, H_{10} , $J = 6.7$ Hz), 3.26 (8H, dd, H_8), 3.65 (24H, s, H_{13}), 7.23 (4H, bt, H_7 , $J = 5.20$ Hz) ppm. ^{13}C NMR (300 MHz, $CDCl_3$): δ 24.03 (CH_2 , C_3), 32.83 (CH_2 , C_{11}), 33.39 (CH_2 , C_5), 37.31 (O- CH_3 , C_{13}), 49.42 (CH_2 , C_8), 50.26 (CH_2 , C_9), 50.92-50.98 (CH_2 , C_4 , C_{10}), 51.76 (CH_2 , C_2), 53.09 (CH_2 , C_1), 172.5 (C=O, C_6), 173.1 (C=O, C_{12}). IR (ATR) $\nu = 1731.38$ cm^{-1} (C=O, ester), 1644.96 cm^{-1} (C=O, amide), 1537.42 cm^{-1} (N-H bend). Elemental analysis $C_{62}H_{112}N_{12}O_{20} \cdot 3CH_2Cl_2$: $C_{cal} = 51.78\%$; $C_{exp} = 51.44\%$; $H_{cal} = 7.87\%$; $H_{exp} = 7.32\%$; $N_{cal} =$

Chapter 2

Synthesis of Unimolecular Dendritic Micelles

11.41%; $N_{\text{exp}} = 11.95\%$. ESI-MS: $C_{62}H_{112}N_{12}O_{20}$ (1345.62); m/z 1367.78 $[M+Na]^+$; m/z 1345.80 $[M+H]^+$; m/z 673.41 $[M+2H]^{2+}$.

G2 cyclam-cored dendrimer (4)

3 (0.633 g, 0.470 mmol) was dissolved in MeOH (4 mL) and added to a Schlenk flask. Ethylenediamine (0.75 mL, 0.0112 mol) was added and the reaction was stirred for 5 days in the dark at room temperature. Excess solvent and ethylenediamine was removed under reduced pressure and the resulting yellow oil was purified by precipitation from MeOH and diethyl ether. Further purification was performed by stirring the resulting product in diethyl ether. This was repeated three times. The final product was dried under vacuum at 40 °C and isolated as a light yellow sticky oil (0.660 g, 89.31%). $^1\text{H-NMR}$ (600 MHz, $\text{DMSO-}d_6$): δ 1.49 (4H, bs, H_3), 2.19 (24H, t, H_5 , H_{11} , $J = 6.29$ Hz), 2.42 (16H, bm, H_1 , H_2), 2.52-2.59 (40H, m, H_9 , H_{15} , H_{16}), 2.64 (24H, t, H_4 , H_{10} , $J = 6.9$ Hz), 3.01-3.08 (24H, m, H_8 , H_{14}), 7.91(4H, s, H_7), 7.92 (8H, s, H_{13}) ppm. $^{13}\text{C NMR}$ (400 MHz, $\text{DMSO-}d_6$): δ 23.52 ($\text{CH}_2\text{-CH}_2\text{-CH}_2$, C_3), 33.09 (NHCO-CH_2 , C_5), 33.39 (NHCO-CH_2 , C_{11}), 41.32 ($\text{CH}_2\text{-N-(CH}_2)_2$, C_9), 42.21 ($\text{CH}_2\text{-NHCO}$, C_8), 49.78 ($\text{CH}_2\text{-NHCO}$, C_{14}), 49.96 ($\text{CH}_2\text{-NH}_2$, C_{15}), 50.02 ($\text{N-CH}_2\text{-CH}_2\text{-N}$, C_1), 50.48 ($\text{N-CH}_2\text{-CH}_2\text{-CH}_2\text{-N}$, C_2), 50.73 (N-CH_2 , C_4), 52.34 ($\text{CH}_2\text{-N-(CH}_2)_2$, C_{10}), 171.56 (C=O , C_6), 171.62 (C=O , C_{12}) ppm. IR (ATR) $\nu = 1633.01\text{cm}^{-1}$ (C=O amide), 1538.96cm^{-1} (C=O ester). Elemental analysis $C_{70}H_{144}N_{28}O_{12}\cdot 13\text{H}_2\text{O}$: $C_{\text{cal}} = 46.60\%$; $C_{\text{exp}} = 46.68\%$; $H_{\text{cal}} = 9.50\%$; $H_{\text{exp}} = 9.40\%$; $N_{\text{cal}} = 21.74\%$; $N_{\text{exp}} = 21.86\%$. ESI-MS: $C_{70}H_{144}N_{28}O_{12}$ (1570.07); m/z 1570.1 (mol. Ion); 785.6 $[M+2H]^{2+}$; 524.1 $[M+3H]^{3+}$.

G1 Cyclam-dendr-(palmitoyl)₄ (5)

2 (0.450 g, 0.685 mmol) was completely dissolved in MeOH (20 mL) followed by the addition of Et_3N (1.4 mL). Palmitoyl chloride (1.1 mL, 3.63 mmol) was added slowly and the reaction mixture was stirred for 3 days at room temperature. Excess solvent was removed under reduced pressure resulting in the formation of a white solid. To remove the excess palmitoyl chloride diethyl ether (30 mL) was added and the reaction was heated under reflux for 2 hours followed by filtration. To the residue was added $\text{Na}_2\text{CO}_3\cdot 10\text{H}_2\text{O}$ (0.543 g) in H_2O (30 mL). The mixture was heated under reflux overnight and filtered, removing residual ammonium salts and deprotonating the dendrimer. The final product was dried under vacuum and isolated as a cream coloured solid (0.851 g, 77.14 %). $^1\text{H-NMR}$ (300 MHz, CDCl_3): δ 0.87 (12H, t, CH_3 , $J = 6.8$ Hz), 1.25 (96H, s, $\text{CH}_2\text{-CH}_3 + \text{CH}_2\text{-CH}_2\text{-CH}_2$), 1.60 (bt, H_3), 2.16

Chapter 2

Synthesis of Unimolecular Dendritic Micelles

(dt, NHCO-CH₂, H₅), 2.28 – 2.34 (m, NHCO-CH₂-CH₂), 2.46 (8H, bt, H₂), 2.53 (8H, s, H₁), 2.69 (8H, t, H₄, $J = 5.7$ Hz), 3.28-3.39 (16H, bs, CH₂-NHCO), 6.18 (2H, s, NHCO), 6.78 (2H, s, NHCO), 8.02 (4H, s, NHCO). ¹³C NMR (300 MHz, CDCl₃): δ 14.27 (CH₃), 22.85 (CH₂-CH₃), 25.12 (NHCO-CH₂-CH₂), 25.88 (N-CH₂-CH₂-CONH), 25.97 (N-CH₂-CH₂-CH₂-N), 29.31-29.86 (CH₂-(CH₂)_n-CH₂), 32.08 (CH₂-CH₂-CH₃), 34.28 (NHCO-CH₂), 36.90 (CH₂-NHCO), 36.93 (CH₂-NHCO), 40.37 (N-CH₂-CH₂-CH₂-N), 51.59 (C₁), 174.69 (NHCO) ppm. IR (ATR): ν = 3295.02 (N-H amide stretch), 3078.36 (sec. amide), 2915.69 (C-H sat.), 1632.96 (C=O amide), 1549.54 (N-H bend). Elemental analysis C₉₄H₁₈₄N₁₂O₈·0.5H₂O·0.5C₄H₁₀O: C_{cal} = 69.60%; C_{exp} = 69.68 %; H_{cal} 11.56%; H_{exp} = 10.81%; N_{cal} = 10.15%; N_{exp} = 9.82%. ESI-MS: C₉₄H₁₈₄N₁₂O₈ (1610.54); m/z 1611.99 (mol. Ion); m/z 1258.14 [C₇₃H₁₄₄N₁₀O₆ + H]⁺; m/z 1074.06 [C₆₀H₁₁₈N₁₀O₆ + H]⁺; m/z 537.46 [M+3H]³⁺; m/z 559.52 [M+Na]³⁺. MP: decomposes at 200°C.

G2 Cyclam-dendr-(palmitoyl)₈ (6)

4 (0.635 g, 0.404 mmol) was completely dissolved in MeOH (20 mL). Et₃N (1.65 mL) was added followed by the dropwise addition of palmitoyl chloride (1.1 mL, 3.64 mmol). The reaction mixture was stirred for 3 days at R.T. Excess solvent was removed resulting in a yellow solid. To remove the excess palmitoyl chloride the yellow solid was refluxed for 1 hour in diethyl ether (30 mL) and filtered. Na₂CO₃ (0.496 g) and H₂O (30 mL) was added and the mixture was refluxed overnight to remove residual ammonium salts and deprotonate the dendrimer followed by filtration. The final product was dried under vacuum and isolated as a cream coloured solid (1.212 g, 86.2%). ¹H-NMR (300 MHz, CDCl₃): δ 0.87 (24H, t, CH₃, $J = 6.6$ Hz), 1.24 (s, CH₂-CH₃ + CH₂-CH₂-CH₂), 1.58 (4H, bs, H₃), 2.17 (8H, t, H₅, $J = 6.5$ Hz), 2.28-2.51 (m, CH₂-N-(CH₂)₂ + CH₂-N-(CH₂)₂), 2.71 (8H, bs, H₄), 3.23 (bs, CH₂-NHCO), 3.33 (bs, CH₂-NHCO), 7.29 (8H, bs, NHCO), 7.79 (8H, bs, NHCO), 8.01 (4H, bs, NHCO) ppm. ¹³C NMR (300 MHz, CDCl₃): δ 14.27 (CH₃), 22.84 (CH₂-CH₃), 25.11 (NHCO-CH₂-CH₂), 25.88 (N-CH₂-CH₂-CONH), 26.01 (N-CH₂-CH₂-CH₂-N), 29.30-29.88 (CH₂-(CH₂)_n-CH₂), 32.08 (CH₂-CH₂-CH₃), 34.28 (NHCO-CH₂), 36.79 (CH₂-NHCO), 36.89 (CH₂-NHCO), 39.54 (CH₂-NHCO), 39.78 (N-CH₂-CH₂-CH₂-N), 50.85 (CH₂-N-(CH₂)₂ + CH₂-N-(CH₂)₂), 51.58 (C₁), 173.62 (NHCO), 174.51 (NHCO), 174.69 (NHCO) ppm. IR (ATR): ν = 3290.83 (N-H amide stretch), 3083.13 (sec. amide), 2915.05 (C-H sat.), 1634.20 (C=O amide), 1548.91 (N-H bend). Elemental analysis C₁₉₈H₃₈₄N₂₈O₂₀·2H₂O·CH₂Cl₂: C_{cal} =

Chapter 2

Synthesis of Unimolecular Dendritic Micelles

66.42%; $C_{\text{exp}} = 66.15\%$; $H_{\text{cal}} = 10.92\%$; $H_{\text{exp}} = 11.40\%$; $N_{\text{cal}} = 10.90\%$; $N_{\text{exp}} = 11.17\%$; MP: 153–170 °C.

2.6. References

1. Y. Chevalier, T. Zemb, *Rep. Prog. Phys.*, **53** (1990) 279
2. M. Liu, K. Kono, J. M. J. Fréchet, *Journal of Controlled Release*, **65** (2000) 121
3. S. Stevelmans, J. C. M. van Hest, J. F. G. A. Jansen, D. A. F. J. van Boxtel, E. M. M. de Brabander-van den Berg, E. W. Meijer, *J. Am. Chem. Soc.*, **118** (1996) 7398
4. M. R. Knecht, J. C. Garcia-Martinez, R. M. Crooks, *Langmuir*, **21** (2005) 11981
5. O. Enoki, T. Imaoka, K. Yamamoto, *Org. Lett.*, **5** (2003) 2547
6. C. Saudan, V. Balzani, P. Ceroni, M. Gorka, M. Maestri, V. Vicinelli, F. Vögtle, *Tetrahedron*, **59** (2003) 3845
7. R. Malgas-Enus, S. F. Mapolie, *Polyhedron*, **47** (2012) 87
8. L. Fabbrizzi, M. Licchelli, P. Pallavicini, D. Sacchi, *Supramol. Chem.*, **13** (2001) 569
9. G. Bergamini, A. Sottilotta, M. Maestri, P. Ceroni, F. Vögtle, *Chem. Asian J.*, **5** (2010) 1884
10. P. Sudik, A. Białońska, S. Wołowicz, *Polyhedron*, **30** (2011) 873
11. H. Stephan, G. Geipel, D. Appelhans, G. Bernhard, D. Tabuani, H. Komber, B. Voit, *Tetrahedron Letters*, **46** (2005) 3209

Chapter 3: Encapsulation of Gold Nanoparticles in Dendritic Micelles

3.1. Introduction

The hydrophobic dendritic micelles discussed in the previous chapter were prepared with the idea of applying them as templates for the encapsulation of gold nanoparticles. As mentioned earlier, when considering the stabilization of nanoparticles it is desirable to use a method that can assist with the nanoparticle formation without reducing the surface area of the particles. The stabilizing agent should also aid the formation of well dispersed particles with a narrow particle size distribution.

Dendrimers are well suited for this purpose. They provide a means of stabilization without reducing the surface area of the nanoparticles, while at the same time assisting with the formation of small, well distributed nanoparticles. Modification of these dendrimers could result in property changes which can be advantageous when used as templates for nanoparticle growth.^[1] The modification of hydrophilic amine-terminated dendrimers with hydrophobic groups on the periphery results in the formation of unimolecular dendritic micelles containing a hydrophilic interior and a hydrophobic exterior. This specific property makes it possible to prepare the dendrimer encapsulated nanoparticles in organic solvents.

3.2. UV/Vis binding study

When considering the preparation of dendrimer encapsulated nanoparticles (DENs) it is important to establish the maximum loading capacity of the dendrimer host. This can be determined by a spectrophotometric titration binding study. The maximum amount of metal ions that can interact with interior functional groups, such as tertiary amines, is largely generation dependent. Crooks *et al*^[2] determined through such a study that hydroxide-terminated G4 PAMAM dendrimers, containing 62 interior tertiary amines, can absorb up to 16 Cu²⁺ ions that primarily binds to outermost tertiary amines. On the other hand, amine-terminated G4 PAMAM dendrimers show a maximum loading of 36 Cu²⁺ ions with binding occurring primarily through the terminal amines. If the maximum loading

Chapter 3

Encapsulation of Gold Nanoparticles in Dendritic Micelles

threshold is exceeded the metal reduction step will result in the formation of nanoparticles on the outside of the dendritic template, i.e. dendrimer stabilized nanoparticles (DSNs).

Unlike Cu^{2+} ions AuCl_4^- ions do not interact with dendrimers in a fixed stoichiometric ratio.^[3] It is also possible to reduce gold ions to metallic gold under spectrophotometric conditions.^[4] Taking this into account it was decided to perform the spectrophotometric titration using CuCl_2 .

Niu and Crooks^[5] performed this study using generation 3-5 palmitoyl modified DAB PPI dendritic micelles and CuCl_2 . They determined that the maximum loading capacity of these unimolecular dendritic micelles is higher than those determined for the PPI/ Cu^{2+} and PAMAM/ Cu^{2+} complexes. In the normal dendrimer systems the interaction between Cu^{2+} and the dendrimer occurs through interactions with the nitrogen-containing functional groups in the dendrimer interior or on the periphery. In the case of PPI dendrimers this interaction is usually limited to the peripheral amine groups. The palmitoyl modified PPI dendritic micelles only contain interior amines and outer amides and thus it is unlikely that the driving force for encapsulation is the interaction with these nitrogen containing functional groups. Taking all of this into account the authors suggested that the driving force for encapsulation is the difference in the solubilisation capacity of the interior of the dendrimer versus that of the solvent used. Since the authors only did this study with generation 3-5 modified dendrimers it was thus necessary to repeat the study with the low molecular weight generation 1 and 2 analogues that we had synthesized.

A spectrophotometric titration binding study was conducted by the addition of 10 μL aliquots of the metal salt solution to a quartz cuvette containing the dendrimer (1.6 mL, 1×10^{-4} M), CHCl_3 (0.8 mL) and MeOH (0.6 mL). The absorption spectrum was recorded after each 10 μL addition. The absorbance recorded at 835 nm was then plotted against the Cu^{2+} /dendrimer ratio present for each experiment (Figure 3.2-1, Figure 3.2-2, Figure 3.2-3).

The maximum loading is indicated by a change in the slope of the graph. The results obtained by this study indicate that the maximum loading is reached at a Cu^{2+} /dendrimer ratio of 12, 21 and 35 for the generation 1, 2 and 3 palmitoyl modified dendrimers respectively. These amounts are significantly higher than the amount of amines present in the dendrimer interior. This then compares well with the results obtained by Niu and Crooks indicating that a

Chapter 3

Encapsulation of Gold Nanoparticles in Dendritic Micelles

difference in solubility of the metal ions in the dendrimer interior versus that in the solvent is the driving force for metal encapsulation.

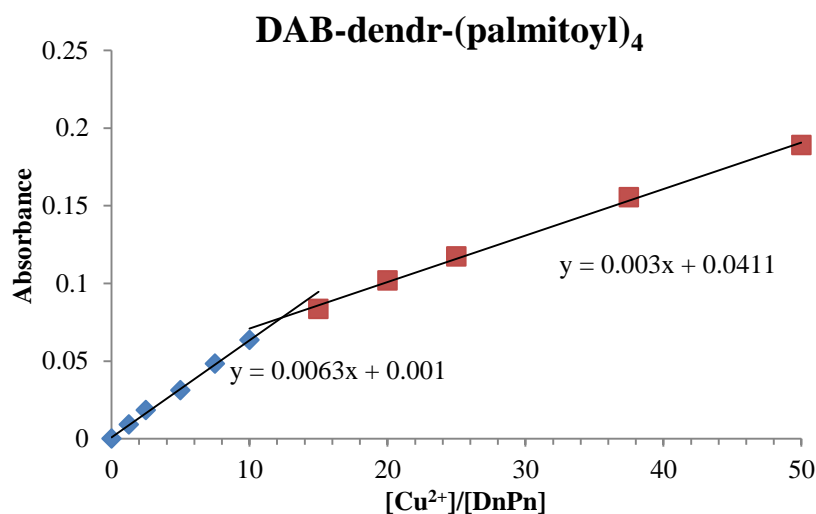


Figure 3.2-1: UV/Vis titration binding study results for DAB-dendr-(palmitoyl)₄ measured at 835 nm

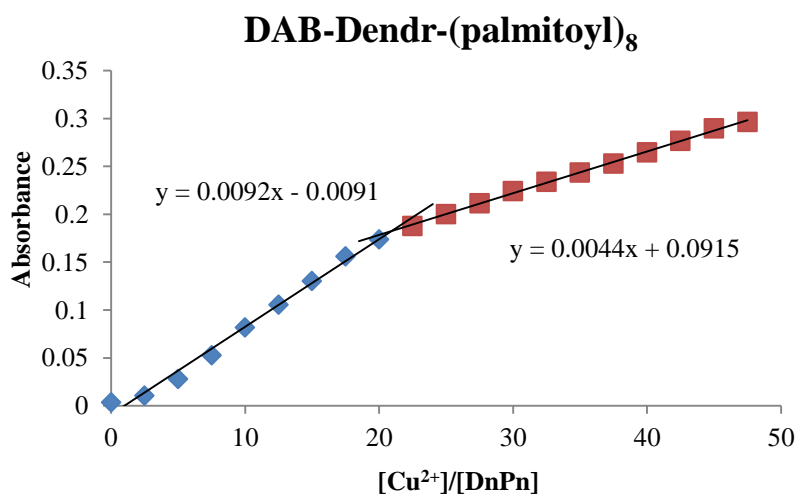


Figure 3.2-2: UV/Vis titration binding study results for DAB-dendr-(palmitoyl)₈ measured at 835 nm

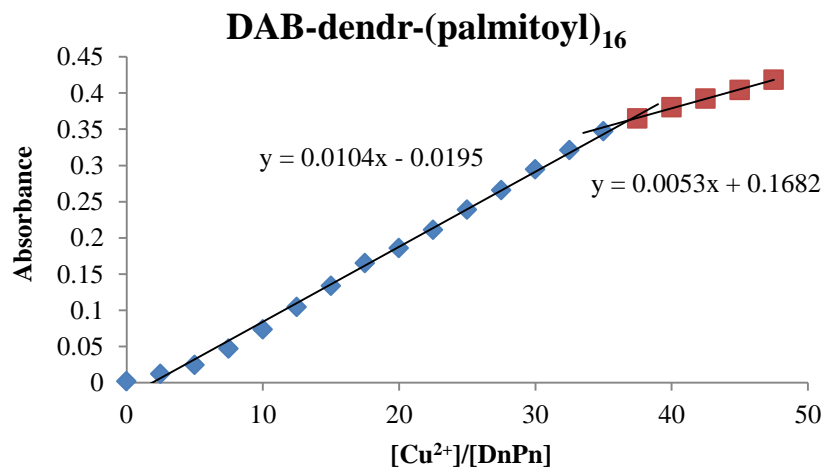


Figure 3.2-3: UV/Vis titration binding study results for DAB-dendr-(palmitoyl)₁₆ measured at 835 nm

Chapter 3

Encapsulation of Gold Nanoparticles in Dendritic Micelles

These studies were also performed using the generation 1 and 2 hydrophobic cyclam-cored dendritic micelles synthesized. Interestingly when performing the spectrophotometric titration binding studies with these cyclam-cored dendrimers no change in slope was observed up to Cu^{2+} /dendrimer ratio of 50. The maximum ratio was then increased to 250 by adding 50 μL aliquots of CuCl_2 instead of 10 μL .

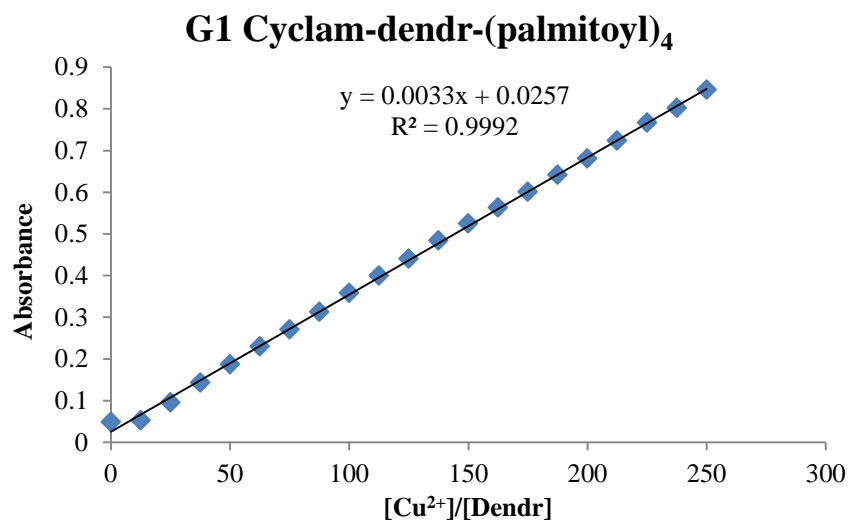


Figure 3.2-4: UV/Vis titration binding study results for Cyclam-dendr-(palmitoyl)₄ measured at 835 nm

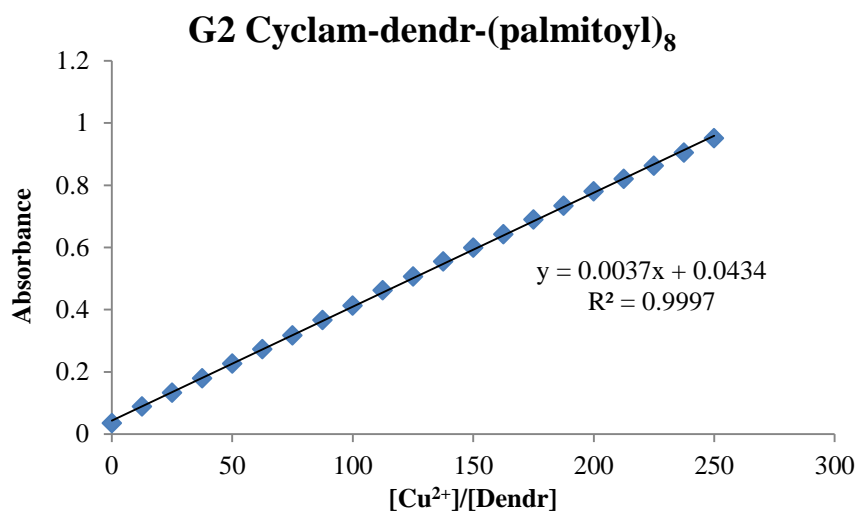


Figure 3.2-5: UV/Vis titration binding study results for Cyclam-dendr-(palmitoyl)₈ measured at 835 nm

Again no change in slope was detected for either of the cyclam based dendrimer hosts. These results thus indicates that the cyclam-cored hydrophobic dendrimers do not have a maximum loading endpoint in the range tested and thus no complexation occurs between the interior amine groups and the Cu^{2+} ions. This result also corresponds with the solubility driven encapsulation theory proposed by Niu and Crooks. The data indicate that no stoichiometric

correlation exists between the amount of metal ions that can be encapsulated within these dendrimer hosts and the tertiary amine functionalities present in the dendrimer interior. A difference in the three dimensional shape of the cyclam-cored hydrophobic dendritic micelles versus that of the DAB PPI hydrophobic dendritic micelles could be the reason for the difference between the results of the two types of dendrimers. Further studies into this phenomenon are however needed to fully confirm this conclusion.

3.3. Encapsulation of Au nanoparticles in dendritic micelles

Using dendrimers as templates for the formation of nanoparticles provides the possibility of preparing nanoparticles of specific cluster sizes. Certain cluster sizes containing full outer shells are considered to be more stable than others. These cluster sizes include M_{13} , M_{55} , M_{147} , M_{309} , M_{561} etc. and are the so-called magic numbers. The clusters are formed by the gradual surrounding of a core atom with a full shell of atoms.^[6]

For this study we focused on the formation of Au_{13} , Au_{31} and Au_{55} nanoparticle clusters. Au_{31} , not being a magic number, was chosen to highlight the difference, if any, of magic numbers against non-magic number cluster sizes when considering stability and application in catalysis.

3.3.1. Method

To encapsulate metal nanoparticles in dendrimer hosts (Figure 3.3-1) the metal salt is reacted with the dendrimer in the desired mole ratio. The mole ratio of dendrimer to metal is adjusted according to the desired cluster size. For example when Au_{55} is desired, a dendrimer to metal ratio of 1:55 is used. The metal ions are then reduced to zero valent metal nanoparticle clusters by the addition of a strong reducing agent.

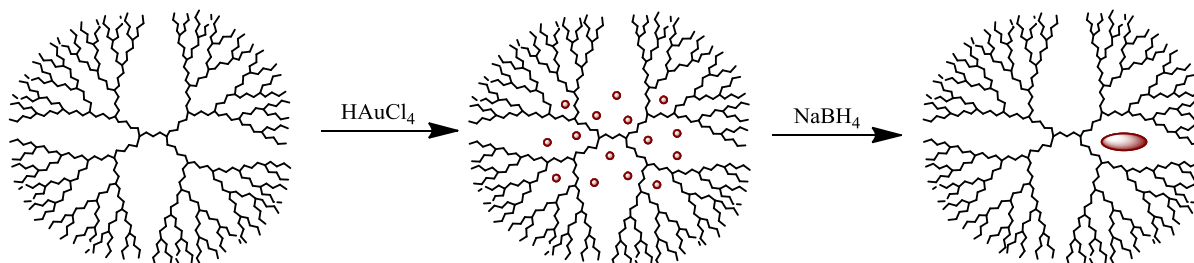


Figure 3.3-1: General method for the preparation of dendrimer encapsulated Au nanoparticles

Chapter 3

Encapsulation of Gold Nanoparticles in Dendritic Micelles

To form the dendritic micelle encapsulated gold nanoparticles a predetermined volume of a HAuCl_4 stock solution of known concentration was added to the dendrimer dissolved in CHCl_3 . A colour change from clear to golden yellow is immediately observed. The mixture is stirred for 5 minutes to allow the dendrimer to interact completely with the metal ions. The reducing agent, NaBH_4 , completely dissolved in MeOH is added dropwise to the mixture. Controlling the rate of addition of the reducing agent is crucial. If the reducing agent is added too fast it will lead to the formation of larger particles and the potential aggregation. The addition of the reducing agent causes an immediate colour change. The colour of the nanoparticle solution gives an idea of the size and morphology of the clusters formed. For spherical Au nanoparticles the colour of the solution is usually in the range of yellow, red and blue. A darker colour usually points to an increase in particle size.^[7] After the addition of NaBH_4 a colour change from golden yellow to dark maroon red, in some cases purple or black, was observed.

3.3.2. Characterization

The characterization of DENs is usually performed by UV/Vis spectroscopy and HR-TEM. If the nanoparticle formation is successful the UV/Vis spectrum will show a systematic increase in absorbance with a decrease in wavelength. Gold nanoparticles also show a characteristic surface plasmon resonance band at around 520 nm that indicates that the particles are larger than 2 nm in size.^[8] The HR-TEM analysis provides insight into the size and distribution of the metal nanoparticles. The average particle size can be determined from the TEM images by the use of ImageJ software. A predetermined amount of particles are counted to give the average particle size.

3.3.2.1. Au_{13} Dendrimer Encapsulated Nanoparticles

Au_{13} nanoparticles were encapsulated in the G1 and 2 cyclam-cored hydrophobic dendrimers and the G1, 2 and 3 hydrophobic DAB PPI dendrimers. UV/Vis spectroscopic characterization indicated that the encapsulation process was successful (Figure 3.3-2).

In each case the spectrum shows the expected systematic increase in absorbance with a decrease in wavelength indicating the presence of metal nanoparticles. Furthermore an absorbance in the range of 520 nm, the surface plasmon resonance of gold, indicates that the particles are larger than 2 nm in size. A larger absorbance and shift to longer wavelengths tend to indicate larger particles.

Chapter 3

Encapsulation of Gold Nanoparticles in Dendritic Micelles

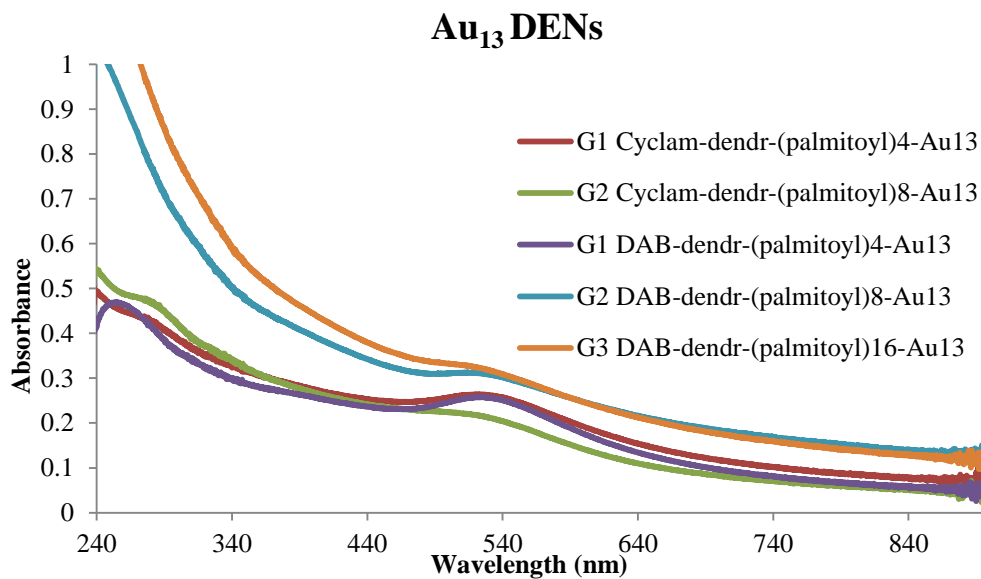


Figure 3.3-2: UV/Vis spectrum of Au₁₃ DENs

The HR-TEM images (Figure 3.3-3, Figure 3.3-4) for the G1 and 2 hydrophobic cyclam-cored dendrimer encapsulated Au₁₃ nanoparticles show well dispersed particles with little aggregation.

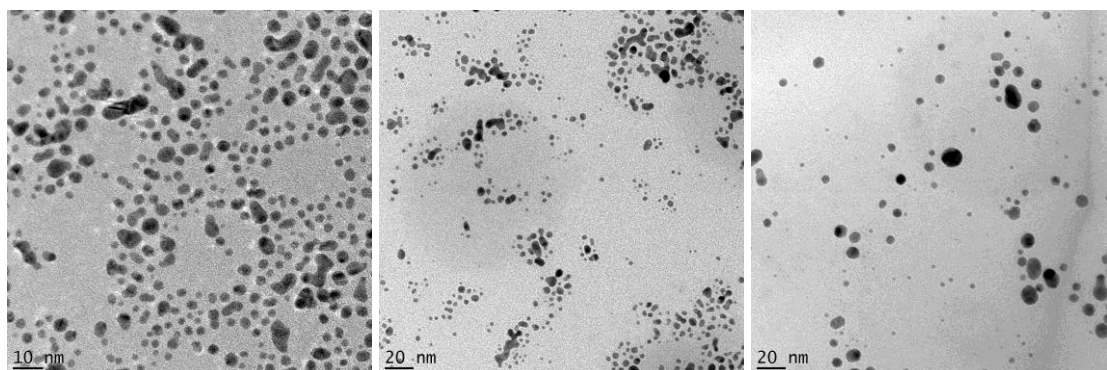


Figure 3.3-3: HR-TEM images of G1 Cyclam-dendr-(palmitoyl)₄-Au₁₃

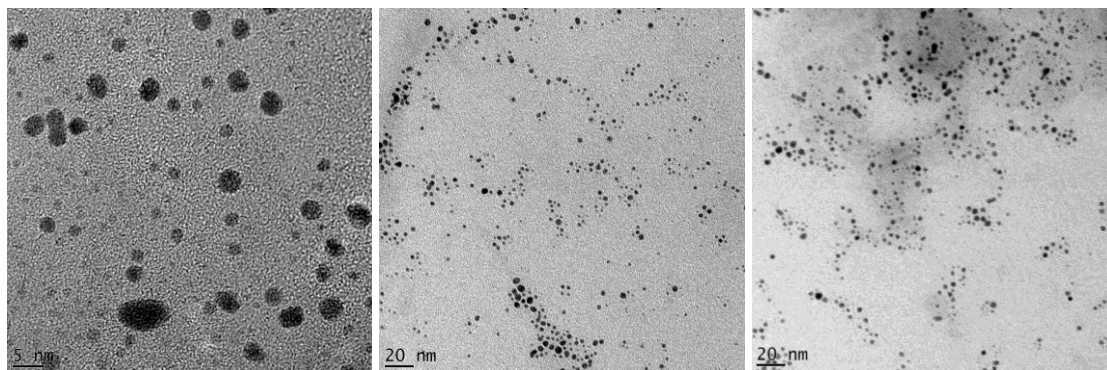


Figure 3.3-4: HR-TEM images of G2 Cyclam-dendr-(palmitoyl)₈-Au₁₃

Chapter 3

Encapsulation of Gold Nanoparticles in Dendritic Micelles

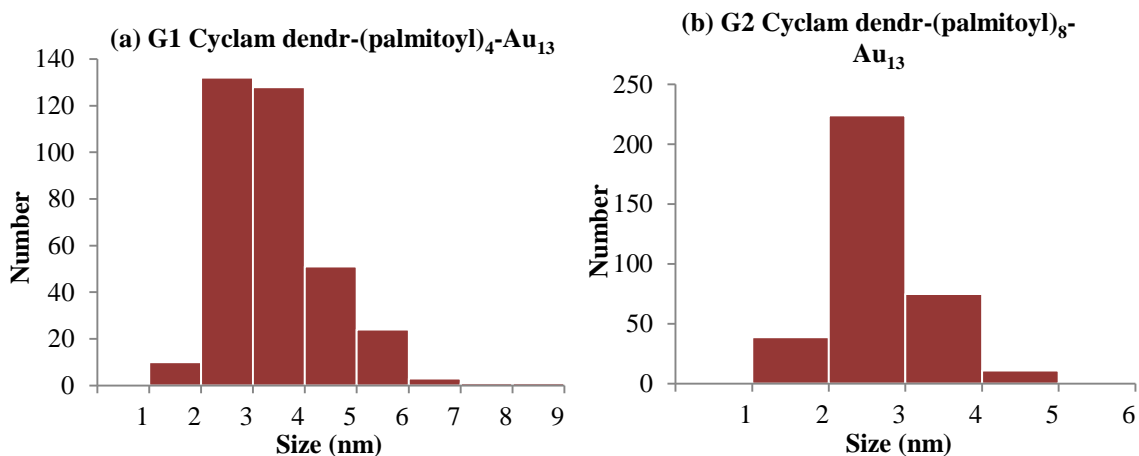


Figure 3.3-5: Particle size distribution (a) Average particle size: 3.41 ± 1.03 nm ; Max: 8.44 nm; Min: 1.45 nm (b) Average particle size: 2.66 ± 0.589 nm; Max: 5.03 nm; Min: 1.43 nm

The average particle size achieved with each dendrimer is 3.41 ± 1.03 nm for the G1 dendrimer and 2.66 ± 0.589 nm for the G2 dendrimer. The particle size distribution is relatively narrow in both cases although the G2 dendrimer results in the narrowest particle size distribution and average particle size. From this data it can be concluded that the G2 cyclam-cored dendrimer provides the best support for nanoparticle formation. This result is expected as this dendrimer is larger, more branched and possibly more spherical and so would potentially be a better template and host for the particles compared to its G1 counterpart.

A comparison between the G1, 2 and 3 hydrophobic DAB dendrimer encapsulated Au₁₃ nanoparticles reveals that the G1 dendrimer by far produces the narrowest size distribution and average particle size.

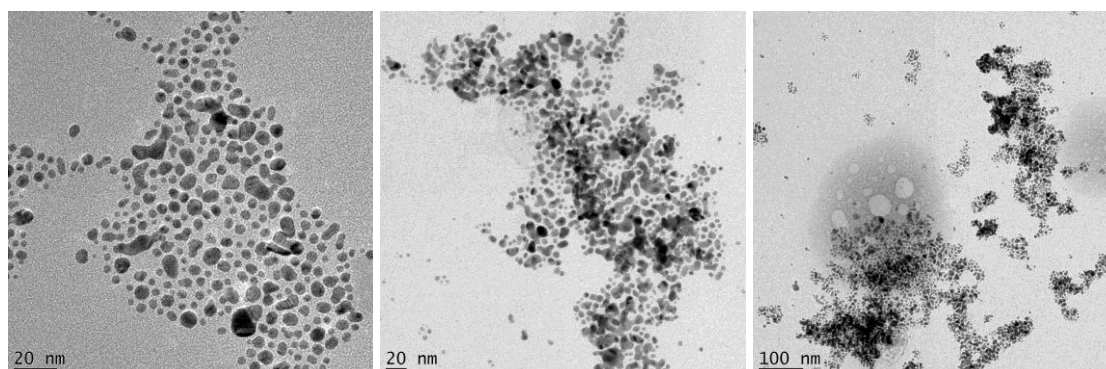


Figure 3.3-6: HR-TEM images of G1 DAB-dendr-(palmitoyl)₄-Au₁₃

Chapter 3

Encapsulation of Gold Nanoparticles in Dendritic Micelles

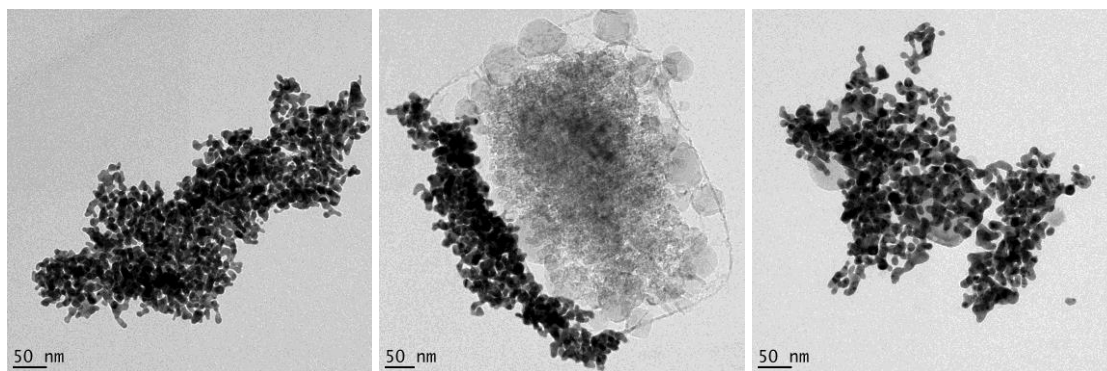


Figure 3.3-7: HR-TEM images of G2 DAB-dendr-(palmitoyl)₈-Au₁₃

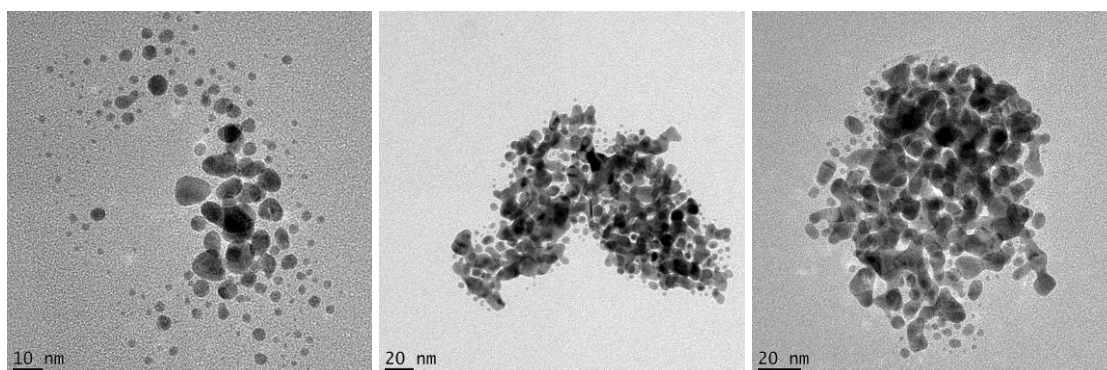


Figure 3.3-8: HR-TEM images of G3 DAB-dendr-(palmitoyl)₁₆-Au₁₃

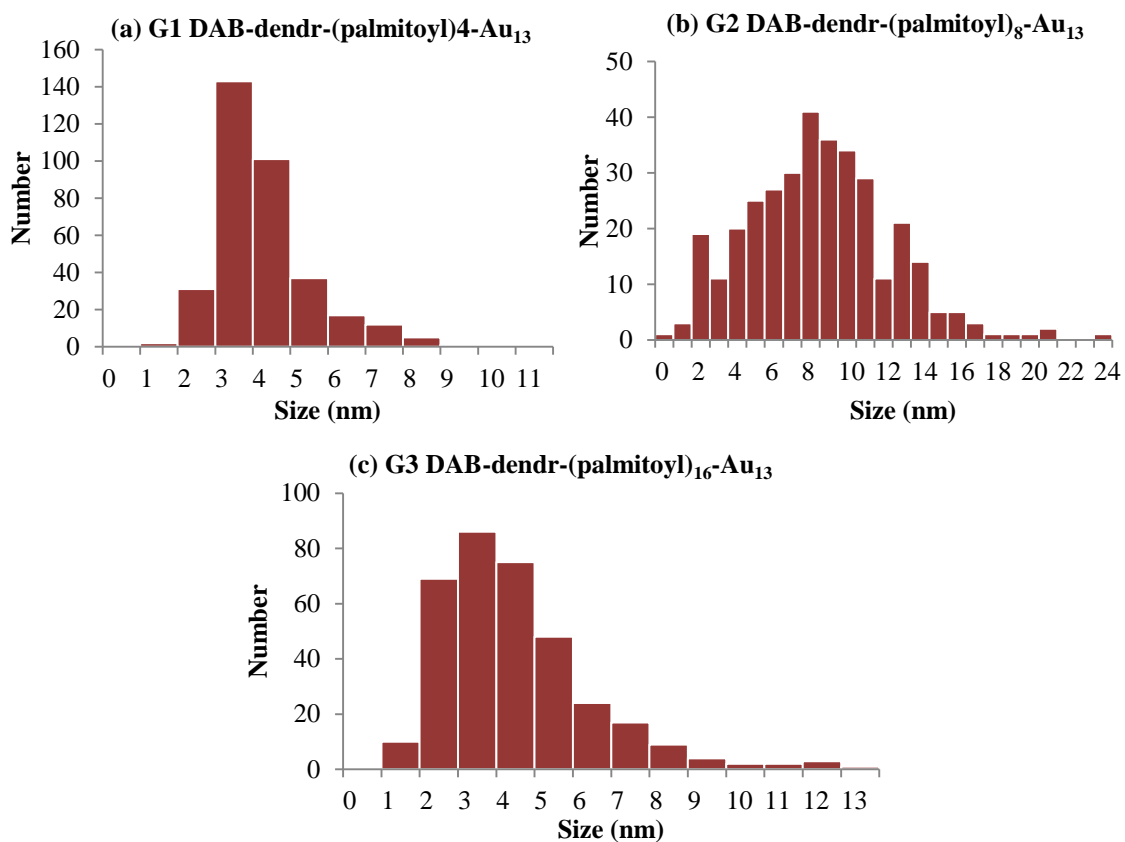


Figure 3.3-9: Particle distribution (a) 4.26 ± 1.31 nm; Max: 11.11 nm; Min: 1.79 nm (b) 8.98 ± 3.87 nm; Max: 24.82 nm; Min: 1.71 nm (c) 4.54 ± 2.02 nm; Max: 13.49 nm; Min: 1.62 nm

Chapter 3

Encapsulation of Gold Nanoparticles in Dendritic Micelles

The HR-TEM results (Figure 3.3-6, Figure 3.3-7, Figure 3.3-8) show some aggregation in all three cases but by far the G2 dendrimer results in the largest amount of aggregation. This dendrimer results in a very wide particle size distribution with a maximum particle size of 24.82 nm, a minimum particle size of 1.71 nm and an average particle size of 8.98 nm. The average particle size is almost double that of the nanoparticles encapsulated in the generation 1 and 3 variations.

Comparing the hydrophobic cyclam-cored dendrimers to the hydrophobic DAB dendrimers leads to a conclusion that the cyclam-cored dendrimers are better hosts for the encapsulation of Au₁₃ nanoparticles. The cyclam-cored dendrimers leads to much smaller size distributions as well as average particle sizes and little aggregation is observed.

3.3.2.2. Au₃₁ Dendrimer Encapsulated Nanoparticles

To get an idea of the difference in stability and size between cluster sizes considered as ‘magic numbers’ and those that do not fall into the category of ‘magic numbers’ Au₃₁ nanoparticles were encapsulated in the G1 and 2 hydrophobic cyclam-cored dendrimers as well as the G1, 2 and 3 hydrophobic DAB dendrimers.

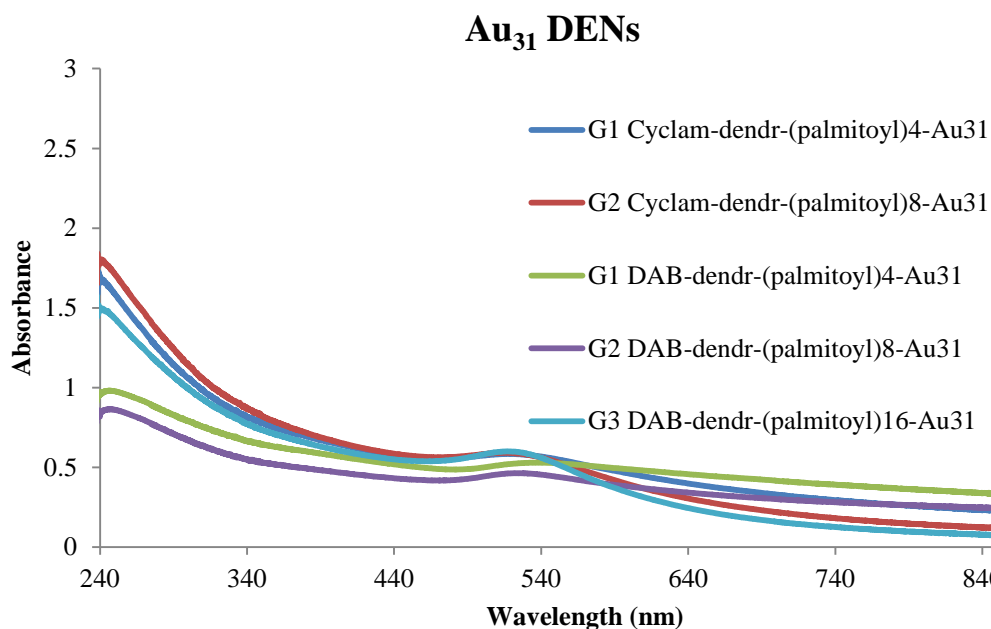


Figure 3.3-10: UV/Vis spectrum of Au₃₁ DENs

UV-Vis spectra (Figure 3.3-10) of the Au₃₁ DENs indicate the presence of the characteristic plasmon band at around 520 nm providing proof of nanoparticle formation. The presence of the surface plasmon resonance band also indicates particles larger than 2 nm in size.

Chapter 3

Encapsulation of Gold Nanoparticles in Dendritic Micelles

The HR-TEM results (Figure 3.3-11, Figure 3.3-12) of the G1 and 2 hydrophobic cyclam-cored dendrimer encapsulated Au₃₁ nanoparticles indicate a relatively large size distribution and some aggregation of particles.

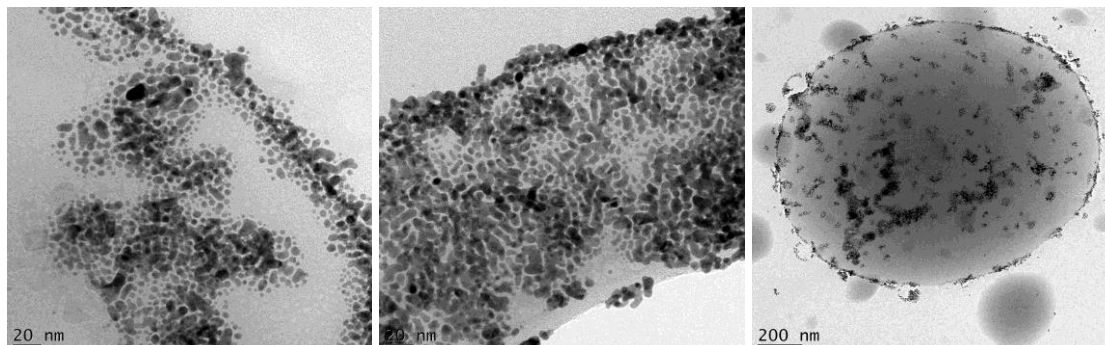


Figure 3.3-11: HR-TEM images of G1 Cyclam-dendr-(palmitoyl)₄-Au₃₁

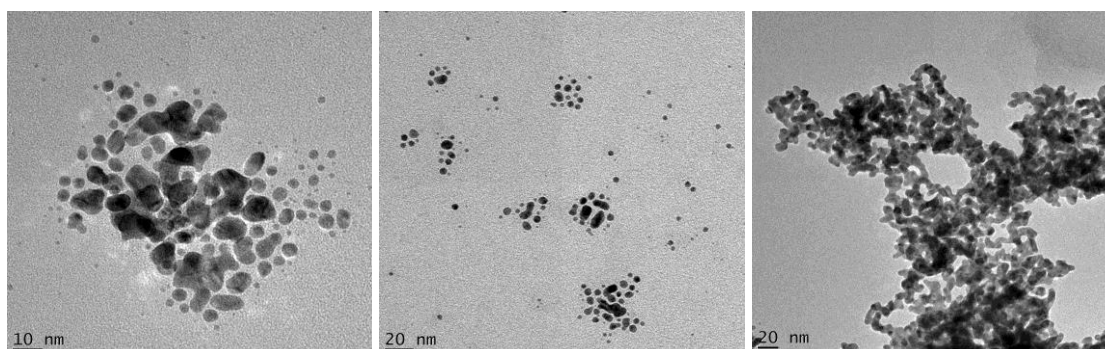


Figure 3.3-12: HR-TEM images of G2 Cyclam-dendr-(palmitoyl)₈-Au₃₁

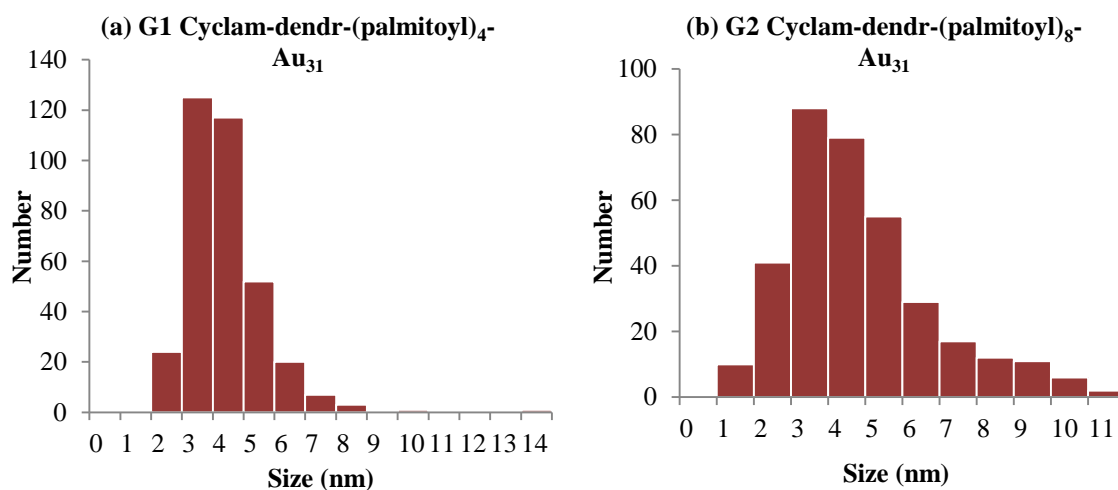


Figure 3.3-13: Particle distribution (a) Average particle size: 4.41 ± 1.31 nm; Min: 2.33 nm; Max: 14.43 nm (b) Average particles size: 4.83 ± 2.00 nm; Min: 1.36 nm; Max: 11.93 nm

The average particle size for both generations are similar with the G1 dendrimer resulting in an average particle size of 4.41 nm and the generation 2 dendrimer resulting in an average

Chapter 3

Encapsulation of Gold Nanoparticles in Dendritic Micelles

particle size of 4.83 nm. A wider size distribution is however observed for the generation 2 dendrimer.

The HR-TEM results (Figure 3.3-16) reveal that the G3 hydrophobic DAB dendrimer produces particles with the smallest size distribution. This is clearly visible in the TEM images. In comparison the TEM images of the G1 and 2 variations (Figure 3.3-14, Figure 3.3-15) show some aggregation and a much wider size distribution.

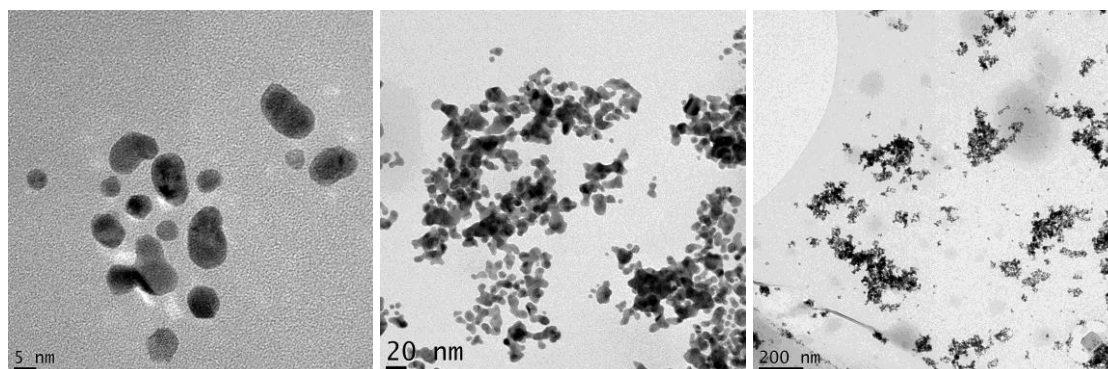


Figure 3.3-14: HR-TEM images of G1 DAB-dendr-(palmitoyl)₄-Au₃₁

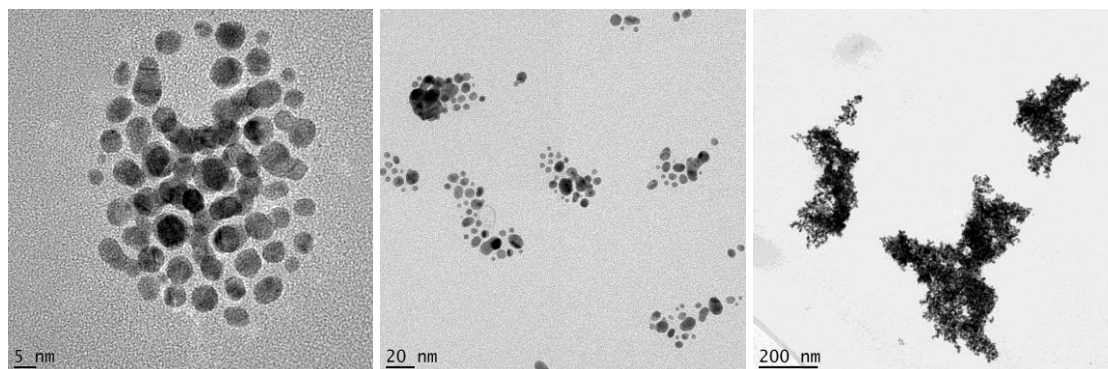


Figure 3.3-15: HR-TEM images of G2 DAB-dendr-(palmitoyl)₈-Au₃₁

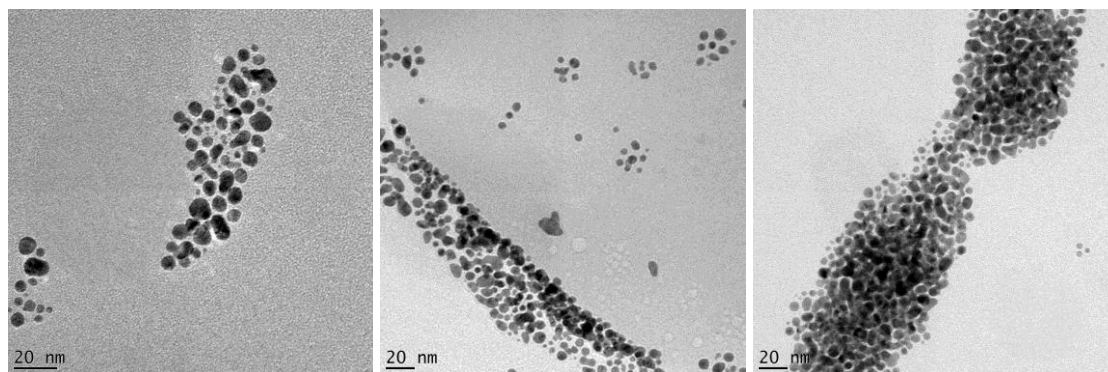


Figure 3.3-16: HR-TEM images of G3 DAB-dendr-(palmitoyl)₁₆-Au₃₁

Chapter 3

Encapsulation of Gold Nanoparticles in Dendritic Micelles

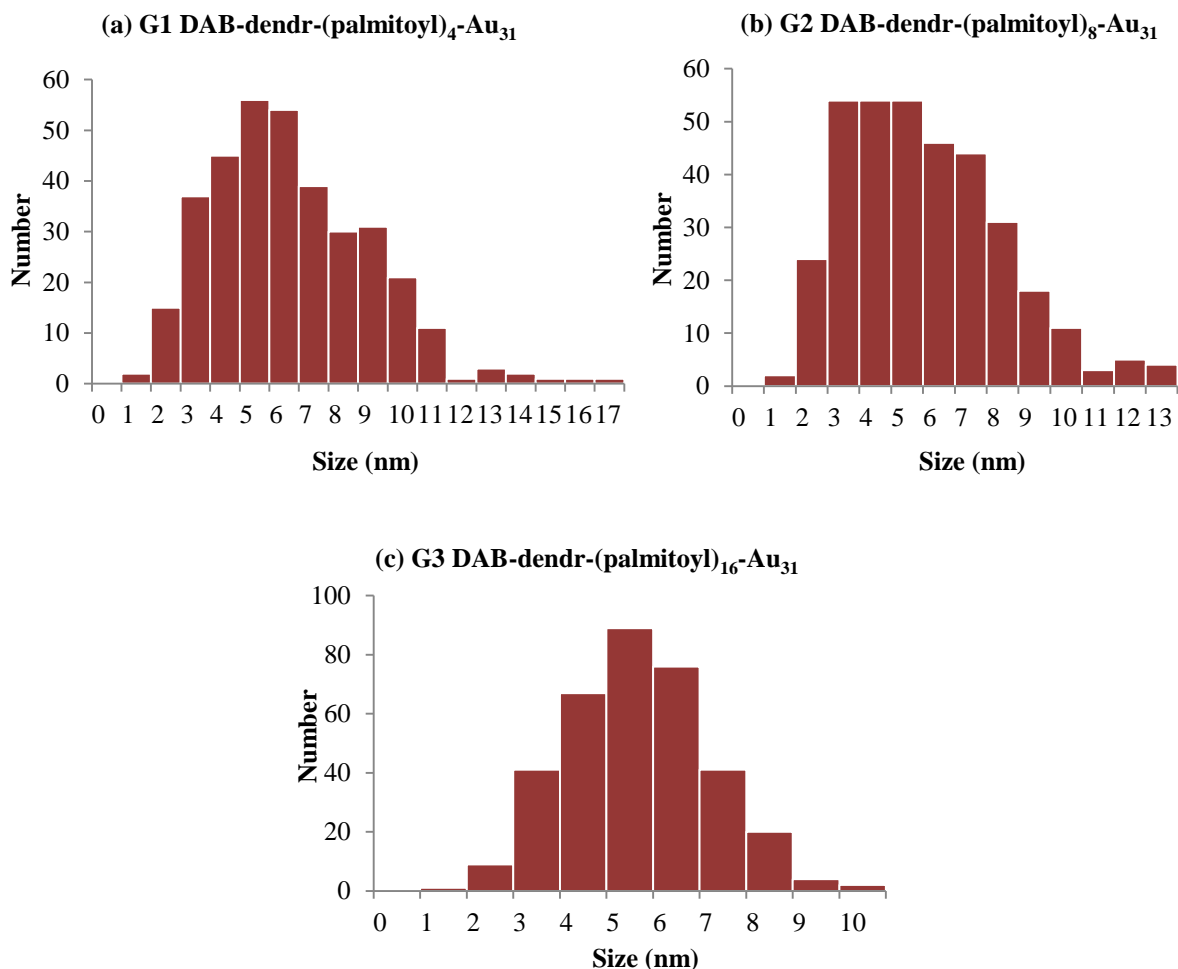


Figure 3.3-17: Particle distribution (a) Average particle size: 6.72 ± 2.69 nm; Min: 1.71 nm; Max: 17.20 nm (b) Average particle size: 6.06 ± 2.42 nm; Min: 1.64 nm; Max: 13.66 nm (c) Average particle size: 5.68 ± 1.54 nm; Min: 1.86 nm; Max: 10.62 nm

The trend observed indicates that a smaller average particle size is expected when using a larger generation dendrimer. This is expected as with an increase in generation there is an increase in branching leading to a more spherical dendritic structure that can provide better stability for the nanoparticle formation process.

As with the Au₁₃ nanoparticles the hydrophobic cyclam-cored dendrimers lead to smaller Au₃₁ nanoparticles. Although the average particle size produced by the G3 DAB dendrimer is slightly larger than that achieved with the cyclam-cored dendrimers it shows a narrower size distribution which could be more desirable.

3.3.2.3. Au₅₅ Dendrimer Encapsulated Nanoparticles

Au₅₅ nanoparticles were encapsulated in the hydrophobic generation 1, 2 and 3 DAB dendrimers as well as the hydrophobic generation 1 and 2 cyclam-cored dendrimers. During

Chapter 3

Encapsulation of Gold Nanoparticles in Dendritic Micelles

the preparation of the dendrimer encapsulated Au₅₅ nanoparticle clusters using the generation 1 hydrophobic DAB dendrimer, a black precipitate formed indicating particle aggregation. The material precipitated completely out of solution resulting in a clear mother liquor with a black precipitate on the bottom of the flask. Given that the solid could not be redissolved in the solvent, characterization by UV-Vis was not possible. The precipitate was however analysed by HR-TEM.

The UV-Vis spectra of the Au₅₅ DENs (Figure 3.3-18) again show a systematic increase in absorbance with a decrease in wavelength. The characteristic gold surface plasmon resonance band is found at around 520 nm in each case indicating particles larger than 2 nm are present, which correlated well with the TEM data.

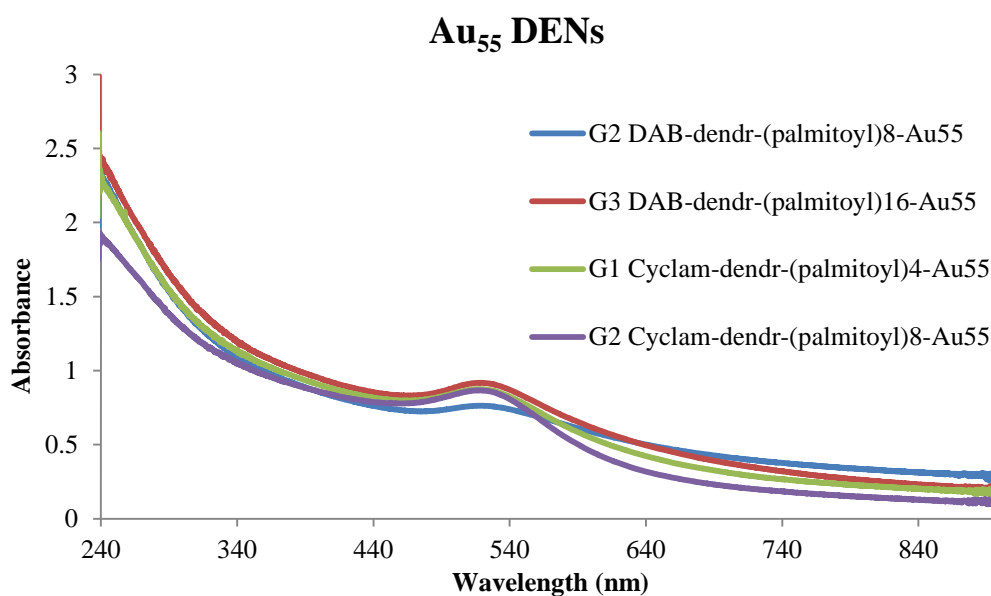


Figure 3.3-18: UV/Vis spectrum of Au₅₅ DENs

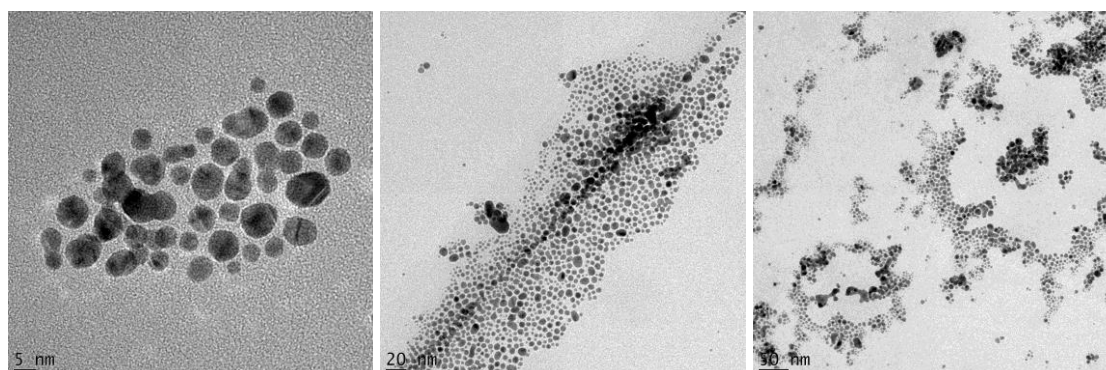


Figure 3.3-19: HR-TEM images of G1 Cyclam-dendr-(palmitoyl)₄-Au₅₅

Chapter 3

Encapsulation of Gold Nanoparticles in Dendritic Micelles

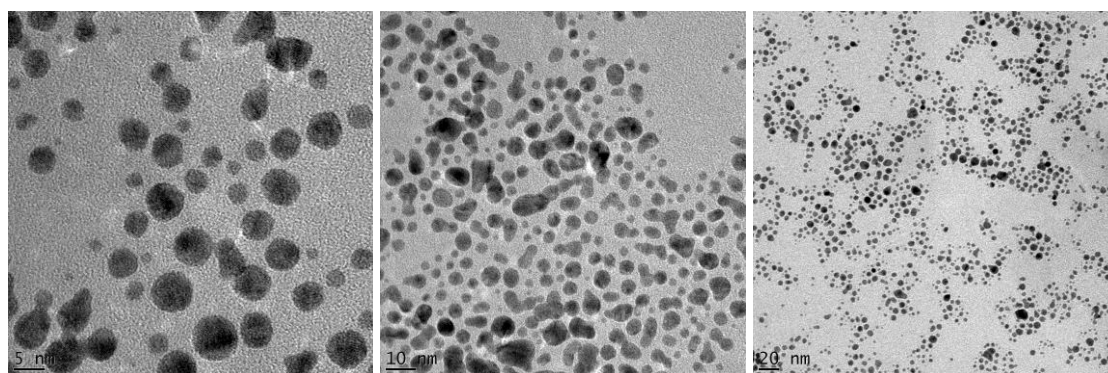


Figure 3.3-20: HR-TEM images of G2 Cyclam-dendr-(palmitoyl)₈-Au₅₅

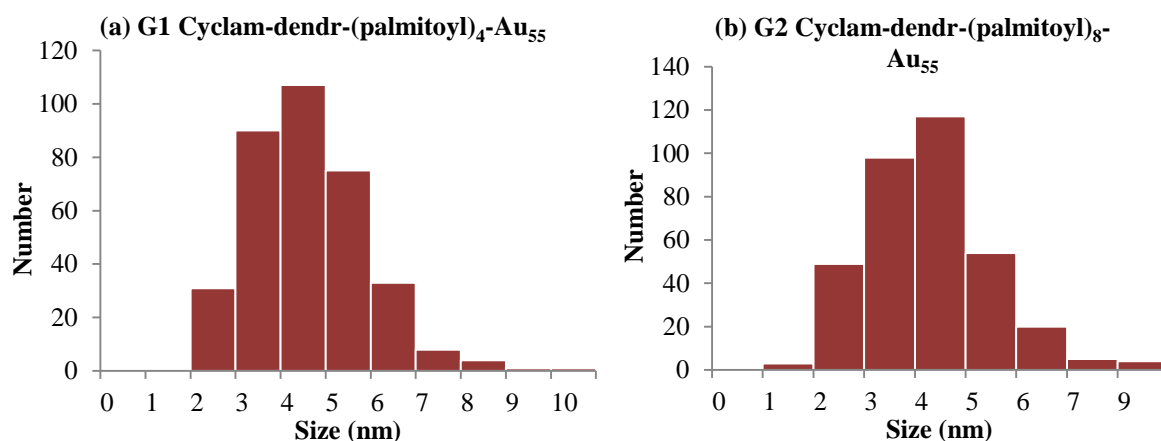


Figure 3.3-21: Particle distribution (a) Average particle size: 4.63 ± 1.29 nm; Min: 2.03 nm; Max: 10.55 nm (b) Average particle size: 4.27 ± 1.23 nm; Min: 1.87 nm; Max: 8.76 nm

HR-TEM images (Figure 3.3-19, Figure 3.3-20) show relatively well dispersed nanoparticles with a moderate size distribution for both the hydrophobic G1 and 2 cyclam-cored Au₅₅ DENs. The average particle size in both cases falls between 4 and 5 nm. The G1 dendrimer leads to a slightly larger maximum particle size, 10.55 nm, compared to that of the generation 2 variation, 8.76 nm.

The HR-TEM images for the hydrophobic G1 DAB Au₅₅ nanoparticles (Figure 3.3-22) show some aggregation as well as the presence of some smaller non-aggregated nanoparticles. Since the average particle size can only be determined by measuring well defined mostly circular particles the particle size distribution given here describes the average particle size of the well-defined particles but does not take into account the large parts of aggregated particles. The images show that even though aggregation and precipitation occurred, some smaller particles are still present with most of them falling in the range of 4-5 nm. The G2 and 3 variations also lead to particles with an average size of about 4-5 nm and a narrow size distribution.

Chapter 3

Encapsulation of Gold Nanoparticles in Dendritic Micelles

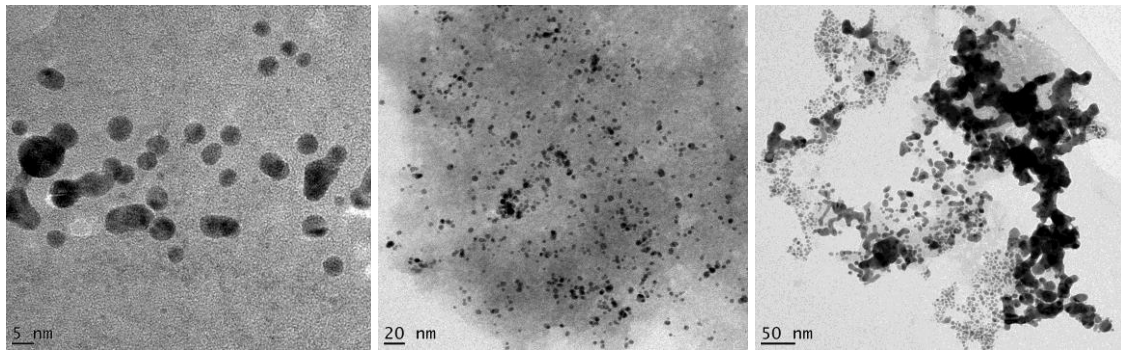


Figure 3.3-22: HR-TEM images of G1 DAB-dendr-(palmitoyl)₄-Au₅₅

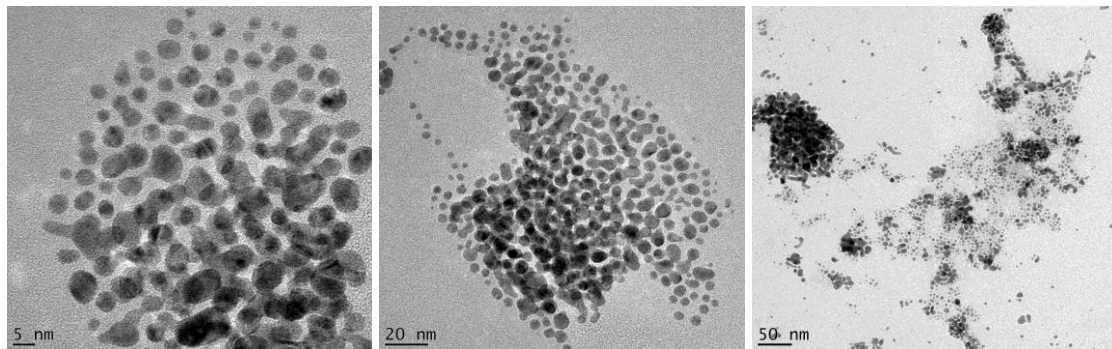


Figure 3.3-23: HR-TEM images of G2 DAB-dendr-(palmitoyl)₈-Au₅₅

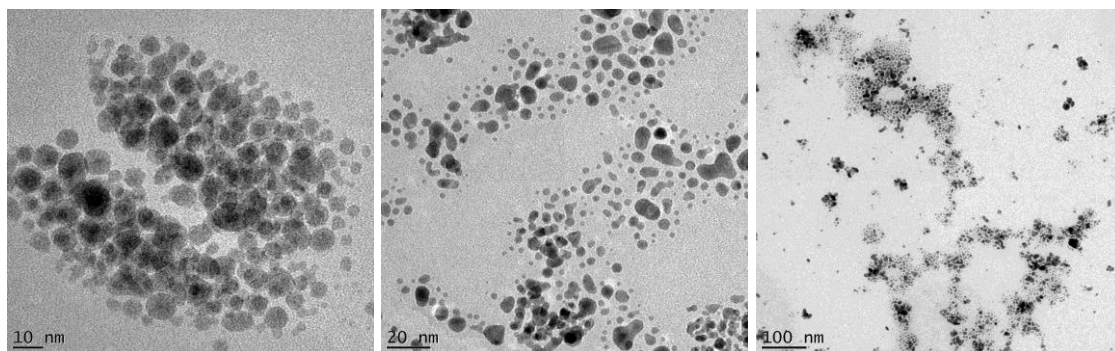
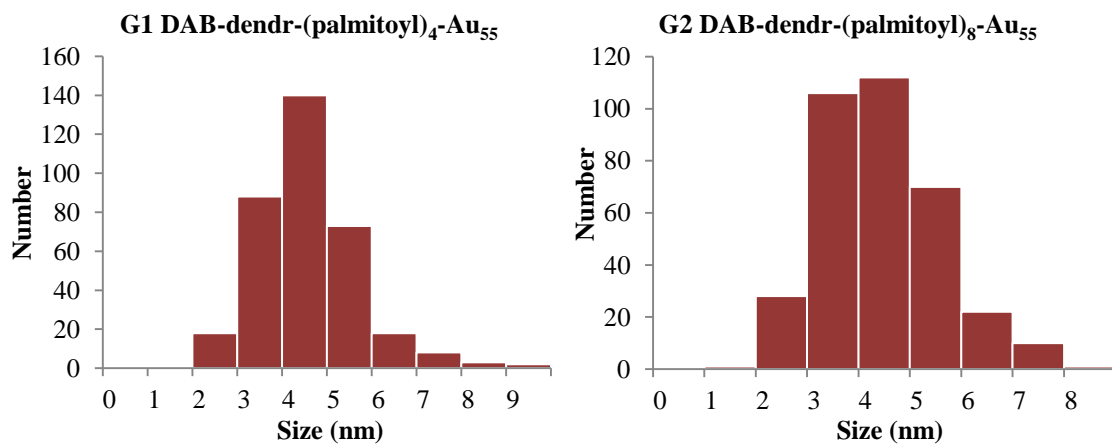


Figure 3.3-24: HR-TEM images of G3 DAB-dendr-(palmitoyl)₁₆-Au₅₅



Chapter 3

Encapsulation of Gold Nanoparticles in Dendritic Micelles

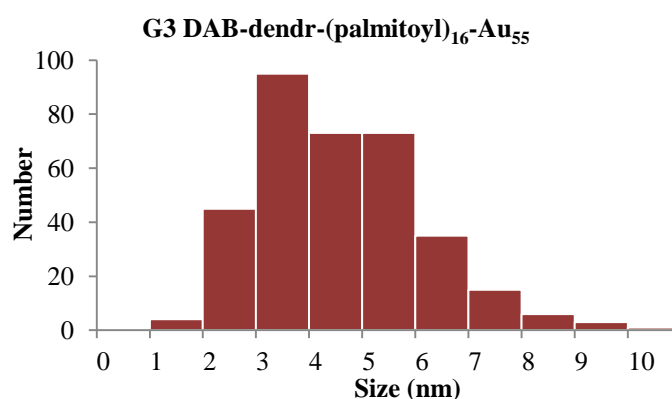


Figure 3.3-25: Particle distribution (a) Average particle size: 4.57 ± 1.12 nm; Min: 2.18 nm; Max: 9.62 nm (b) Average particle size: 4.44 ± 1.14 nm; Min: 1.94 nm; Max: 8.33 nm (c) Average particle size: 4.61 ± 1.53 nm; Min: 1.66 nm; Max: 10.01 nm

It is expected that when using the same dendrimer to metal ratio, similar nanoparticle sizes would be achieved regardless of the template as the encapsulation in this case is solubility and not complexation driven. The Au₅₅ DENs synthesized agrees with this as all of the DENs have an average particle size of approximately 4.5 nm. The only exception to this is that the G1 DAB analogue shows some degree of aggregation and precipitation. This is expected when taking the binding study results mentioned previously into account as well as the dendrimer structure. The binding studies showed that the G1 hydrophobic DAB dendrimer has a maximum loading capacity of approximately 12 metal ions. The dendrimer interior appears to be too small to encapsulate nanoparticle clusters of this size resulting in them aggregating or forming dendrimer stabilized (DSNs) rather than dendrimer encapsulated (DENs) nanoparticles (refer to section 1.1.2.2). In the case of dendrimer stabilized nanoparticles the particles are situated on the periphery of the dendrimer and stabilized by more than one dendrimer. The structure of the dendrimer is also perceived to be relatively flat compared to the more spherical higher generation dendrimers and thus encapsulation within the interior voids cannot occur.

3.3.3. Cluster size vs average particle size

One of the advantages of using dendrimers as templates for the encapsulation of NPs is the fact that specific cluster sizes, for example Au₅₅, can easily be produced by manipulating the dendrimer to metal ratio. As briefly stated in section 3.3, different cluster sizes are produced by the gradual addition of full shells of atoms around a core atom.

Chapter 3

Encapsulation of Gold Nanoparticles in Dendritic Micelles

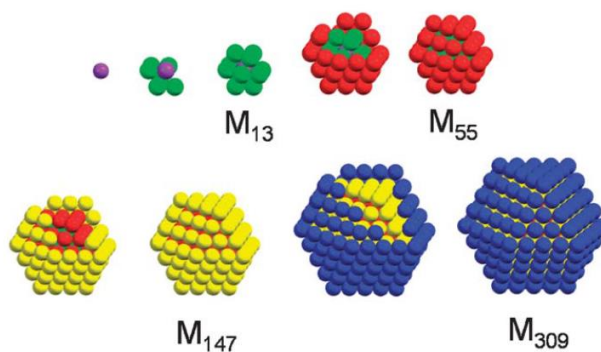


Figure 3.3-26: The organization of full shells of atoms around a central core atom to produce 'magic number' cluster sizes^[9]

The cluster size denotes the total number of atoms used to produce that specific cluster size. The increase in cluster size goes hand in hand with an increase in the diameter of the particles as indicated in Table 3.3-1 for Pt NPs.

Table 3.3-1: Approximate size of specific Pt nanoparticle cluster sizes^[10]

# of shells (n)	# of atoms in n th shell (=10n ² +2)	Total # of atoms	# of atom on a diameter (=2n+1)	Surface atoms [%]	Size of Pt NPs [nm]
0		1	1	–	0.3
1	12	13	3	92	0.8
2	42	55	5	76	1.4
3	92	147	7	63	1.9
4	162	309	9	52	2.4
5	252	561	11	45	3.0
6	362	923	13	39	3.5
7	492	1415	15	35	4.1
8	642	2057	17	31	4.6
9	812	2869	19	28	5.1

Table 3.3-1 shows the calculated approximate particle diameter expected for each cluster size containing complete full shells. For a face-centered cubic (fcc) structure $(10n^2 + 2)$ atoms are needed to completely fill a shell while $(2n + 1)$ atoms gives the diameter of the crystal where n denotes the number of shells.^[10] Taking into account the atomic radius of Au, 0.1442 nm,^[11] the approximate theoretical size of Au₅₅ and Au₁₃ could be calculated. The size of Au₃₁ cannot be calculated as it is not a full shell cluster. As the diameter of the particles increase with cluster size, its size should be in between that of Au₁₃ and Au₅₅. The calculated values are shown in Table 3.3-2.

Chapter 3

Encapsulation of Gold Nanoparticles in Dendritic Micelles

Table 3.3-2: Approximate theoretical size of Au₁₃ and Au₅₅ nanoparticles

Number of shells (n)	Total number of atoms	(2n + 1)	Size of Au NP (nm)
1	13	3	0.864
2	55	5	1.44

It is clear from these sizes calculated that although a dendrimer to gold ratio of 1:13 and 1:55 was used we did not produce the expected Au₁₃ and Au₅₅ nanoparticles. The approximate cluster sizes achieved are provided in Table 3.3-3.

Table 3.3-3: Calculated cluster sizes of Au nanoparticles synthesized

	Experimental size (nm)	Std dev	Theoretical shell (n)	Theoretical total number of atoms/cluster size
Au₁₃				
G1 DAB	4.36	1.31	7	1415
G2 DAB	8.98	3.87	15	12431
G3 DAB	4.54	2.02	7	1415
G1 Cyclam	3.41	1.03	5	561
G2 Cyclam	2.66	0.589	4	309
Au₅₅				
G1 DAB	4.57	1.12	7	1415
G2 DAB	4.44	1.14	7	1415
G3 DAB	4.61	1.53	7	1415
G1 Cyclam	4.63	1.29	7	1415
G2 Cyclam	4.27	1.23	7	1415

The fact that larger cluster sizes than desired were achieved can be explained by the difference in encapsulation methods between conventional dendrimers and dendritic micelles. In conventional dendrimers nanoparticle encapsulation is driven by metal coordination while in the case of dendritic micelles solubility of the metal salts within hydrophobic cavities is the driving force. There is also a possibility that with the optimum amount of stabilization (for example seen with the Au₅₅ DENs) the dendritic micelle template can limit the growth of the particles to a certain size. There is a fair possibility that the particles aren't encapsulated in the interior voids of the dendrimer but rather entangled in the hydrophobic chains on the exterior of the dendrimer micelle. Another possibility is the formation of dendrimer stabilized rather than dendrimer encapsulated nanoparticles. Although dendrimer structures become more

Chapter 3

Encapsulation of Gold Nanoparticles in Dendritic Micelles

spherical with an increase in the generation, we have used lower generation dendrimers that are not completely spherical and thus does not provide enough stabilization for the particles to be encapsulated in the voids.

3.4. Conclusion

The encapsulation of Au₁₃, Au₃₁ and Au₅₅ nanoparticles in hydrophobic generation 1-3 DAB dendrimers as well as hydrophobic generation 1 and 2 cyclam-cored dendrimers was attempted. It was found that the particle size of the nanoparticles produced pointed to much larger cluster sizes having formed. In all cases average particle sizes smaller than 10 nm and relatively narrow particle size distributions were achieved. The smallest average particle size produced, 2.66 ± 0.589 nm, was achieved using the G2 cyclam-cored dendrimer and a dendrimer: Au ratio of 1:13. In general the hydrophobic cyclam-cored dendrimers tend to be better stabilisers than the hydrophobic DAB dendrimers. This could be the result of a difference in the nature of the core molecule or the difference in the interior architecture of the dendrimer. The cyclam core should potentially have a more spherical structure compared to the more planar diaminobutane cored dendrimers. This could have an effect on the encapsulation ability of the dendrimer. The two types of dendrimers also consist of different interior groups. The DAB dendrimers has a polypropyleneimine interior while the cyclam dendrimers has a polyamidoamine interior. The polyamidoamine interior results in a higher amide concentration in the interior of the cyclam-cored dendrimers compared to the DAB dendrimers which could have an influence on the encapsulation ability of the dendrimer.

3.5. Experimental Section

3.5.1. General Considerations and Materials

All reagents were acquired from Sigma-Aldrich and used without any further purification. All solvents were purchased from Sigma-Aldrich or Kimix. CHCl₃ was used without any further purification while MeOH was purified by distillation over a mixture of magnesium filings and iodine prior to use.

3.5.2. Instrumentation

UV/Vis spectra were recorded on a GBC 920 UV/Vis spectrometer equipped with Cintral software using quartz cuvettes with a 10 mm pathway. A wavelength scan was performed and

Chapter 3

Encapsulation of Gold Nanoparticles in Dendritic Micelles

the absorbance recorded in the range of 200-800 nm at a speed of 500 nm/min using a step size of 0.213 nm and a slit width of 2.0 nm. CHCl₃ was used as reference solvent.

HR-TEM was recorded using a Tecnai F20 Field Emission Transmission Electron Microscope operated at 200 kV. The samples were prepared by placing a drop of the sample on a holey-carbon Cu or Ni grid.

3.5.3. Procedures and Characterization

General Procedure for the encapsulation of Au nanoparticles in dendritic micelles

The dendrimer was completely dissolved in CHCl₃ (25 mL). HAuCl₄, dissolved in MeOH, was added and stirred for 5 min. NaBH₄ (50 eq.) was completely dissolved in MeOH and added dropwise with vigorous stirring. The mixture was stirred for 5 min and diluted to give a final volume of 50 mL.

Au₁₃ DENs

The specific amounts used for each dendrimer:

Table 3.5-1: Amount of the dendrimer template used

Dendrimer	Mass	Mol
G1 Cyclam-dendr-(palmitoyl) ₄	0.0044 g	2.5 x 10 ⁻⁶
G2 Cyclam-dendr-(palmitoyl) ₈	0.0093 g	2.5 x 10 ⁻⁶
G1 DAB-dendr-(palmitoyl) ₄	0.00350 g	2.76 x 10 ⁻⁶
G2 DAB-dendr-(palmitoyl) ₈	0.0065 g	2.42 x 10 ⁻⁶
G3 DAB-dendr-(palmitoyl) ₁₆	0.0134 g	2.44 x 10 ⁻⁶

A HAuCl₄ stock solution was prepared by dissolving a predetermined amount of HAuCl₄ in MeOH. To form the Au₁₃ nanoparticles a 1:13 dendrimer to Au mole ratio was needed. The required volume of HAuCl₄ solution in each case is as follows:

Chapter 3

Encapsulation of Gold Nanoparticles in Dendritic Micelles

Table 3.5-2: Amount of H₂AuCl₄ solution required

Dendrimer	[H ₂ AuCl ₄]	Vol added
G1 Cyclam-dendr-(palmitoyl) ₄	0.0556 M	0.585 mL
G2 Cyclam-dendr-(palmitoyl) ₈	0.0556 M	0.585 mL
G1 DAB-dendr-(palmitoyl) ₄	0.0538 M	0.666 mL
G2 DAB-dendr-(palmitoyl) ₈	0.0538 M	0.586 mL
G3 DAB-dendr-(palmitoyl) ₁₆	0.0538 M	0.588 mL

Au₃₁ DENs

The specific amounts used for each dendrimer:

Table 3.5-3: Amount of dendrimer template used

Dendrimer	Mass	Mol
G1 Cyclam-dendr-(palmitoyl) ₄	0.0045 g	2.79×10^{-6}
G2 Cyclam-dendr-(palmitoyl) ₈	0.0087 g	2.50×10^{-6}
G1 DAB-dendr-(palmitoyl) ₄	0.0031 g	2.44×10^{-6}
G2 DAB-dendr-(palmitoyl) ₈	0.0066 g	2.46×10^{-6}
G3 DAB-dendr-(palmitoyl) ₁₆	0.0136 g	2.47×10^{-6}

A 0.0572 M H₂AuCl₄ stock solution was prepared by dissolving a predetermined amount of H₂AuCl₄ in MeOH. To form the Au₃₁ nanoparticles a 1:31 dendrimer : Au mol ratio is needed. The required volume of H₂AuCl₄ solution in each case is as follows:

Table 3.5-4: Amount of H₂AuCl₄ solution required

Dendrimer	[H ₂ AuCl ₄]	Vol added
G1 Cyclam-dendr-(palmitoyl) ₄	0.0572 M	1.514 mL
G2 Cyclam-dendr-(palmitoyl) ₈	0.0572 M	1.356 mL
G1 DAB-dendr-(palmitoyl) ₄	0.0572 M	1.323 mL
G2 DAB-dendr-(palmitoyl) ₈	0.0572 M	1.334 mL
G3 DAB-dendr-(palmitoyl) ₁₆	0.0572 M	1.340 mL

Chapter 3

Encapsulation of Gold Nanoparticles in Dendritic Micelles

Au₅₅ DENs

The specific amounts used for each dendrimer:

Table 3.5-5: Amount of dendrimer template used

Dendrimer	Mass	Mol
G1 Cyclam-dendr-(palmitoyl) ₄	0.0044 g	2.73 x 10 ⁻⁶
G2 Cyclam-dendr-(palmitoyl) ₈	0.0086 g	2.47 x 10 ⁻⁶
G1 DAB-dendr-(palmitoyl) ₄	0.0035 g	2.76 x 10 ⁻⁶
G2 DAB-dendr-(palmitoyl) ₈	0.0067 g	2.46 x 10 ⁻⁶
G3 DAB-dendr-(palmitoyl) ₁₆	0.0138 g	2.56 x 10 ⁻⁶

A H₂AuCl₄ stock solution was prepared by dissolving a predetermined amount of H₂AuCl₄ in MeOH. To form the Au₅₅ nanoparticles a 1:55 dendrimer : Au mol ratio is needed. The required volume of H₂AuCl₄ solution in each case is as follows:

Table 3.5-6: Amount of H₂AuCl₄ required

Dendrimer	[H₂AuCl₄]	Vol added
G1 Cyclam-dendr-(palmitoyl) ₄	0.0572 M	2.627 mL
G2 Cyclam-dendr-(palmitoyl) ₈	0.0572 M	2.378 mL
G1 DAB-dendr-(palmitoyl) ₄	0.0556 M	2.482 mL
G2 DAB-dendr-(palmitoyl) ₈	0.0572 M	2.367 mL
G3 DAB-dendr-(palmitoyl) ₁₆	0.0572 M	2.464

3.7. References

1. R. W. J. Scott, O. M. Wilson, R. M. Crooks, *J. Phys. Chem. B*, **109** (2005) 692
2. M. Zhao, L. Sun, R. M. Crooks, *J. Am. Chem. Soc.*, **120** (1998) 4877
3. J. C. Garcia-Martinez, R. M. Crooks, *J. Am. Chem. Soc.*, **126** (2004) 16170
4. K. Esumi, A. Suzuki, N. Aihara, K. Usui, K. Torigoe, *Langmuir*, **14** (1998) 3157
5. Y. Niu, R. M. Crooks, *Chem. Mater.*, **15** (2003) 3463
6. E. M. Mulder, R. C. Thiel, L. J. de Jongh, P. C. M. Gubbens, *Nanostruct. Mater.*, **7** (1996) 269
7. M. Antonietti, F. Grohn, J. Hartmann, L. Bronstein, *Angew. Chem. Int. Ed. Engl.*, **36** (1997) 2080
8. G. Schmid, in *Metal Nanoclusters in Catalysis and Materials Science: The Issue of Size Control*, ed. B. Corain, G. Schmid, N. Toshima, Elsevier, Amsterdam, 1st Edn., 2008, ch. 1, p.3
9. G. Schmid, *Chem. Soc. Rev.*, **37** (2008) 1909
10. K. An, G. A. Somorjai, *ChemCatChem*, **4** (2012) 1512
11. C. H. Suresh, N. Koga, *J. Phys. Chem. A*, **105** (2001) 5940

Chapter 4: Application of Dendritic Micelle Encapsulated Gold Nanoparticles as Alkane Oxidation Catalysts

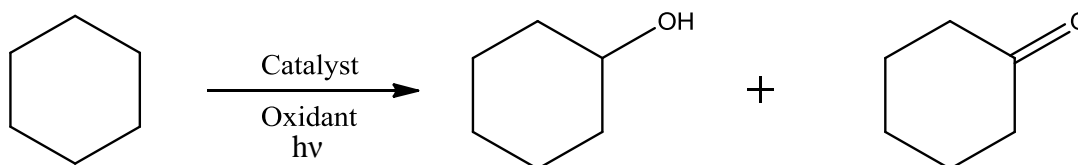
4.1. Introduction

Saturated hydrocarbons, otherwise known as paraffins, are without affinity or otherwise stated mostly inert. ^[1] The incorporation of an oxygen containing functionality into the unreactive hydrocarbon backbone can lead to the production of value-added products that can be used as precursors in the fine chemicals industry. ^[2,3] Although alkanes tend to be more reactive under higher temperatures and harsher conditions this tends to lead to their combustion and thus the formation of less desirable carbon dioxide and water as products. The problem remains trying to achieve controlled oxidation of alkanes to specific oxygenated products in a selective manner, for example activation of the primary carbon to produce the primary alcohol product selectively. ^[1]

The catalytic oxidation of alkanes is a greener and more efficient approach than a stoichiometric approach. ^[4,5] A lot of success has been achieved in recent years with various different catalysts ranging from metal nanoparticles to discrete organometallic complexes.

4.1.1. Oxidation of cyclic hydrocarbon substrates

Most commonly found are reports of the catalytic oxidation of cyclic substrates such as cyclohexane. The selective oxidation of cyclohexane to cyclohexanol and cyclohexanone (Scheme 4.1-1) has been widely studied because these mixtures of products, otherwise known as KA oil, are important intermediates in the production of Nylon-6 and Nylon-66. ^[6]



Scheme 4.1-1: General scheme for the photocatalytic oxidation of cyclohexane

Some interesting approaches to this transformation have been reported with most of the work involving gold-based catalysts. R. Liu *et al* and J. Liu *et al* both employed photocatalysis for the oxidative transformation of cyclohexane making use of different gold-based catalysts.

Chapter 4

Application of Dendritic Micelle Encapsulated Gold Nanoparticles as Alkane Oxidation Catalysts

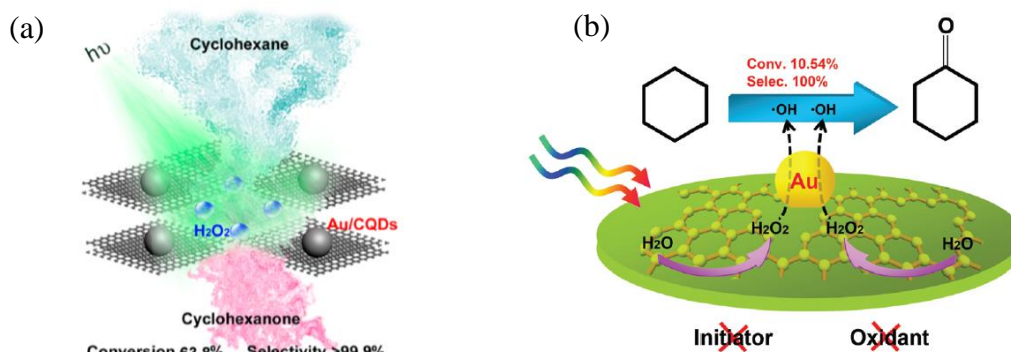


Figure 4.1-1: Photocatalysed oxidation of cyclohexane via (a) Au/CQD composites in the presence of H₂O₂ [7] and (b) C₃N₄/Au using water as oxidant [8]

R. Liu et al [7] applied gold nanoparticle/carbon quantum dot (Au/CQD) composites as photocatalysts in the oxidation of cyclohexane [Figure 4.1-1 (a)]. They found that when applying light at a wavelength corresponding to the surface plasmon resonance zone of gold nanoparticles (490-590 nm) the best conversion was achieved. Furthermore utilizing H₂O₂ as oxidant, high conversions (63.8%) and selectivity towards cyclohexanone (>99.9%) were achieved compared to Au/SiO₂ (30.3 %, 54.1%), Au/carbon nanotube (22.1%, 49.7%), Au/graphene (23.9%, 50.1%) and Au/graphite composites (14.2%, 64.2%). J. Liu et al [8] used carbon nitride/Au nanoparticle (C₃N₄/Au) nanocomposites in a completely green approach to the oxidation of cyclohexane [Figure 4.1-1 (b)]. The reaction was performed in the absence of any conventional oxidant or initiator. This was made possible by performing the oxidation under irradiation with visible light (>420 nm) using water as oxidant. A conversion of 10.54% and 100% selectivity towards cyclohexanone was achieved.

4.1.2. Oxidation of linear hydrocarbon substrates

Fewer reports are available for the oxidation of acyclic alkanes, especially the longer chain linear alkanes. Usually these types of reactions result in low conversions as shown by Hutchings *et al* (Figure 4.1-2). [9]

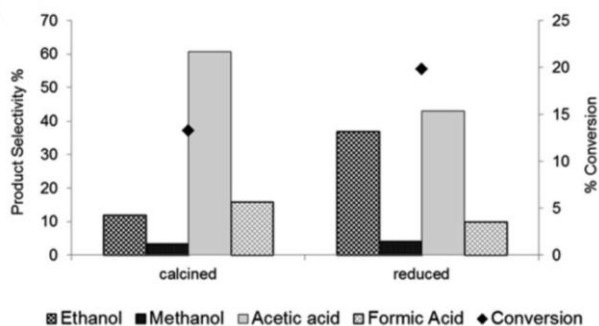
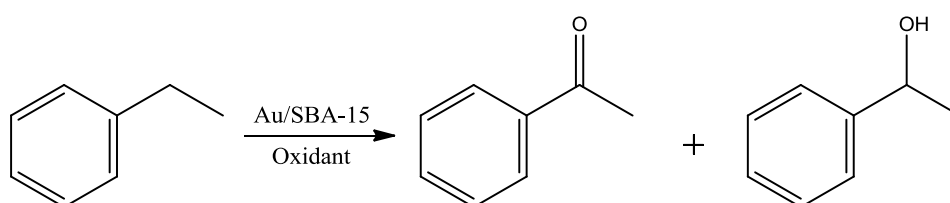


Figure 4.1-2: Product distribution and % conversion achieved for the oxidation of ethane using a Fe/ZSM-5 catalyst prepared by calcination and reduction [9]

Chapter 4

Application of Dendritic Micelle Encapsulated Gold Nanoparticles as Alkane Oxidation Catalysts

They reported the oxidation of ethane using 1.1 wt% Fe/ZSM-5 catalysts. The highest percentage conversion achieved was $\pm 20\%$ with 36% selectivity towards ethanol. Chen *et al* ^[10] produced Au/mesoporous silica composites and applied these as catalysts in the oxidation of n-hexadecane. The catalyst was found to be easily recoverable and reusable. Although relatively high conversions were achieved (52.3%) under aerobic oxidation conditions, selectivity remained an issue as a range of different alcohol and ketones products were identified. Biradar *et al* ^[11] synthesized Au nanoparticles supported on SBA-15 mesoporous silica for the oxidation of ethylbenzene (Scheme 4.1-2), other alkyl-substituted benzenes, hexane and n-hexadecane and found that the catalyst was very active and selective.



Scheme 4.1-2: Au/SBA-15 catalysed oxidation of ethylbenzene ^[11]

Ethylbenzene was used to determine the optimized conditions and they found that the highest conversion (79%) was achieved when using TBHP as oxidant and acetonitrile as solvent. The reaction was mostly selective towards the ketone product (93%). To test the scope of the catalyst the authors also tested its activity in the oxidation of other alkyl-substituted benzenes as well as hexane. They achieved a 95% conversion of hexane to mostly 2-hexanone (92%) in only 8 hours.

Table 4.1-1: Oxidation of n-hexadecane catalyzed by Au/SBA-15 under various reaction conditions ^{a, [11]}

Entry	Reaction solvent/condition	% Conversion	% Selectivity		
			2-hexadecanone	4-hexadecanone	3-hexadecanone
1	In Acetonitrile ^b	9	58	41	1
2	In Methanol ^b	5	57	42	1
3	Neat ^c	15	40	47	13
4	Neat ^d	74	42	47	11

^a This reaction is particularly chosen to show both the catalyst's versatility as well as relatively high efficiency and selectivity compared to other closely related materials/catalysts in similar reactions

^b Reaction condition: substrate, n-hexadecane (1 mmol) in 10 mL, solvent (acetonitrile or MeOH); oxidant: 80% TBHP (aq.), 2 mmol; catalyst: Au/SBA-15 (15 mg); reaction temperature: 70 °C; internal standard: chlorobenzene, 0.5 mL; and reaction time: 36 h

^c Reaction condition: substrate, n-hexadecane (25 mmol), neat (no solvent); oxidant: 80% TBHP (aq.), 2 mmol; catalyst: Au/SBA-15 (15 mg); reaction temperature: 70 °C; and reaction time: 24 h

^d Reaction condition: n-hexadecane (25 mmol), neat (no solvent); oxidant: 80% TBHP (aq.), 50 mmol; catalyst: Au/SBA-15 (15 mg); reaction temperature: 150 °C in a Parr reactor; and reaction time: 6 h

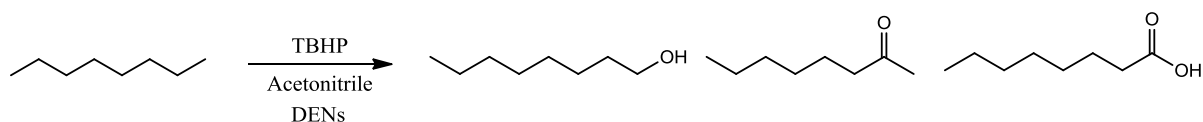
Chapter 4

Application of Dendritic Micelle Encapsulated Gold Nanoparticles as Alkane Oxidation Catalysts

Further studies were also conducted using n-hexadecane as substrate and again only ketone products were observed (Table 4.1-1). Lower conversions were achieved for this substrate under the conditions used for the ethylbenzene oxidation reactions, however when performing a solventless reaction at higher temperatures a conversion of 74% was achieved.

4.2. Catalysed oxidation of n-octane

To the best of our knowledge the use of unsupported dendrimer encapsulated nanoparticles have not previously been reported as catalysts in the oxidation of linear alkanes. As indicated in sections 4.1.1 and 4.1.2, the field of catalysed alkane oxidation is dominated by the use of gold nanoparticles. As the gold nanoparticles seem to be very effective oxidation catalysts it was decided to also use gold for the preparation of the dendrimer encapsulated nanoparticle (DEN) catalysts. The substrate chosen for this study is n-octane (Scheme 4.2-1).



Scheme 4.2-1: General reaction for the oxidation of n-octane

Usually dendrimer encapsulated nanoparticles are stored and used in solution to prevent the dendrimer from collapsing onto the metal nanoparticles. This makes it very difficult when applying DENs in catalysis as the solvent used for the DEN preparation is not always the most suitable solvent to use in the catalytic reaction. The use of dendritic micelles however widens the choice of a suitable solvent as it provides the possibility of using organic media for the preparation of the DENs and the subsequent use of these DENs in catalysis. Given that the DENs were prepared as a chloroform solution, it was initially decided to conduct the catalysis in this solvent. However preliminary results indicated poor performance of the catalytic system in this solvent. Changing the solvent from chloroform to toluene for the DEN preparation had an impact on the subsequent catalytic process. In this case we observed that the solvent was in fact more reactive than the substrate resulting in toluene oxidation. We next considered acetonitrile as solvent and it proved to be very effective. Considering that the DENs do not dissolve in acetonitrile we could not prepare the DENs in acetonitrile. We decided that the best approach would be to prepare the catalyst in chloroform and then remove the chloroform for the catalysis and replace it with acetonitrile. This then resulted in a heterogeneous catalytic system which has the potential of easy catalyst recovery.

Chapter 4

Application of Dendritic Micelle Encapsulated Gold Nanoparticles as Alkane Oxidation Catalysts

The dendritic micelle encapsulated gold nanoparticles were applied as catalysts in the oxidation of n-octane using TBHP as oxidant. Preliminary investigations were conducted using the conditions reported by Biradar *et al.* [11] As stated in section 4.1.2 these authors investigated the catalysed oxidation of ethylbenzene and other alkane substrates such as n-hexadecane using gold nanoparticles supported on SBA-15 mesoporous silica as catalyst and TBHP as oxidant. In our reactions we employed similar conditions as employed for the oxidation of ethylbenzene and n-hexadecane. These conditions included a 1:2 ratio of substrate to oxidant (80% TBHP), a temperature of 70 °C and 3.86 wt% (2.94 mmol Au) catalyst. Optimisation of our catalytic reaction conditions were performed using the G2 Cyclam Au₅₅ catalyst employing acetonitrile as solvent. Firstly the effect of metal loading was tested using a substrate to oxidant ratio of 1:1. The results obtained indicated that increasing the metal loading resulted in a decrease in the percentage conversion achieved (Figure 4.2-1). The activity was tested at a metal loading of 0.1, 0.21, 0.5 and 1.0 mol%. This resulted in a decrease in percentage conversion from 90% to 71% over the range of metal loadings tested. One would usually expect the opposite to be true. This result could possibly be explained by the fact that an increase in the amount of metal present could result in the particles aggregating and thus leading to a reduction in the overall surface area. This would impact negatively on the activity of the catalyst.

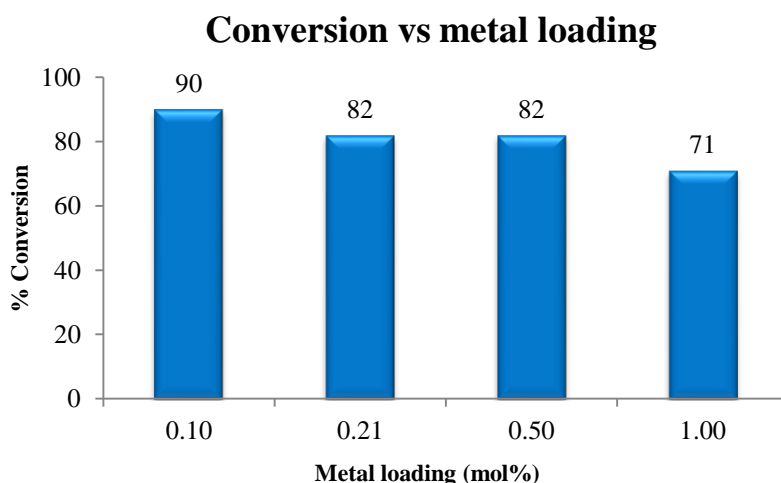


Figure 4.2-1: Results of the effect of metal loading experiments; Reaction conditions: n-octane (2 mmol), 80% TBHP (2 mmol), 70 °C, acetonitrile (5 mL), 72 hours

A metal loading of 0.21 mol% was chosen to perform the rest of the experiments. An investigation into the effect of the reaction time on the conversion was done using the same conditions employed for the metal loading study (Figure 4.2-2). It was found that increasing the reaction time from 24 hours to 72 hours led to an increase in percentage conversion from

Chapter 4

Application of Dendritic Micelle Encapsulated Gold Nanoparticles as Alkane Oxidation Catalysts

11 % at 24 hours to 82% at 72 hours. Although such a long reaction time is not necessarily optimum, it does show that the catalyst is stable for long periods under the reaction conditions employed.

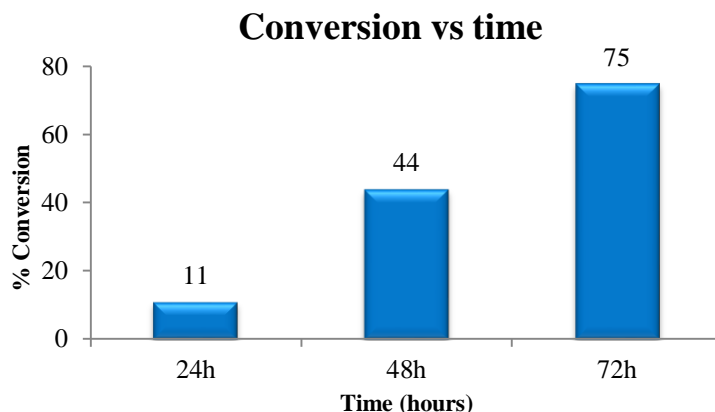


Figure 4.2-2: Results of the effect of time experiments; Reaction conditions: n-octane (2 mmol), 80% TBHP (2 mmol), 70 °C, acetonitrile (5 mL), 0.21 mol% catalyst (G2 Cyclam Au₅₅)

After deciding on the metal loading (0.21 mol%) and the reaction time (72 hours) the activity and selectivity of the different catalysts could be tested. Taking into account the dendrimer to metal ratio used for the preparation of the catalysts, the difference in the nature of the dendrimer templates as well as the different generations of dendrimer templates used, a comparison between all of the catalysts could be made. The idea was to investigate if any of these properties have an effect on the catalyst activity and selectivity.

Dendrimer to gold ratios of 1:13 (Au₁₃), 1:31 (Au₃₁) and 1:55 (Au₅₅) were used when encapsulating gold nanoparticles in the generation 1-3 hydrophobic DAB dendrimers as well as the generation 1-2 hydrophobic cyclam-cored dendrimers.

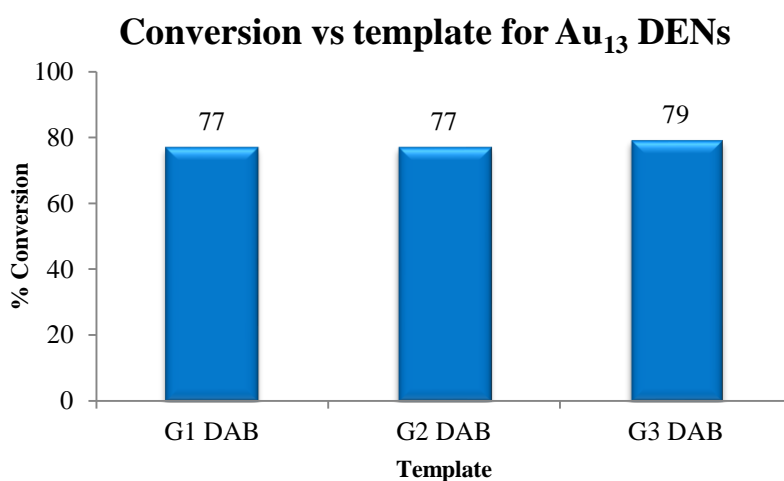


Figure 4.2-3: Effect of the dendrimer template on the conversion for the Au₁₃ DENs; Reaction conditions: n-octane (2 mmol), 80% TBHP (2 mmol), 70 °C, 72 hours, acetonitrile (5 mL), 0.21 mol% catalyst

Chapter 4

Application of Dendritic Micelle Encapsulated Gold Nanoparticles as Alkane Oxidation Catalysts

As stated in chapter 3, these ratios did not result in the intended Au₁₃, Au₃₁ and Au₅₅ nanoparticles but rather much larger clusters. However, to avoid confusion the catalysts will be referred to as Au₁₃, Au₃₁ and Au₅₅ DENs pointing to the ratio used and not the cluster formed. The G1-3 hydrophobic DAB – Au₁₃ DENs were tested using the optimised reaction conditions and this resulted in high conversions (77% - 79%) in all three cases (Figure 4.2-3). The generation of the dendrimer did not seem to have any significant effect on the percentage conversion achieved.

The G1-3 hydrophobic DAB and G1-2 cyclam-cored Au₃₁ DENs were tested in the catalytic oxidation of n-octane and gave some interesting results (Figure 4.2-2). It was found that when using the DAB dendrimer templates there was an increase in the percentage conversion achieved with an increase in the generation of the dendrimer from 76% for the G1 DENs to 93% for the G3 DENs. The opposite effect was observed for the hydrophobic cyclam-cored DENs. Here a decrease in conversion from 88% for the G1 DENs to 71% for the G2 DENs was observed. We also found that the positive generation effect observed for the DAB dendrimers as well as the negative effect observed for the cyclam-cored dendrimers can be correlated to the average particle sizes of the gold nanoparticles produced using these dendrimer templates. With an increase in the average particle size a decrease in percentage conversion is observed. This is expected as an increase in particle size results in a decrease in the surface area of the catalyst and thus a decrease in the area available for substrate activation.

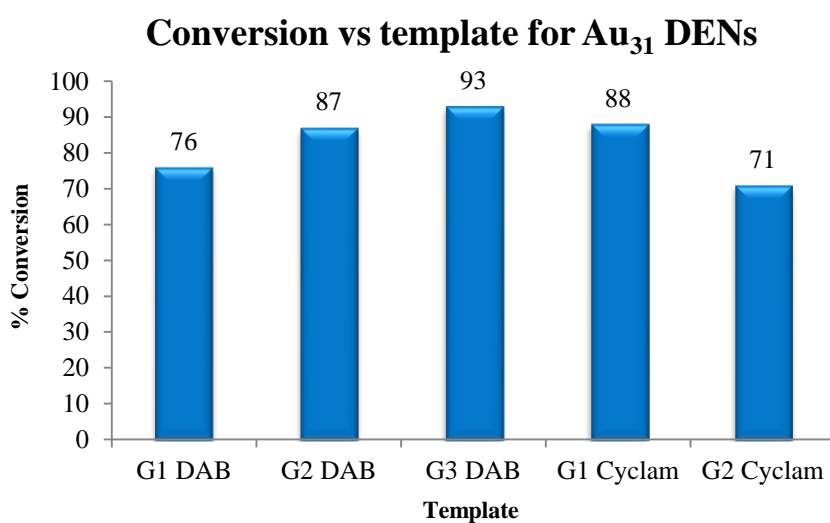


Figure 4.2-4: Effect of the dendrimer template on the conversion for the Au₃₁ DENs; Reaction conditions: n-octane (2 mmol), 80% TBHP (2 mmol), 70 °C, 72 hours, acetonitrile (5 mL), 0.21 mol% catalyst

Chapter 4

Application of Dendritic Micelle Encapsulated Gold Nanoparticles as Alkane Oxidation Catalysts

All of the prepared Au₅₅ catalysts, except for the G1 DAB dendrimer encapsulated Au₅₅ DENs, were tested as alkane oxidation catalysts. The G1 analogue could not be tested as it aggregated immediately after preparation. The rest of the analogues resulted in high conversions of octane. Unlike the Au₃₁ DENs, the Au₅₅ DENs showed a decrease in percentage conversion with an increase in the dendrimer generation. This could again be correlated to an increase in the average particle size observed. A decrease in conversion from 87% to 79% was observed with an increase in the DAB dendrimer generation while a decrease from 83% to 75% was observed for the cyclam-cored DENs (refer to Figure 3.3-21 and 3.3-25).

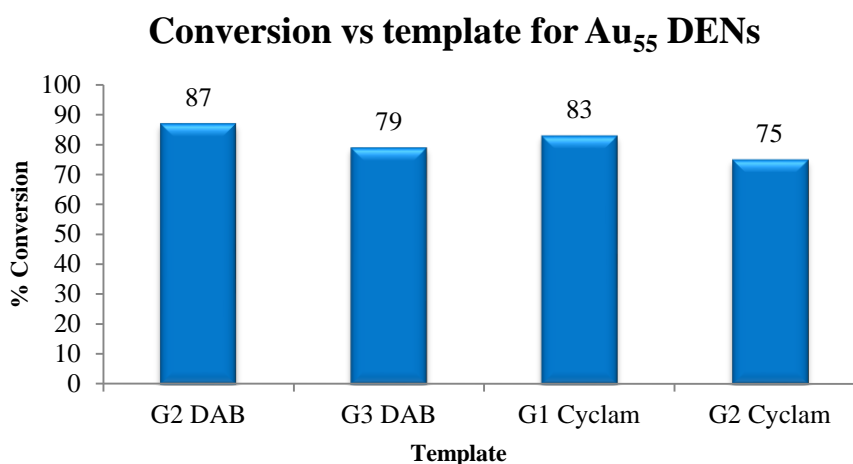


Figure 4.2-5: Effect of the dendrimer template on the conversion for the Au₅₅ DENs; Reaction conditions: n-octane (2 mmol), 80% TBHP (2 mmol), 70 °C, 72 hours, acetonitrile (5 mL), 0.21 mol% catalyst

Drawing a comparison between the different dendrimer to gold ratios used in each specific dendrimer template shows that the ratio does not make such a big difference (Figure 4.2-6).

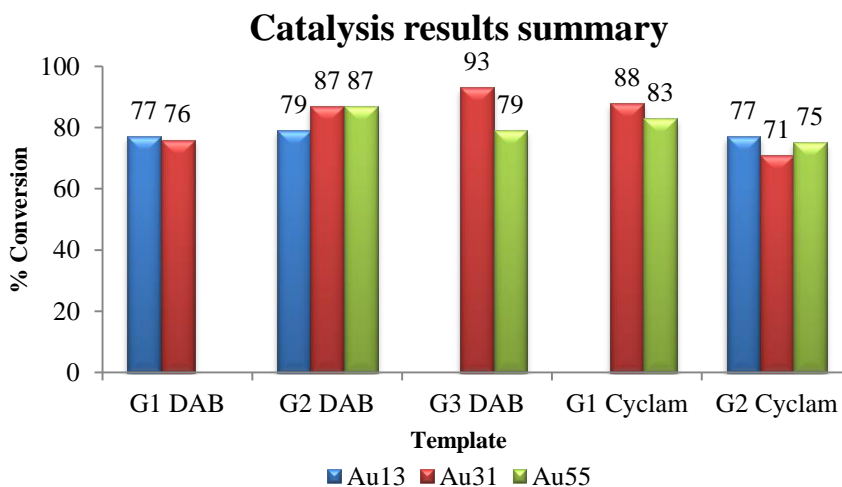


Figure 4.2-6: Effect of the different Au/dendrimer ratios used for each specific dendrimer template on the conversion achieved; Reaction conditions: n-octane (2 mmol), 80% TBHP (2 mmol), 70 °C, 72 hours, acetonitrile (5 mL), 0.21 mol% catalyst

Chapter 4

Application of Dendritic Micelle Encapsulated Gold Nanoparticles as Alkane Oxidation Catalysts

Fairly similar results are achieved when utilizing the same dendrimer template regardless of the metal to dendrimer ratio used. Some outliers are however observed as seen for example in the results of the G2 and G3 DAB dendritic micelles encapsulated nanoparticles. The G2 DAB Au₁₃ DENs result in a slightly lower percentage conversion (77%) than the G2 Au₃₁ and Au₅₅ analogues (87%). In the case of the G3 DAB dendrimer template, the Au₁₃ and Au₅₅ DENs give the same percentage conversion (79%) while the Au₃₁ analogue performs much better and gives the highest percentage conversion achieved for any of the catalysts tested (93%).

Table 4.2-1: Summary of catalyst activity in turn over number (TON) and percentage conversion

Entry	Catalyst	TON ^a	% Conversion
1	G1 DAB - Au ₁₃	365.16	76.68
2	G2 DAB - Au ₁₃	365.01	76.65
3	G3 DAB - Au ₁₃	373.84	78.51
4	G1 DAB - Au ₃₁	361.89	76.00
5	G2 DAB - Au ₃₁	413.23	86.78
6	G3 DAB - Au ₃₁	440.95	92.60
7	G2 DAB - Au ₅₅	414.16	86.97
8	G3 DAB - Au ₅₅	378.00	79.38
9	G1 Cyclam - Au ₃₁	419.51	88.10
10	G2 Cyclam - Au ₃₁	339.22	71.24
11	G1 Cyclam - Au ₅₅	394.40	82.82
12	G2 Cyclam - Au ₅₅	357.34	75.04

^a TON calculated as mmol substrate consumed/mmol catalyst used

The product selectivity in most cases included roughly equal amounts of 1-octanol (32.44%)^a, 2-octanone (36.12%)^a and 3-octanone (31.43%)^a.

According to our knowledge gold DENs have not previously been applied as catalysts in the oxidation of n-octane and thus cannot be compared directly to work reported in the literature. A comparison to the catalyst of Biradar et al, Au/SBA-15, used in the oxidation of another

^a Selectivity for G3 DAB Au₃₁ DENs

Chapter 4

Application of Dendritic Micelle Encapsulated Gold Nanoparticles as Alkane Oxidation Catalysts

linear alkane substrate, n-hexadecane, indicates that our catalyst is much more active in solution however the selectivity of their catalyst is better as only the ketone products are produced in this case. They also tested their catalyst in a solventless system producing results much more comparable to what we achieved.

A comparison between the gold DENs catalysts and other catalysts used for the oxidation of n-octane was also needed to provide an idea of how our system performs. Poladi *et al* ^[12] used a Ti doped microporous mesoporous material (Ti-MMM-1) catalyst and achieved a relatively high conversion for this transformation, 19.8%. The catalyst does not however seem to be very selective as a range of alcohol and ketone products are formed. The conditions used should however also be taken into account before concluding that our system performs better than the Ti-MMM-1 catalyst. The authors used a milder oxidising agent (H₂O₂), a higher temperature (95 °C) and a much shorter reaction time (8h) compared to our conditions indicating that although we achieve much higher conversions their catalyst is probably more effective but not as selective. Cele *et al* ^[13] produced iron metal organic frameworks (Fe₄-MOF -5) as catalysts for the oxidative transformation of n-octane utilizing H₂O₂ as oxidant. They achieved a conversion of 10.5% after 4 hours at 80 °C. All possible oxygenated products were formed with selectivity leaning more towards the C₂ and C₃ oxygenates. Again, these authors achieved a much lower conversion and the catalyst is less selective than our Au DENs but a slightly higher temperature (80 °C), much lower reaction time (4h) and milder oxidant (H₂O₂) is used in their case. Kadwa *et al* ^[14] prepared montmorillonite (Mt) supported Fe-salen complexes (Mt-Fe-salen) for the oxidation of n-octane using conditions more comparable to ours. They used TBHP as oxidant and a reaction time of 48 hours with a catalyst to substrate to oxidant ratio of 1:50:150. An 8.78% conversion was achieved with mostly octanone products forming. Compared to the 44% conversion the gold DENs achieved after 48 hours this is not very high. In our case a catalyst to substrate to oxidant ratio of 1:476:476 was used.

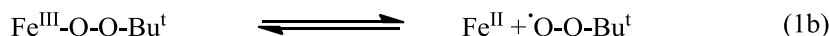
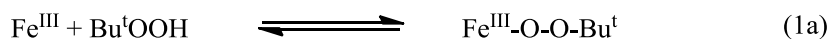
Taking all of this into account it seems that the gold DENs under our reaction conditions achieved higher conversion than the aforementioned catalysts and in some cases appears more selective than the other catalysts. However it should be noted that our reactions were conducted over much longer reaction times and using a different oxidising agent.

Chapter 4

Application of Dendritic Micelle Encapsulated Gold Nanoparticles as Alkane Oxidation Catalysts

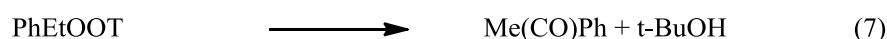
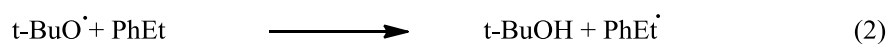
4.2.1. Mechanistic insight into the product selectivity

The metal-mediated decomposition of TBHP via a radical chain mechanism is well known. [15,16,17] Barton *et al* [16] investigated the iron-induced radical chemistry of TBHP and proposed the following reaction pathway:



Scheme 4.2-2: Iron-induced radical chain decomposition of TBHP^[16]

Equations 1 and 3 show the formation of tert-Butylperoxyl radicals while equation 2 shows the formation of tert-Butoxyl radicals. Similarly Macedo *et al* [15] described the use of ceria nanorods (CeNR) in the oxidation of ethylbenzene:



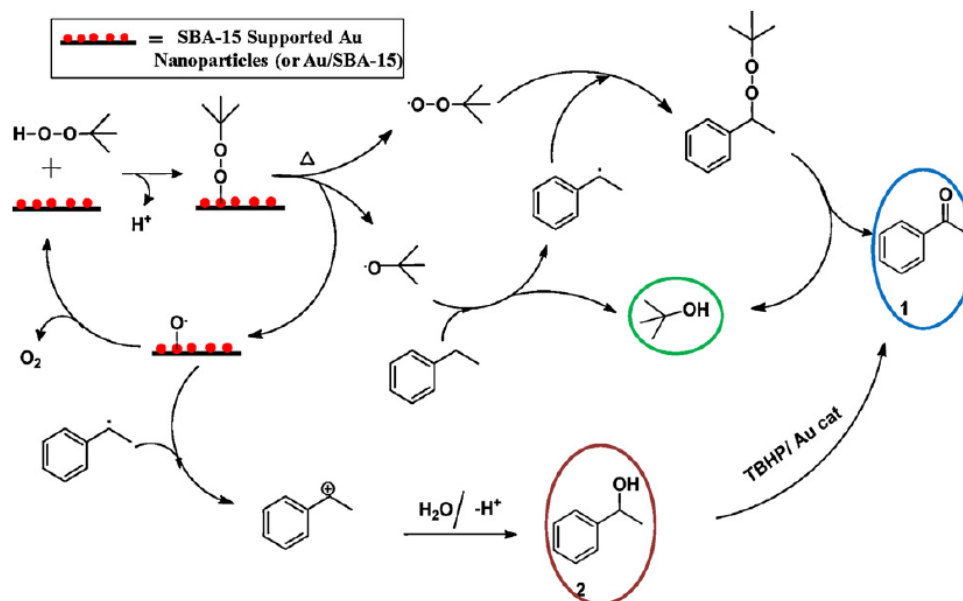
Scheme 4.2-3: CeNR induced decomposition of TBHP^[15]

CeNR initiates the homolysis of TBHP to tert-butylperoxyl ($\text{t-BuO}_2\cdot$) and tert-butoxyl ($\text{t-BuO}\cdot$) radicals and water. The tert-butoxyl radical is then able to abstract a proton from ethylbenzene (PhEt) resulting in the formation of the ethylbenzene radical and the byproduct tert-butanol (t-BuOH). The reaction of the ethylbenzene radical and the tert-butylperoxyl radical forms the intermediate 1-phenylethyl-tert-butyl-peroxide (PhEtOOT), which can then be transformed to the final product, acetophenone [Me(CO)Ph], coupled to the formation of t-BuOH .

Chapter 4

Application of Dendritic Micelle Encapsulated Gold Nanoparticles as Alkane Oxidation Catalysts

Biradar *et al*^[11] hypothesized a similar pathway using a catalyst more comparable to gold DENs. As previously stated they used Au/SBA-15 catalyst for the oxidation of ethylbenzene resulting in only the alcohol and ketone products. The authors found that increasing the TBHP to substrate ratio from 1:1 to 2:1 had no effect on the product selectivity. This led them to conclude that the alcohol is not transformed into the ketone but rather that two different pathways exist for the formation of the two different products.



Scheme 4.2-4: The mechanism proposed by Biradar *et al*^[11]

The homolysis of TBHP into $t\text{-BuO}\cdot$ and $t\text{-BuOO}\cdot$ is induced by Au nanoparticles and heat. Similar to the mechanism suggested by Macedo *et al*, the $t\text{-BuO}\cdot$ abstracts a hydrogen from the substrate to produce its radical and the by-product tert-butanol. The ethylbenzene radical reacts with $t\text{-BuOO}\cdot$ to produce 1-phenylethyl-tert-butyl-peroxide which can then be transformed into acetophenone. In the process of TBHP homolysis oxygen radicals form which reacts with the ethylbenzene radical to produce positively charged ethylbenzene. The positively charged ethylbenzene can then react with water to produce 1-phenylethanol.

As the catalyst used and products observed are similar to what is seen with the Au DENs in the oxidation of *n*-octane, this mechanism gives some insight into what is possibly occurring in our catalytic system.

4.2.2. Possibility of catalyst recovery

It was found that the catalyst remains insoluble under the reaction conditions used, although a colour change of the solid from purple to white is observed. The colour change could be an

Chapter 4

Application of Dendritic Micelle Encapsulated Gold Nanoparticles as Alkane Oxidation Catalysts

indication that the nanoparticles are oxidized back to the Au(III) ions. Preliminary FT-IR analysis indicates the presence of an organic substance that could be the broken down dendrimer template. An extensive further investigation is needed to determine if the catalyst could be recoverable and reusable. If the gold nanoparticles are oxidised is it possible to re-reduce the gold ions to gold nanoparticles? What exactly happens to the dendrimer template in these reaction conditions? These are just some of the questions that need further investigation to completely optimise this catalytic system.

In these types of systems there are many different factors that can play a role in the properties and activity of the DENs including the particle size and distribution as well as the nanoparticle cluster sizes as this plays a role in the amount of metal present in the system. It is very difficult to control each of these properties. One would expect that an increase in the dendrimer to metal ratio used would result in an increase in the particle sizes as explained in section 3.3.3. As the nanoparticles are kept in solution there is also a possibility that particle growth occurs over time. This can be determined by HR-TEM analysis over time.

4.3. Conclusion

To conclude, dendritic micelle encapsulated gold nanoparticles were applied as catalysts in the oxidation of n-octane. To our knowledge this is the first application of gold DENs as catalyst for the oxidation of n-octane. The results indicated that the catalysts gave high substrate conversions and thus show great potential. We determined that the dendrimer template and generation does not have as great an effect on the conversion as the average particle size of the gold nanoparticles. Longer reaction times resulted in a higher percentage conversion of the substrate while a higher metal loading had the opposite effect. We attributed this to the fact that the higher amount of catalyst results in a higher chance of particle aggregation and thus leads to a decrease in the particle surface area. As previously stated, these catalysts show great potential however there are still many questions regarding the product distribution, catalyst stability, chance of recovery and reusability.

4.4. Experimental Section

4.4.1. General Considerations and Materials

All reagents were acquired from Sigma-Aldrich or Fluka and used without any further purification. All solvents were purchased from Sigma-Aldrich or Kimix. Toluene was purified by a Pure SolvTM Micro solvent purifier fitted with activated alumina columns while acetonitrile was purified by distillation over phosphorous pentoxide. 1-decanol, purified by distillation, was used as internal standard for all GC-FID analysis.

4.4.2. Instrumentation

A Radleys 12-stage carousel parallel reactor equipped with a gas distribution system was used for the catalytic reactions. Products were analysed on a Varian 3900 gas chromatograph containing a Cyclosil- β (30 m x 0.25 mm x 0.25 μ m) column. 1-Decanol was used as internal standard.

4.4.3. Procedures and Characterization

A representative example of a typical catalytic oxidation of n-octane reaction using the conditions employed for entry 6 in table 4.2-1 is as follows:

A catalyst stock solution containing 1.532×10^{-3} M Au was prepared for the catalytic reaction as stated in section 3.4.3. The solvent (chloroform) was removed from the catalyst solution (2.742 mL, 4.2×10^{-3} mmol, 0.21 mol % relative to 2 mmol n-octane) under vacuum. The flask was refilled with nitrogen followed by the immediate addition of acetonitrile (5 mL). The mixture was brought up to temperature (70 °C) followed by the addition of TBHP (2 mmol, 0.320 mL) and n-octane (2 mmol, 0.325 mL). The reaction mixture was stirred for 72 hours and then analysed by GC-FID. For this purpose the syringe filtered reaction mixture (0.9 mL) and 1-decanol internal standard (0.1 mL) was added to a GC vial. Substrate conversion and product distribution was calculated relative to the internal standard.

4.5. References

1. J. A. Labinger, J. E. Bercaw, *Nature*, **417** (2002) 507
2. M. Ayala, E. Torres, *Appl. Catal. A*, **272** (2004) 1
3. E. G. Chepaikin, *J. Mol. Catal. A: Chem*, **385** (2014) 160
4. P. T. Anastas, M. M. Kirchhoff, T. C. Williamson, *Appl. Catal. A*, **221** (2001) 3
5. F. Cavani, *Catalysis Today*, **157** (2010) 8
6. B. P. C. Hereijgers, B. M. Weckhuysen, *J. Catal.*, **270** (2010) 16
7. R. Liu, H. Huang, H. Li, Y. Liu, J. Zhong, Y. Li, S. Zhang, Z. Kang, *ACS Catal.*, **4** (2014) 328
8. J. Liu, Y. Yang, N. Liu, Y. Liu, H. Huang, Z. Kang, *Green Chem.*, **16** (2014) 4559
9. M. M. Forde, R. D. Armstrong, R. McVicker, P. P. Wells, N. Dimitratos, Q. He, L. Lu, R. L. Jenkins, C. Hammond, J. A. Lopez-Sanchez, C. J. Kiely, G. J. Hutchings, *Chem. Sci.*, **5** (2014) 3603
10. L. Chen, J. Hu, R. Richards, *J. Am. Chem. Soc.*, **131** (2009) 9
11. A. V. Biradar, T. Asefa, *Appl. Catal. A*, **435-436** (2012) 19
12. R. H. P. R. Poladi, C. C. Landry, *Microporous and Mesoporous Mater.*, **52** (2002) 11
13. M. N. Cele, H. B. Friedrich, M. D. Bala, *Catal. Commun.*, **57** (2014) 99
14. E. Kadwa, M. D. Bala, H. B. Friedrich, *Applied Clay Science*, **95** (2014) 340
15. A. G. Macedo, S. E. M. Fernandes, A. A. Valente, R. A. S. Ferreira, L. D. Carlos, J. Rocha, *Molecules*, **15** (2010) 747
16. D. H. R. Barton, V. N. Le Gloahec, H. Patin, F. Launay, *New J. Chem.*, (1998) 559
17. F. Launay, A. Roucoux, H. Patin, *Tetrahedron Letters*, **39** (1998) 1353

Chapter 5: A Summary of the Preceding Chapters and Suggestions for Future Work

5.1. Summary of preceding chapters

This study was conducted to explore the catalytic potential of dendrimer encapsulated nanoparticles. The aim was to produce hydrophobic dendritic micelles that could be used as templates in the encapsulation of gold nanoparticles. The gold DENs could then ultimately be applied as catalysts in the oxidation of alkanes, specifically n-octane.

With this in mind **Chapter one** gives a brief overview on the synthesis, stabilization and application of metal nanoparticles. Two popular methods of nanoparticle stabilization are discussed including preparation methods and applications. The first method involves the use of ligands to provide stabilization for metal nanoparticles. Ligand-stabilized nanoparticles are considered to be very stable as it involves a formal bond between the ligand and the nanoparticle. This however has the disadvantage of passivating the surface of the particles reducing the particle surface area. The second method involves the use of dendrimers as templates for the encapsulation of metal nanoparticles, thereby stabilizing these metallic particles. The chapter also includes a short history of dendrimers followed by a brief discussion of the different synthetic pathways utilized to prepare dendrimers. The chapter concludes with a section exploring the advantages and applications of dendrimer encapsulated nanoparticles (DENs) as catalysts.

The **second chapter** introduces the concept of dendritic micelles and how they differ from conventional polymeric micelles. The synthetic routes to two types of dendritic micelles are discussed. The first section deals with the modification of generation 1-3 commercially available DAB PPI dendrimers with palmitoyl chloride to give hydrophobic DAB PPI dendritic micelles of three different generations. The second section deals with the preparation of novel cyclam-cored dendritic micelles containing a poly(amido amine) interior architecture. Two generations of cyclam-cored dendrimers were synthesized by repetitive Michael addition and amidation steps. The amine-terminated dendrimers were then modified on the periphery with palmitoyl chloride to produce cyclam-cored hydrophobic dendritic

Chapter 5

A Summary of the Preceding Chapters and Suggestions for Future Work

micelles. The characterization of all intermediate and final products by IR spectroscopy, ^1H -NMR and ^{13}C NMR spectroscopy, mass spectrometry and elemental analysis is also discussed.

Following the successful synthesis of two different dendritic micelles it was possible to apply them as templates for the encapsulation of gold nanoparticles. **Chapter three** contains the preparation methods and characterization details of the gold DENs. The chapter commences with a discussion about the maximum loading capacity of the dendritic micelles. By performing a UV/Vis titration binding study we determined that the nanoparticles are driven into the voids of the dendrimers by solubility forces rather than stabilization by complexation to the interior amine groups, as is the case with conventional dendrimers. The chapter continues with a description of the methods followed to produce gold DENs using 1:13, 1:31 and 1:55 dendrimer to gold ratios. The advantage of using dendrimers as templates is that specific cluster sizes, in this case Au_{13} , Au_{31} and Au_{55} , can be produced by changing the dendrimer to metal ratio. Characterization of the gold DENs performed by UV/Vis spectroscopy and HR-TEM is discussed. Relatively small, well dispersed nanoparticles are produced with an average particle size in the range of 4-6 nm. The chapter concludes with a comparison between the particle sizes achieved and those expected for Au_{13} , Au_{31} and Au_{55} DENs. Calculations indicate that Au_{1415} rather than Au_{55} or Au_{13} was formed. This could be explained by the fact that the encapsulation is solubility driven instead of complexation driven. Another explanation could be that the particles are entangled in the hydrophobic chains on the exterior of the dendrimer rather than situated in the interior voids. The formation of DSNs rather than DENs is also a possibility.

The final chapter, **Chapter four**, involves the application of the gold DENs as catalysts in the oxidation of n-octane. A brief overview of catalysts used in the oxidation of cyclic and linear alkanes is provided followed by the results of our catalytic studies. The catalysts tested were found to be very active producing substrate conversions between 70 and 93% and selectivity towards mostly ketone products. The optimum conditions determined included a reaction temperature and time of 70 °C for 72 hours using a 1:1 ratio of substrate to oxidant (TBHP) and 0.21 mol % catalyst loading. It was determined that the nanoparticle size has a greater effect on the percentage conversion achieved than the nature of the dendrimer template or dendrimer generation. A comparison between the gold DENs and other catalysts reported in the literature for the oxidation of n-octane revealed that our catalyst gives a much higher

Chapter 5

A Summary of the Preceding Chapters and Suggestions for Future Work

conversion. The chapter concluded with some mechanistic insight into the catalytic cycle and product distribution.

5.2. Suggestions for future work

Considering that gold nanoparticle growth easily occurs in solution over time it would be interesting to investigate if these catalysts could be stored and used in solid form and what the effect of this would be on its catalytic activity and selectivity. HR-TEM analysis over time of solid DENs as well as DENs in solution is necessary.

The preliminary catalytic results indicate that the gold DEN catalysts show great potential as oxidation catalysts. There is however still many questions that need to be answered. For example an in-depth investigation into the catalytic mechanism and how it can be tuned to further improve selectivity is necessary. A study into the recovery and reusability of the catalyst is also needed. If the Au nanoparticles are oxidised back to Au ions in the oxidation conditions is it possible to re-reduce them to be used in another cycle? Is the dendrimer template inert enough to survive the harsh oxidation conditions? Furthermore the use of milder and more environmentally friendly oxidizing agents (H_2O_2 , O_2 or air) and reaction conditions is typically desired.